HISTORIC AND FUTURE WEATHER EXTREMES IN THE SOUTH SASKATCHEWAN RIVER WATERSHED, ALBERTA

ROYA SADAT MOUSAVI

DOCTOR OF PHILOSOPHY, BU-ALI SINA UNIVERSITY, 2017

A thesis submitted
in partial fulfilment of the requirements for the degree of

DOCTOR OF PHILOSOPHY

in

EARTH, SPACE, AND PHYSICAL SCIENCE

Department of Geography and Environment
University of Lethbridge
LETHBRIDGE, ALBERTA, CANADA

HISTORIC AND FUTURE WEATHER EXTREMES IN THE SOUTH SASKATCHEWAN RIVER WATERSHED, ALBERTA

ROYA SADAT MOUSAVI

Date of Defense: September 15, 2023

Dr. J. M. Byrne	Professor Emeritus,	Ph.D.
Dr. D. L. Johnson	Professor	Ph.D.
Thesis Co-Supervisors		
Dr. R. Kroebel		
Thesis Examination Committee Member	Adjunct Professor	Ph.D.
Dr. Aaron Berg		
External Examiner	Professor	Ph.D.
University of Guelph, Ontario		
Dr. Craig Coburn		
Chair, Thesis Examination Committee	Associate Professor	Ph.D.

DEDICATION

To Mojtaba and Hana for their companion, patience, help, and love that supported and encouraged me tremendously in my journey.

ABSTRACT

Extreme weather events can cause catastrophic and long-lasting impacts on water availability, environment, agriculture, economies, and societies. This study investigates the historical and future conditions of drought- and temperature-related extreme events in the South Saskatchewan River Watershed (Alberta, Canada), which is dominated by activities related to agriculture and environment. We studied interdecadal drought variation as well as future projections of drought condition based on CMIP6 ensemble of 26 GCMs and 3 SSP scenarios. Our results showed increased occurrence rates of drought, with more intensified droughts occurring after year 2000 in the historical period. Future projections reveal that more occurrence of droughts and at higher severity levels are plausible under climate change scenarios. Similarly, the extreme temperature events showed increased numbers of hot summer days, fewer frost days and icing days, longer growing seasons, and increased occurrence of extreme temperatures are expected under climate change scenarios.

ACKNOWLEDGEMENTS

I would like to express my heartful thanks to my family and friends whose love, support, and encouragement helped me a lot during my PhD program. I would like to sincerely thank my supervisor Dr. James Byrne and co-supervisor Dr. Dan Johnson and my committee member Dr. Roland Kroebel for their invaluable support and remarkable advice. Their great knowledge and guidance were so constructive for my dissertation. I also would like to thank the professors and instructors at the Department of Geography and Environment who I collaborated with during my PhD program.

My warm thanks go to my fellow friends and lab mates Dr. Shima Javaheri, Adnan Aftab, Dr. Shaghayegh Mirmasoudi, and Hadis Honarvari, who were exceptionally supportive and helpful and their kindness helped me a lot in my journey.

I would like to extend my great appreciation to the University of Lethbridge, Department of Geography and Environment, School of Graduate Studies, and exceptional staff at the University Library, IT solution Center, and International Students Office.

I am extremely grateful for financial support I received from the University of Lethbridge, The Prentice Institute, Siksika SRDL Business Group, Old Sun Community College, the Alberta Real Estate Foundation, Lethbridge County, the Government of Canada and the Government of Alberta through the Canadian Agricultural Partnership for related northern Alberta research, and the MITACS National R&D Consortium.

TABLE OF CONTENTS

LIST OF TABLES

LIST OF FIGURES

LIST OF ABBREVIATIONS

AR4	Fourth Assessment Report
AR5	Fifth Assessment Report
AR6	Sixth Assessment Report
BCCAQv2	Bias Correction/Constructed Analogues with Quantile delta mapping algorithm version 2
CMIP6	Coupled Model Intercomparison Project Phase 6
CSDI	Cold spell duration index
DTR	Daily temperature range
ETCCDI	Expert Team on Climate Change Detection, Monitoring and Indices
FD	Number of frost days
GCM	Global Circulation Model
GSL	Growing season length
ID	Number of icing days
IPCC	Inter-governmental Panel on Climate Change
PDSI	Palmer Drought Severity Index
PET	Potential Evapotranspiration
RDI	Reconnaissance Drought Index
SPI	Standardized Precipitation Index
SPEI	Standardized Precipitation-Evapotranspiration Index
SSP	Shared Socioeconomic Pathways
SSRW	South Saskatchewan River Watershed
SU	Number of summer days (> 25°C)
SU30	Number of summer days (> 30°C)
TN	Minimum temperature
TN10p	Percentage of days when TN < 10^{th} percentile
TN90p	Percentage of days when TN > 90^{th} percentile
TNn	Monthly minimum value of TN
TNx	Monthly maximum value of daily TN
TR	Number of tropical nights
TX	Maximum temperature
TXn	Monthly minimum value of TX
TXx	Monthly maximum value of daily TX
TX10p	Percentage of days when TX < 10^{th} percentile
TX90p	Percentage of days when TX > 90^{th} percentile
WMO	World Meteorological Organization
WNA	Western North America RDI (Reconnaissance Drought Index)
WSDI	Warm spell duration index

CHAPTER 1: INTRODUCTION

The current trends of weather indicators show anomalies and intensification of climate extremes (Tabari, 2020). These variations can be seen on extreme events, such as occurrence of extreme temperature, precipitation, heat waves, and drought condition, and can have disastrous consequences for different sectors. Based on the most recent projections in AR6 the risk of severe extreme events such as heatwaves, droughts, and floods are evaluated to be high with 1.5 to 2°C warming, a shift from AR5 projections in which the extreme outcomes and events were expected to happen by temperature increases of 1.6 to 2.6°C (IPCC, 2018). Also, the current warming due to accumulation of greenhouse gasses in the atmosphere caused more temperature rise in Canada compared to other regions because of its location in higher latitudes and being adjacent to north pole. Reduction of ice cover, decreased Albedo, and subsequently more heat absorption are amongst the main reasons for more warming in Canada (especially closer to polar regions), compared to other regions.

Drought and heat waves will become more prevalent under global climate change. These phenomena have resulted in severe consequences in many regions, such as Western Europe-2003 (Luterbacher et al., 2004); Central Europe and Russia-2010 (Grumm, 2011); and California-2014 (Aghakouchak et al., 2014; Swain, 2014).

Due to global warming, coincidence of heat waves and droughts have been more frequent in recent years (IPCC., 2012; Aghakouckak et al., 2014; Xu et al., 2020). Many studies suggest an increase in drought intensity for the 21st century (Cook et al., 2014; Sheffield and Wood, 2008; Huang et al., 2016; Guo, 2012). Similar results are reported for extreme temperature and heatwaves (French et al., 2019; Parente et al., 2018;

Bandyopadhyay et al., 2016)

These extreme events need to be analyzed as they could happen simultaneously and superimpose effects (Parente et al., 2018). Moreover, heat waves could limit the suitable condition for convective precipitation, leading to less moisture and continuation of drought (Mazdiyasni and Aghakouchak, 2015).

Based on the definition, drought is a prolonged period with relatively low precipitation and reduced amount of available water. This broad definition could be interpreted differently from meteorological, hydrological, agricultural, and socioeconomic points of view, leading to different indices pertaining to each of these concepts (Danandeh Mehr and Vaheddoost, 2019; Tran et al., 2019). Among different types of droughts, the meteorological drought is normally considered as the cause to other types of droughts (Zhang and Jia, 2013). Meteorological drought is the result of dominancy of dry weather and can change rapidly. Other types of droughts are evident when the impacts of meteorological drought develop over time and can be apparent through available water and crop yields, and can result in socioeconomic changes. There are several indices proposed for drought analysis (Zargar et al., 2011, Eslamian et al., 2017) among which the SPI (Standardized Precipitation Index) and SPEI (Standardized Precipitation-Evapotranspiration Index) are frequently used because of their acceptable performance and simplicity. The SPI is proposed by the World Meteorological Organization (WMO) as a standard tool for countries to monitor drought (Svoboda and Fuchs, 2016). The SPI which is developed by McKee et al. (1993) is a simple method based on precipitation only. But as it does not account for temperature role in drought, SPEI index was later proposed by Vicente-Serrano et al. (2010) that uses a simple water balance equation by

replacing the precipitation parameter with the difference of precipitation and evapotranspiration. Both indices could be calculated for different timescales from one month to multiple months and can represent different characteristics of short-term and long-term droughts.

A heat wave is another extreme event that refers to higher rates of temperature that persist for several days, and usually is measured based on magnitude and duration. Heat wave impacts are multifold and can directly affect the environment and living organisms (including human, plants, and marine life), overburden the medical and power supply sectors, and damage the infrastructures (Perkins, 2013). Heat waves occur under high pressure of the upper atmosphere while a mass of air remains stationary for a number of days or weeks and acts as a blanket, and as a result of accumulation of heat and preventing convective currents, the temperature rises abnormally (www.worldatlas.com). Heat waves do not necessarily lead to droughts, but if they occur during a dry period, the impacts of the drought could be intensified.

Also, as a result of global warming, the amount of vapor in the atmosphere is altered due to greater vapor-holding capacity that can translate into more extreme precipitations and can cause floods and associated damage (Tabari, 2020). In addition, changes in dry and wet spells are reported in different regions (Alexander et al., 2006). As the impacts are not uniform in all the regions, they need to be studied locally to unveil the new routines under changing climatic conditions.

Extreme events are projected to occur more frequently and severely in Canada under climate change (Bush and Lemmen, 2019). Some of the impacts that are expected

to be intensified in Canada due to global warming include more droughts, floods, extreme heat, longer growing seasons, glacier melting and thawing permafrost (Bush and Lemmen, 2019). In Prairies, however, the extreme events are not rare, and the region has a history of long and severe drought and significant variation of temperature and precipitation (Wheater and Gober, 2013). The region known as the Palliser Triangle that covers a vast area in southern parts of Alberta and Saskatchewan and parts of Manitoba provinces was seemed a not suitable region for agricultural development, however, thanks to modern farming and irrigation technologies and weather and soil conditions of the region, today most of Canada's irrigated farms are located in the two western provinces (Wheater and Gober, 2013).

This study is focused on the South Saskatchewan River Watershed (SSRW) in Alberta which is the most populated area in the Alberta province and is dominated with agricultural land, ranches and related industries. The SSRW is home to rural communities, a number of First Nation's reserves and communities, and four large cities. This region has a heterogenous climate but most of it is defined by semi-arid climate, with dry and cold winters. It is in the leeward side of the Rocky Mountains and receives less amount of precipitation than other parts of the province and Canada (Chipanshi et al., 2006). Summer days could be hot and dry, especially recently. The summer of 2023 has experienced multiple days of record-breaking high temperatures. Recently, due to global warming, the region experiences longer growing seasons than the past. The communities and economy of the region are heavily relied on surface water resources in the four sub-basins of the SSRW (Red Deer River, Bow River, Oldman River, and South Saskatchewan River) with an overall discharge close to 9 BCM (Grinder and Peterson,

2010). The discharge of the rivers in the SSRW is mostly from snow melt water that originates in the Rocky Mountains in the western border of the Alberta and flows to the east through southern Alberta and Saskatchewan, where South Saskatchewan and North Saskatchewan Rivers join and make the Saskatchewan River that flows to the north end of Lake Winnipeg Lake, and finally into the Hudson's Bay (Wheater and Gober, 2013).

In this study, we investigate the recent and future changes that have occurred or are expected to occur in SSRW, with regards to extreme events such as drought, temperature extremes and heat wave. To this aim, we use a number of suitable indices and measures introduced and recommended by peer-reviewed scientific papers and organizations, depending on the data availability and their robustness for this type of analysis.

1.2 THESIS STRUCTURE

This thesis contains 5 chapters. This introduction provides highlights of the importance of this research and summarizes previous works and background of this study. The next three chapters are dedicated to the findings related to the thesis objectives explained below. The findings of this research are summarized in chapter 5, and recommendations are presented.

1.3 THESIS OBJECTIVES

This study has four main objectives that provide detailed insights regarding the long-term patterns of droughts and temperature related extremes and their changes in recent decades and in future time horizons in the South Saskatchewan River Watershed.

1- Studying the historical changes of drought in the South Saskatchewan River

Watershed using two drought indices and comparing the rate of drought occurrence rate in the past four decades (1980-2018) and the areas that showed significant trends of drought.

2- Investigating the impact of climate change on drought conditions in the study area using three SSP climate change scenarios (SSP1-2.6, SSP2-4.5, and SSP5-8.5) and comparing the results with the base period (1951-1990).

3- Identifying the areas most vulnerable to drought within the study area.

4- Investigating the impact of climate change temperature-related extreme events in the study area using three SSP climate change scenarios (SSP1-2.6, SSP2-4.5, and SSP5-8.5) and comparing the results with the base period (1951-1990).

This information is important to consider for adapting to climatic change and variability, increasing the resiliency of local communities, decreasing the vulnerability against damaging or unpleasant consequences of climatic change, and increasing preparedness of the healthcare sector, urban development plans, power supply, and infrastructure design in order to prevent/reduce the disastrous damages and losses.

CHAPTER 2: ANALYSIS OF HISTORICAL DROUGHT CONDITIONS BASED ON SPI AND SPEI AT VARIOUS TIMESCALES IN THE SOUTH SASKATCHEWAN RIVER WATERSHED, ALBERTA

2.1 INTRODUCTION

Drought is one of the most disastrous extreme events, and can have long-lasting impacts on water resources, agriculture, and environment (Sheffield, 2012) at a large spatial scale (Bonsal et al., 2011a). There are concerns regarding future potential of more severe and frequent droughts with global warming (Sheffield, 2012; Dai, 2004). The Sixth Assessment Report (AR6) of the Intergovernmental Panel on Climate Change (IPCC) indicates that continued global warming and increased atmospheric evaporative demand will cause more severe and frequent droughts and Western North America will experience increased agricultural, ecological, and hydrological droughts (IPCC, 2021b). More severe and longer droughts are also projected to occur by the end of the 21st century in the Canadian Prairies (Bonsal et al., 2020). Drought is a temporary but prolonged period with lack of moisture and may occur in all climates (Mishra and Singh, 2010). This concept could be interpreted differently based on different physical impacts on precipitation, soil moisture, and surface water resources (Zargar et al., 2011). Drought and the impacts of drought can be assessed from meteorological, hydrological, agricultural, and socioeconomic points of view, leading to different indices pertaining to each of these concepts (Tran et al., 2019). Among different types of droughts, meteorological drought is normally considered a fundamental cause of other types of droughts (Zhang and Jia, 2013). Meteorological drought is the result of a substantial period of dry weather, which can change rapidly. Other types of droughts, for example with impacts on available water and

crops and resulting in environmental and socioeconomic consequences, are evident when the impacts of meteorological drought extend over time (Zargar et al., 2011; Eslamian et al., 2017). Numerous drought indices have been proposed and employed that deal with different types and characteristics of droughts (for lists of different indices, their definitions and characteristics, refer to Zargar et al., 2011; Svoboda and Fuchs, 2016; Eslamian et al., 2017; Kchouk et al., 2021). Many studies have employed SPI (Standardized Precipitation Index) and SPEI (Standardized Precipitation-Evapotranspiration Index), which are considered useful because of their relative simplicity, robustness, and applicability in analyzing distinct aspects and consequences of drought, in part because they can be computed at different timescales. SPI with multi-scalar features was introduced by McKee et al. (1993). It does not have the shortcomings of previous methods such as PDSI (Palmer Drought Severity Index) in addressing the temporal variability of the drought (Li et al., 2015), and especially with regard to analyzing short-term droughts. Also, PDSI requires more variables, and is preferable and more accurate for analyses of arid and semi-arid regions (Yang et al., 2016). The calculation of SPI is simple (based only on precipitation) and recommended by the World Meteorological Organization (WMO) for monitoring meteorological drought by all countries (Svoboda and Fuchs, 2016). However, SPI does not account for the impact of temperature on drought and water demand. Therefore, Vincente-Serrano et al. (2010) adjusted the SPI by adding potential evapotranspiration (PET) to the calculations and substituting the P (precipitation) with the term D (defined as moisture deficit), resulting in the SPEI. This improved method estimates the cumulative difference between precipitation and potential evapotranspiration, and therefore it accounts for surface water balance and the role of temperature variability during drought condition (Zhang et al., 2015).

Both SPI and SPEI could be applied on multiple timescales, representing variation in drought conditions and characteristics (Pei et al., 2020). This feature has led to widespread application of these indices in many recent studies (Hong et al., 2015; Spinoni, 2014; Pei et al., 2020; Kchouk et al., 2021). The multi-scalar feature makes these indices useful tools for drought assessments related to water resources, and for different applications. The time lag until the consequences of meteorological drought emerge on available water resources (such as available moisture, small river, snowpack and snow melt water and groundwater recharge) and usage, causes the timescales of hydrological, environmental, agricultural, and socio-economic drought effect to vary significantly. In order to address these differences, different timescales of these indices can be applied as representative of different types of droughts; with 1-month being better reflective of meteorological drought, 3-months and 6-months better for evaluating hydrological drought, and longer timescales being more suitable for assessing the agricultural and socioeconomic droughts (Pei et al., 2020; Wang et al., 2021a). Gurrapu et al. (2014) showed that SPEI could accurately represent the variability of streamflow in Western Canada.

The Canadian Prairies are prone to long periods of droughts impacting large areas (Shabbar and Skinner, 2004; Chipanshi et al., 2006; Sun et al., 2012; Stewart et al., 2012; Bonsal et al., 2013, Masud et al., 2015). Some studies on drought in Canada were conducted (see the review by Bonsal et al., 2011b) that have shown that drought in the prairies is mainly due to high spatial and temporal precipitation variability that combined with temperature anomalies impact the drought frequency and severity (Bonsal et al., 2011b). Past drought events imposed significant costs on agriculture and economy of Western Canada. For example, the estimated loss from the 2001-2002 drought is estimated

to be 3.6 billion dollars in agricultural production in the Prairies (Sun et al., 2012), around 4 billion dollars in Canada's grain revenue (Khandekar 2004), and 6.14 billion dollars in the economy of the western Canada (Shabbar and Skinner 2004). In addition, ancillary factors resulting from drought such as insect outbreaks, additional transportation costs in reducing herds, soil damage, environmental damage, and costs of carrying hay and water, likely add to these figures considerably. Global scale drought study by Spinoni et al. (2014) showed that western Canada suffered from more frequent but less severe droughts between 1971-1990. They also found that more frequent droughts have been occurring between 1991-2010 in Canada, with 2001-2002 being a remarkable drought, as described by Weathon et al. (2008) and Sun et al. (2012). Spinoni et al. (2019) showed that Western North America experienced dramatic increases in extreme drought events during 1981-2016 compared to 1951-1980 period. Another global study by Dai et al. (2004) based on PDSI showed increasing drought trends in two periods of 1900-1949 and 1950-2002 in most parts of Canada, with hot spots in the Canadian Prairies. Similar increasing trends were identified by Sheffield et al. (2012) for western North America between 1950-2008 by using different evaporation models in PDSI.

The South Saskatchewan River Watershed (SSRW) is located in Southern Alberta (province) and in the rain shadow zone of the Rocky Mountains (Chipanshi et al., 2006), and far from other moisture sources (Bonsal et al., 2013). These conditions, as for other parts of the Prairies, cause generally low soil moisture and water supply (Sun et al. 2012). This region is highly dependent on water supply from Rocky Mountain streams, which are susceptible to snow droughts (Dierauer et al., 2019). With increased water consumption for agricultural use, this region faces future water insecurity (Wheater and Gober, 2013) that

could be exacerbated under drought conditions. Therefore, including more recent data is necessary to enhance our understanding of drought definition and history. In this study, we investigated interdecadal variability of drought condition as well as its long-term monotonic trends in the past four decades in the SSRW. High-resolution Daymet data (Thornton et al., 2017) is used to provide spatio-temporal series of monthly SPI and SPEI drought indices. The fine resolution of these data provides detailed drought surface maps that are required for historical analysis, forecasting, and development plans in Southern Alberta. This study differentiates the shorter timescale and longer time scale droughts that can have different impacts indicating different types of droughts, considering that longer periods of drought with accumulated moisture deficit can impact more resistant systems such as crops and groundwater recharge (O'Brien and Stroich, 2005). Also, this study aims at identifying the areas most vulnerable to drought by studying the rate of drought occurrence and drought trends. This information is important to adapt with gradual climatic shifts and variability, increase the resiliency of local communities, and decrease the vulnerability to detrimental consequences of drought, in order to prevent or reduce impacts and losses to agriculture, environment, and urban systems.

2.2 STUDY AREA

The South Saskatchewan River Watershed, located in Southern Alberta, Canada, consists of four sub-basins (Table 2.1) which drain an area of 112,800 km2 (Figure 2.1). The region lies between latitudes of 52º 58′ 6″and 48º 59′ 50″ and longitudes of 110º 0′ 3″ and 116º 35′ 55″, and includes parts of the Rocky Mountains in the West, foothills, and grassland, extending east to the border of Alberta and Saskatchewan. There are currently 12 major irrigation districts in this area that have a significant share in crop and livestock

production of Canada. The average annual discharge from this watershed is 8.842 Bm3, which originates from the Rocky Mountains, flows eastward, joining the Oldman River, Bow River, Red Deer River, and ultimately forms the South Saskatchewan River, which flows through Saskatchewan into the Northwest Territories, and drains into Hudson Bay.

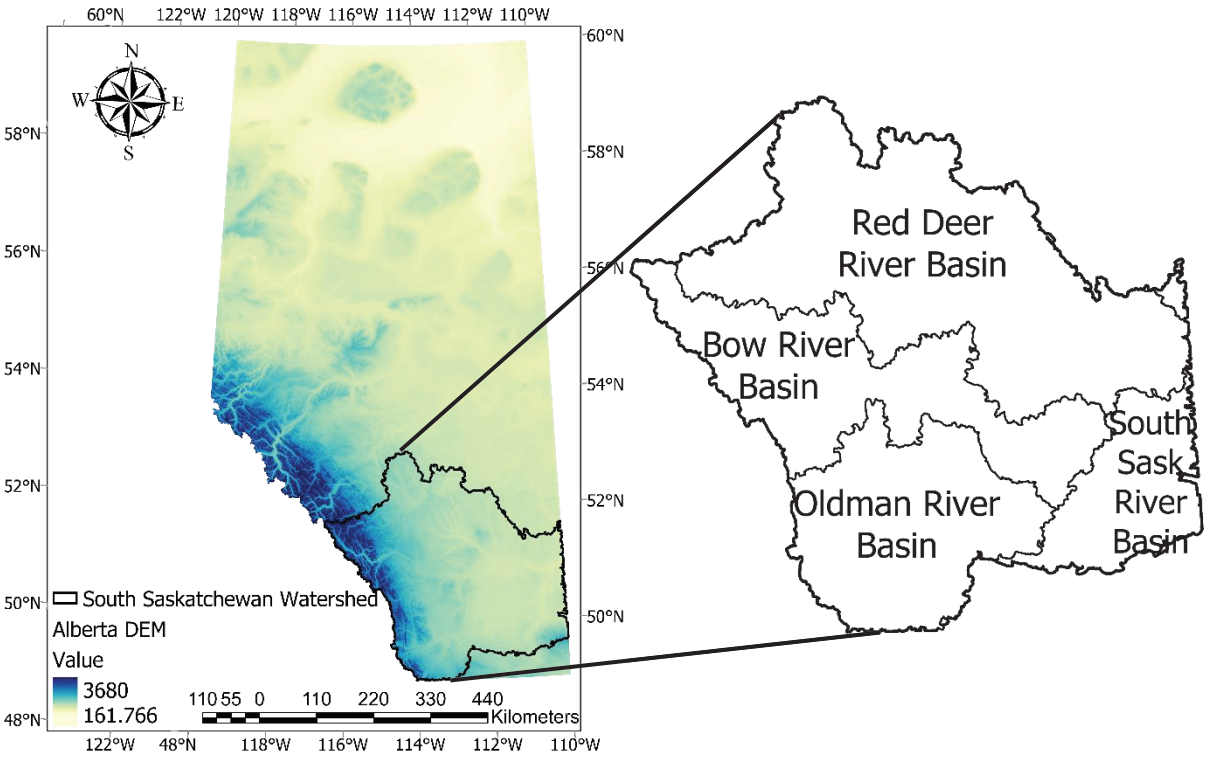

Fig. 2.1 Location of the South Saskatchewan River Watershed in Southern Alberta and its four sub-basins (Created by Alberta DEM adopted from Government of Alberta website: https://open.alberta.ca/licence)

Table 2.1 Characteristics of the sub-basins in the SSRW in Alberta (Grinder and Peterson, 2010)

Sub-basins	Drainage Area (km^2)	Annual Precipitation (mm)	Annual discharge (Mm^3)
Red Deer River Basin	46800	393	1666
Bow River Basin	25300	538	3829
Oldman River Basin	27500	488	3434
South Saskatchewan River Basin	13200	278	4
Total SSRW	112800	435	8842

2.3 DATASET

In this study, the Daymet high-resolution daily historical weather database, which provides gridded dataset of daily maximum and minimum temperatures and precipitation (Thornton et al., 2017), is used to calculate the drought indices. This dataset is used in many studies and is validated against recorded data by different scholars (Mourtzinis et al., 2017; Mehdipour et al., 2018; Walton and Hall, 2018).

Daymet uses daily maximum temperature, minimum temperature, and precipitation station data with algorithms to estimate weather data on individual 2°×2° tiles. The interpolation to estimate data at each point is based on the iterative estimation of station density using the spatial convolution of a truncated Gaussian filter which is described by Thornton et al. (1997). It uses various search radii for stations depending on the density of stations. In the Daymet software, spatially and temporally explicit empirical relationship of temperature and precipitation with the elevation change are analyzed and used. Daymet daily data is available from 1980 at the spatial resolution of 1 km×1 km for Canada, Mexico, the United States of America, and Puerto Rico.

The analysis period in this study is 1980-2018 which is used to compare inter-decadal variations and the long-term monotonic trends in the SSRW. Our analysis of the quality of the Daymet data with daily observed data showed a good fit between the Daymet data (daily precipitation, minimum temperature, and maximum temperature) and recorded data from weather.

2.4 METHODOLOGY

2.4.1 DROUGHT INDICES

2.4.1.1 SPI

The SPI index proposed by McKee et al. (1993) is one of the drought indices recognized by the WMO for worldwide application (Li et al., 2021). The SPI is based on precipitation only and is a multi-scalar index. Since this method is simple and accounts for different timescales, it received considerable acceptance and is widely used to study drought, for application in different sectors.

Equations 1 to 6 represent the procedure of calculating the SPI based on the Gamma distribution. For the precipitation value of x over a given period, the distribution of probability density function of Γ is as follows:

$$F(x) = \frac{1}{\beta^{\gamma}\Gamma(\gamma_0)} x^{\gamma-1} e^{-x/\beta}, x > 0 \qquad (1)$$

where β and γ are scale and shape parameters of the distribution function (Γ), respectively.

The probability of all precipitation events (x) that are smaller than the x0 for a given year is:

$$F(x < x_0) = \int_0^{\infty} f(x)dx \qquad (2)$$

and

$$F(x = 0) = m/n \qquad (3)$$

where m is the number of days with no precipitation (x=0) and n is the total number of days.

The normal standardizing of the Γ probability function is done through substitution of the result of probability value in the standardized normal distribution function:

$$f(x < x_0) = \frac{1}{\sqrt{2\pi}} \int_0^{\infty} e^{-x^2/2} dx \qquad (4)$$

By solving the above equation, the SPI would be as follows:

$$SPI = S \frac{t-(c_2 t+c_1)+c_0}{[(d_3+d_2)t+d_1]t+1} \qquad (5)$$

where

$$t = \sqrt{ln \frac{1}{F^2}} \qquad (6)$$

$$c_0 = 2.515517;\ c_1 = 0.802853;\ c_2 = 0.010328;$$

$$d_1 = 1.432788;\ d_2 = 0.189269;\ d_3 = 0.001308$$

c0, c1, c2, d1, d2 and d3 are constant parameters of SPI. The sign of the SPI index is identified by coefficient S that is based on the value of F. For F>0.5, S equals 1 and for F≤0.5, S equals -1.

2.4.1.2 SPEI

Vicente-Serrano et al. (2010) proposed the SPEI based on the SPI method with a simple climatic water balance by adding the PET as an input. SPEI has both the

multiscale characteristic of the SPI and sensitivity to atmospheric water demand of the PDSI. These advantages combined with its relative simplicity makes it more advantageous compared to other methods (Tan et al., 2015). The computation procedure of SPEI is presented by Vicente-Serrano et al. (2010) (Eqs. (7) to (14)).

There are different methods that could be used to estimate the PET (such as Thornthwaite method, Penman-Monteith method, and Hargreaves method). After computing the PET by any of the available methods, the moisture deficit of the month i would be as follows:

$$D_i = P_i - PET_i \qquad (7)$$

The standardization is followed by selection of the probability density function of a three-parameter log-logistic distributed variable as follows:

$$f(x) = \frac{\beta}{\alpha}\left(\frac{x-\gamma}{\alpha}\right)^{\beta-1}\left(1+\left(\frac{x-\gamma}{\alpha}\right)^{\beta}\right)^{-2} \qquad (8)$$

in which, α, β and γ are scale, shape, and origin parameters, respectively; with D values in the range $\gamma > D < \infty$. These parameters are obtained through Eqs. (9) to (11):

$$\beta = \frac{2w_1 - w_0}{6w_1 - w_0 - 6w_2} \qquad (9)$$

$$\alpha = \frac{(w_0 - 2w_1)\beta}{\Gamma(1+1/\beta)\Gamma(1-1/\beta)} \qquad (10)$$

$$\gamma = w_0 - \alpha\,\Gamma\left(1+\frac{1}{\beta}\right)\Gamma\left(1-\frac{1}{\beta}\right) \qquad (11)$$

where Γ(β) is the gamma function of β.

The probability density function of D based on the given distribution of three-parameter log-logistic is as follows:

$$F(x) = \left[a + \left(\frac{\propto}{x-\gamma}\right)^{\beta}\right]^{-1} \qquad (12)$$

Then, the SPEI is calculated as the standardized values of F(x) as follows:

$$SPEI = W - \frac{c_0 + c_1 W + c_2 W^2}{1 + d_1 W + d_2 W^2 + d_3 W^3} \qquad (13)$$

Given P is the probability of exceeding a given D value (P=1-F(x)), for P≤0.5, the W is:

$$W = \sqrt{-2\ln(P)} \qquad (14)$$

And, if P>0.5, then P is replaced by 1-P and the sign of the resultant SPEI is reversed.

Six constant parameters of the SPEI equation are as follow:

$$c_0 = 2.515517;\ c_1 = 0.802853;\ c_2 = 0.010328;$$

$$d_1 = 1.432788;\ d_2 = 0.189269;\ d_3 = 0.001308$$

2.4.2 DROUGHT CATEGORIES BASED ON SPI AND SPEI

In this study, we used different drought classes as presented in Table 2.2 to determine the drought severity based on the categories adapted from McKee et al. (1993). When the index value drops below 0, it indicates the start of the drought; and the drought ends when the sign become positive once more. The more negative the value of the index,

the more severe the drought condition (McKee et al., 1993). Other classifications are used by other researchers for different regions. For example, Spinoni et al. (2018) used a combined measure based on three indices, including SPI and SPEI and RDI to study the drought in the past and future in Europe and used "normal/dry" category instead of "mild dry" for when their combined index values were between -1 and 0; Bonsal et al. (2011a) described SPI between -0.5 and 0.5 as near normal and Bonsal et al. (2017) identified -1 to +1 as near normal. Use of different classes to describe the drought condition depends on study design and the climate regime of the study area. In more humid areas values above -1 might describe minor dryness that could be considered as normal with minimal impact, but it is necessary to reassess such categories in areas with arid and semi-arid climates, such as the Canadian Prairies, which are vulnerable to even mild but long-lasting droughts.

Table 2.2 Drought classification based on the SPI and SPEI values

Drought category	Index values
No drought	0<Index
Mild drought	-1< Index≤0
Moderate drought	-1.5< Index≤-1
Severe drought	-2<Index≤-1.5
Extreme drought	Index≤-2

2.4.3 ESTIMATION OF PET

There are different methods to estimate the maximum evaporative potential of the atmosphere, which vary in their simplicity, data requirement, and timestep, such as Penman (1948), Thornthwaite (1948), Hargreaves (1994), Penman-Monteith (Allen et al. 1998), and Modified Hargreaves (Droogers and Allen, 2002). In this study, the

Hargreaves method is used for calculating the PET (Hargreaves and Samani, 1985). This method is simple and is based on maximum and minimum temperature. It is widely used and recommended for estimating PET (Hargreaves, 1994). Satisfactory performance of the Hargreaves method is apparent in multiple studies especially when data are scarce or uncertainty is high (Hargreaves and Allen, 2003; Beguería et al., 2014). There are recommendations for using more sophisticated models that account for surface energy balance, like Penman-Monteith, however its application is limited by extensive data requirement (Beguería et al., 2014). Also, to achieve acceptable accuracy some local calibrations of wind and solar radiation equation might be required, especially in arid areas (Allen et al. 1998; Sabziparvar et al., 2013; Mousavi et al., 2015).

2.4.4 TREND ANALYSIS OF THE DROUGHT TIMESERIES

For detecting trends in the computed drought indices, the Mann-Kendall trend method at 95% significance level is employed at each cell to produce the trend maps. The power of this method is in detection of the trends in nonparametric datasets and, as most of the hydro-climatic datasets are not normal, it is therefore recommended and widely used for hydrologic and climatologic studies (Mousavi et al., 2019).

2.4.5 DATA ANALYSIS

Data processing and analysis is done by employing ArcGIS Pro and RStudio (R Core Team 2020). R packages used to compute indices (SPEI package, version 1.7) and trend analysis (modifiedmk package, version 1.6).

2.5 RESULTS AND DISCUSSION

2.5.1 DECADAL AVERAGE OF DROUGHT CONDITION

To assess the long-term trends of drought in the SSRW, the spatial time-series of SPI and SPEI at 1-, 3-, 6-, 9-, and 12-months timescales were prepared. Figure 2.2 summarizes the percentage of areas within the SSRW that experienced drought in the past four decades. Drought has impacted nearly half of the watershed during the study period. The decadal average shows that the drought was more extensive during 2001-2010. Also, Yang et al. (2020) found that southern parts of Canada experienced more severe droughts between 1999-2005, compared to other 5-years periods within the 1950-2016 period. Further, the percentage of the area characterized as severely or extremely dry is shown to be significantly higher in 2001-2010 than in other decades and it is more pronounced for both the SPI and SPEI at longer timescales (i.e., 6-, 9-, and 12-months). This increase in the severity of drought with increasing timescale could be interpreted in relation to the different types of droughts that each index timescale is representing. Thus, based on the results, mild or moderate meteorological droughts (1-month timescale) caused severe or extreme conditions in the region that can lead to a significant drought impact on the available water and agricultural sector, shown by the increase in areas with higher severity of drought when longer timescales of the indices were applied.

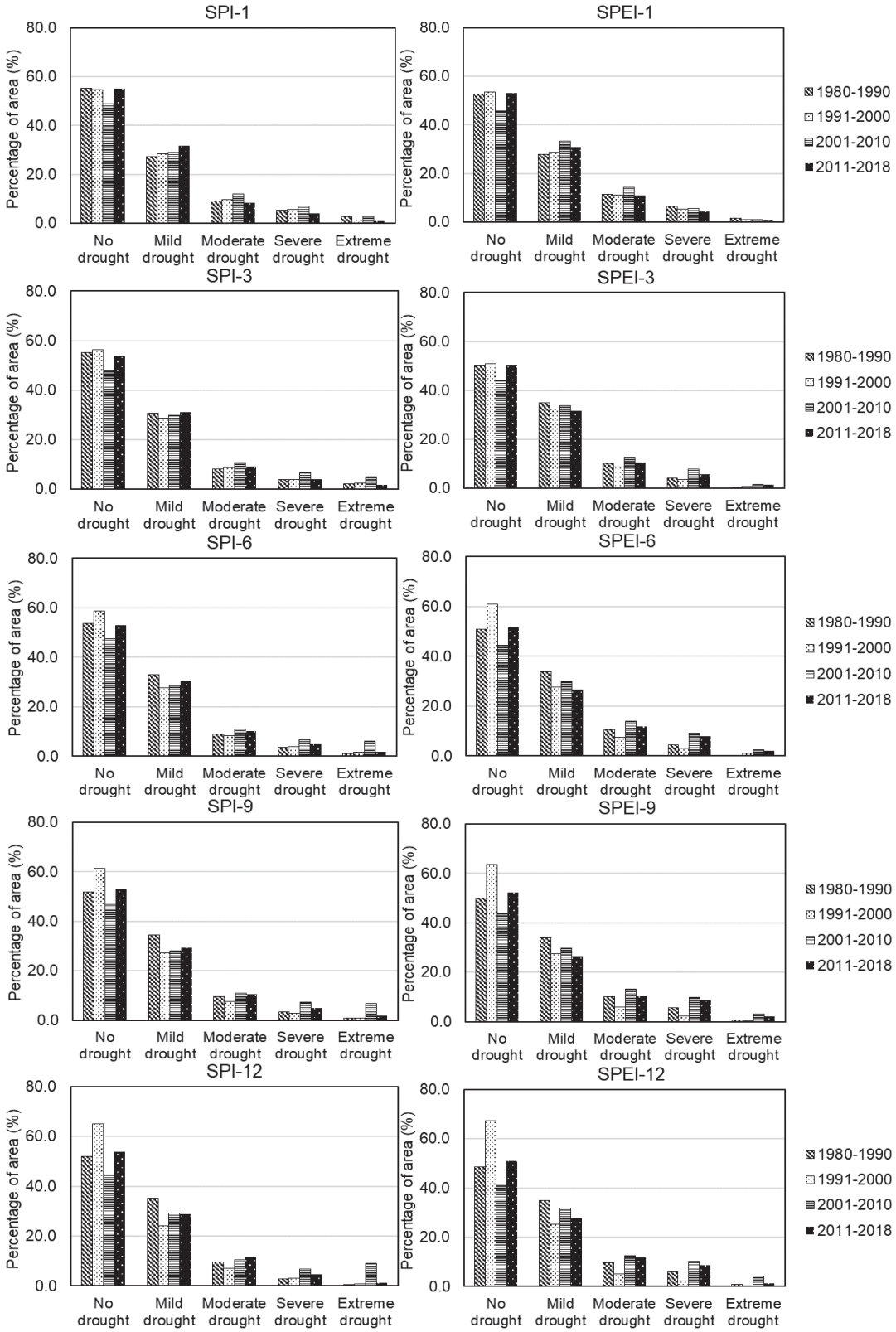

Fig. 2.2 Percentage of areas within the SSRW that experienced different degrees of drought based on SPI and SPEI at 1-, 3-, 6-, 9-, and 12-months timescales (1980-1990; 1991-2000; 2001-2010; and 2011-2018)

2.5.2 DROUGHT TRENDS

Figures 2.3 and 2.4 illustrate the significant trends observed in drought, based on SPI and SPEI. We use terms of increasing and decreasing trends for drought, implying increased and decreased drying, respectively, regardless of the sign of the index. Both indices show similar patterns regarding decreasing or increasing trends in both upstream and downstream areas. Significant decreasing drought trends are visible in the headwaters of the Bow River in the Rocky Mountains, which at longer timescales are more extensive. Decreasing drought trends are visible on some spots located on the eastern boundary of the SSRW. Increasing drought trends are more indicated in the northern parts at 1-month and 3-months for both indices.

At longer timescales, the area of increasing drought trends expands towards central and southern parts of the watershed and encompasses a significantly larger area. This indicates propagation of the effects of meteorological droughts, extended at longer timescales, to the extent that drought could affect the available moister of a larger region. Therefore, even a low-range drought at shorter timescales (meteorological drought) can function as an indicator of extended droughts affecting soil water content and water resources condition of the wider region. In the same way, the areas with decreasing drought trends can enlarge as the timescale increases, which shows expansion of the moisture availability and suitability of agricultural and economic conditions followed by decreasing trends of drought.

Table 2.3 represents the percentages of the area of SSRW that have increasing, decreasing, or no drought trends based on the SPI and SPEI at different timescales. The

significantly greater size of the areas with increasing or decreasing trends at longer timescale implies that the trends are more pronounced at longer timescales. In addition, the values presented in Table 2.3 clearly show that, based on SPEI, a larger portion of the SSRW is subject to increasing drought trends and much less area to decreasing drought trends.

Table 2.3 Percentage of the area in the SSRW with increasing, decreasing, or not significant drought trends, based on SPI and SPEI at 1-, 3-, 6-, 9-, and 12-months

Timescale	Increasing trend		Decreasing trend		No trend	
	SPI	SPEI	SPI	SPEI	SPI	SPEI
1-month	7.95	7.11	2.87	3.16	89.18	89.72
3-months	23.20	30.39	8.35	5.73	68.45	63.87
6-months	37.98	49.72	8.67	6.61	53.35	43.67
9-months	40.08	51.96	12.27	9.48	47.65	38.56
12-months	43.53	56.96	14.89	10.68	41.58	32.36

Yang et al. (2020), using 1950-2016 data, showed Southern Alberta experienced drying trends in the winter season. They also reported decreased frequency and duration of droughts for most southern parts of Canada. However, their results were generalized over a large region and do not represent localized long-term variations.

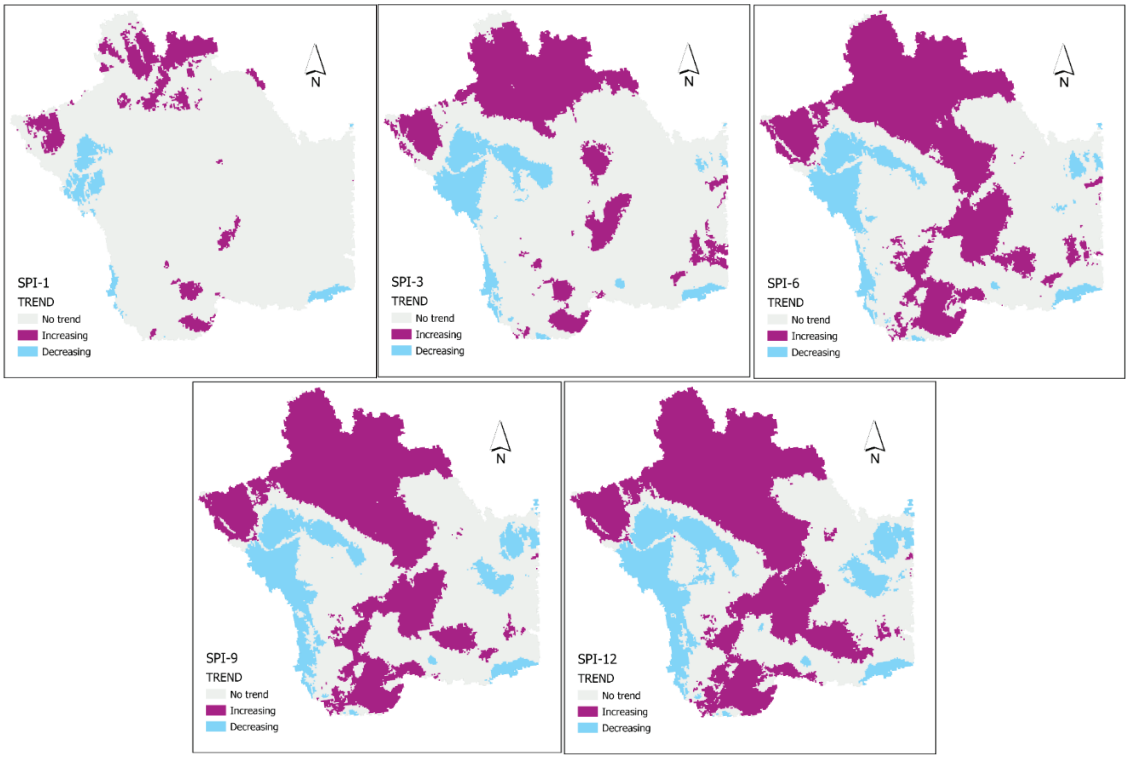

Fig. 2.3 Trends of SPI drought index at 1-, 3-, 6-, 9-, and 12-months timescales in the SSRW with the Mann-Kendall trend test (1980-2018) at 95% significance level

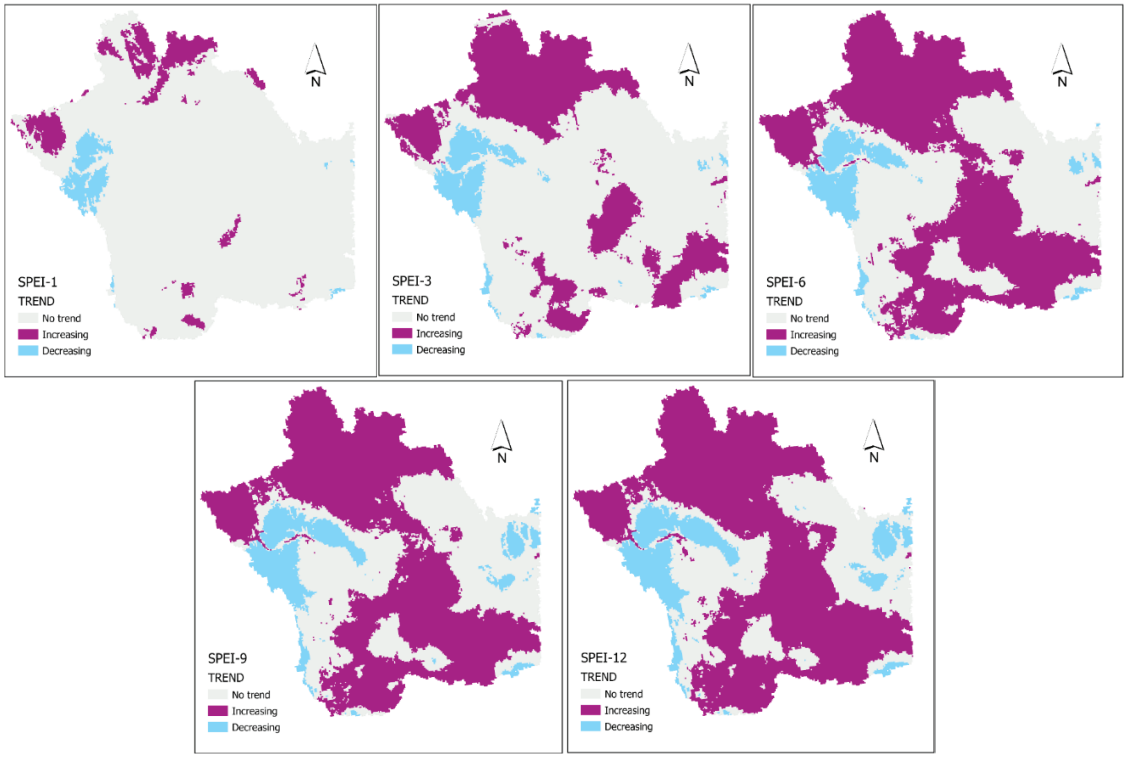

Fig. 2.4 Trends of SPEI drought index at 1-, 3-, 6-, 9-, and 12-months timescales in the SSRW with the Mann-Kendall trend test (1980-2018) at 95% significance level

2.5.3 DROUGHT OCCURRENCE

To identify the areas within the watershed that are more prone to drought, the drought occurrence rate is illustrated by the proportion of dry months to the total count of months during the study period. The ratios are presented as percentages in Figures 2.5 and 2.6 for SPI and SPEI, respectively. Based on these results, all parts of the watershed have experienced some sort of drought during the past four decades and the percentage of drought occurrence at each point ranges between 36 and 55% of time in the SSRW. These results are comparable to findings of global and regional studies, such as Bonsal et al. (2013), Spinini et al. (2014) and Masud et al. (2015), showing hot spots of droughts in this part of Prairies in Western Canada.

The frequency of dry months is slightly different between SPI and SPEI. Based on the SPI, lower drought frequencies are evident in the northern part of the region, especially at timescales of 6-months and longer. Based on SPEI, higher occurrence rates of drought (darker spots) are spread out in almost all parts of the region and do not form a distinguishable, consolidated pattern. Overall, it can be seen in Figures 2.5 and 2.6 that the SPEI showed higher rates of drought, than the SPI.

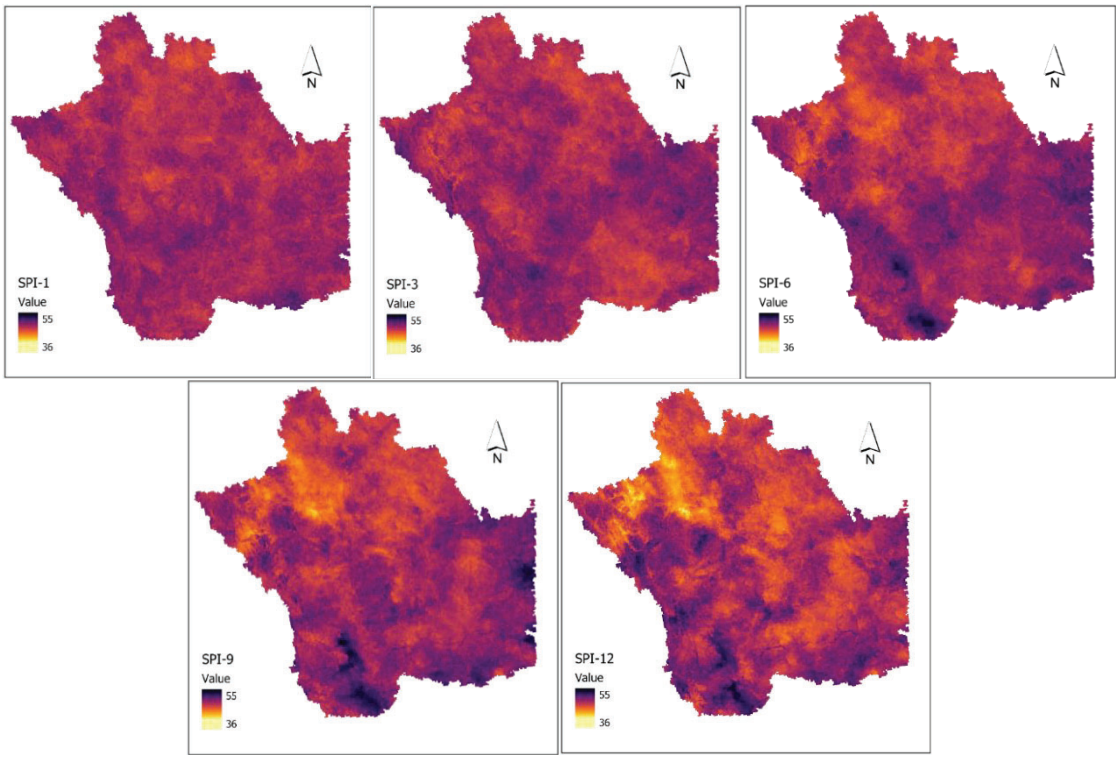

Fig. 2.5 Drought occurrence rate as percentage of dry months to the whole study period based on SPI at 1-, 3-, 6-, 9-, and 12-months timescale in the SSRW (1980-2018)

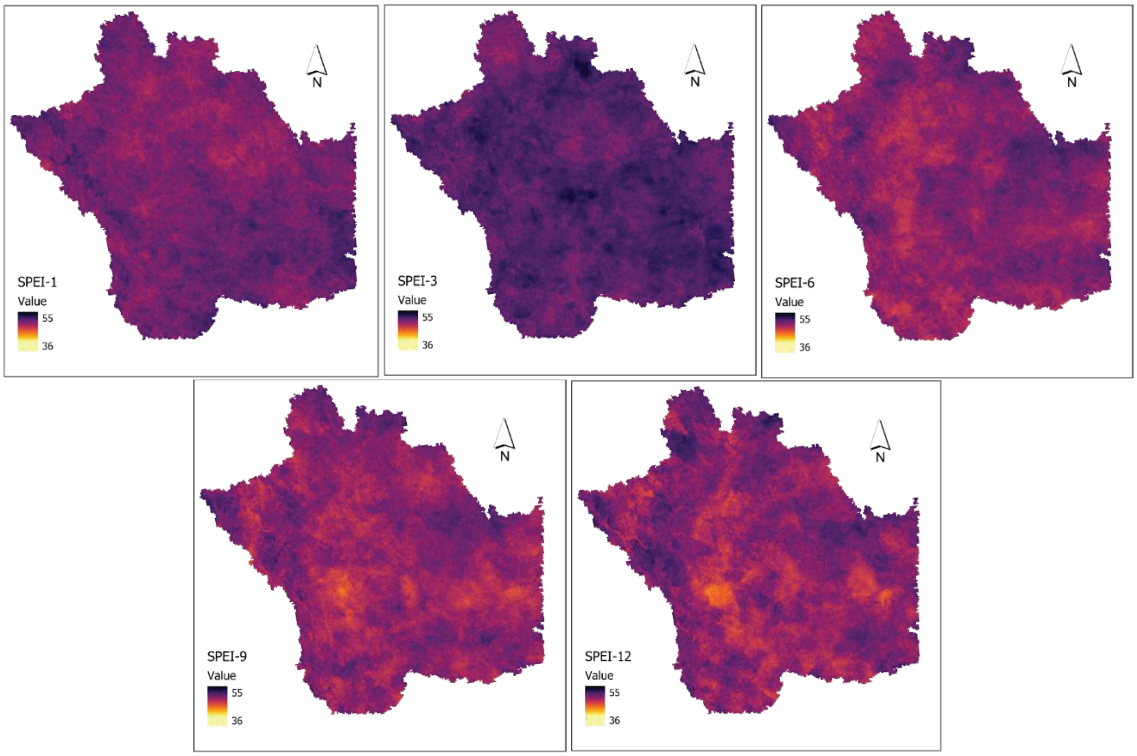

Fig. 2.6 Drought occurrence rate as percentage of dry months to the whole study period based on SPEI at 1-, 3-, 6-, 9-, and 12-months timescale in the SSRW (1980-2018)

Masud et al. (2015) using 1961-2003 data, identified the southern parts of the Saskatchewan River Basin and areas closer to Alberta and Saskatchewan border as areas with higher risk of drought. Our results confirm both the high rate of occurrence of drought and also the increasing drought trends (especially at higher timescales) in most parts of the Red Deer, Oldman River, and Albertan part of the South Saskatchewan River Basins, as well as the downstream of the Bow River basin, which suggests increased risk and vulnerability of this part of the Saskatchewan River Basin to drought.

2.5.4 CONSISTENCY OF SPI AND SPEI

Results of the trend test (applied to both indices) and maps of the occurrence rate of drought (calculated as the percentage of dry months to the whole of the study period) were compared for the two indices.

Comparing trend maps of SPI and SPEI at different timescales shows that the detected trends are significantly different between the two indices. At timescales of 1-, 3-, 6-, 9-, and 12-months 2.95%, 50.60%, 46.63%, 44.64%, and 11.86% of overlayed cells show inconsistent trend results, respectively.

Dry months occurrence rates (as percentage) were also compared based on the applied index. Table 2.4 shows the percentage of the area with different drought occurrence rates for SPI and SPEI at various difference levels. The values suggest that the two indices were showing slight differences (less than 5%) in 54.74%, 24.93%, 68.62%, 63.53, and 53.28% of the area at 1-, 3-, 6-, 9-, and 12-months, respectively. The percentages of the areas with different occurrence rates for SPI and SPEI are significant at 5-10% difference level as well (ranging from 26.79% to 54.07%). But, for difference

levels above 10% the percentages of the areas with inconsistent SPI and SPEI results drop down to 2.93%, 21.00%, 4.59%, 6.36, and 14.33%, at 1-, 3-, 6-, 9-, and 12-months, respectively.

Table 2.4 Percentage of area showing different values of drought occurrence rates for SPI and SPEI

Difference Level (DL)	1-month	3-months	6-months	9-months	12-months
<5%	54.74	24.93	68.62	63.53	53.28
5≤DL<10%	42.33	54.07	26.79	30.12	32.39
10≤DL<15%	2.91	19.27	4.50	5.85	11.14
15≤DL<20%	0.01	1.70	0.09	0.46	2.62
20≤DL<25%	0.00	0.02	0.00	0.05	0.52
25≤DL<30%	0.00	0.00	0.00	0.00	0.05

Masud et al. (2015) reported small differences between SPI and SPEI in the Saskatchewan River Basin. Conversely, Spinoni et al. (2019) reported that by examining the role of temperature in drought assessment using SPEI, many areas including Canada, showed a drying pattern, which were representing a wetting trend based on SPI. They concluded that this difference is related to greater impact of increased PET that offsets the impact of increasing precipitation trend. Our results also show a significant difference between SPI and SPEI at a significant percentage of the study area. The difference between the results of different studies might come from different resolution of the applied gridded data, the time period of the study or different parametrization and model set up for calculation of the indices.

Histograms of the number of dry months as a percentage of all months during the study period are shown in Figure 2.7. On average, around 47 to 50% of the area of the watershed experienced drought at different severity levels. When the SPEI is employed,

the number of detected dry months is slightly higher than when the SPI is used. The standard deviations are higher for SPI than for SPEI.

Tefera et al. (2019) reported that there is a high degree of agreement between the two indices in Northern Ethiopia. Comparison of the results obtained by the SPI and SPEI in this study suggests that the differences between the two drought indices in identifying dry months is less than 15% at most of the study area. Although differences of occurrence rates are small in the SSRW, the performances of two indices are not consistent when they are used for trend analysis. This result is in line with the reports of some other studies that reported notable differences of the two indices and better performance of the SPEI (Pei et al., 2020).

This could be explained based on the weather indicators that are used in the calculation of each index. Including evapotranspiration in calculation of the drought index can change the outputs significantly and can be more realistic, which denotes the determining role of evapotranspiration in the assessment of drought condition.

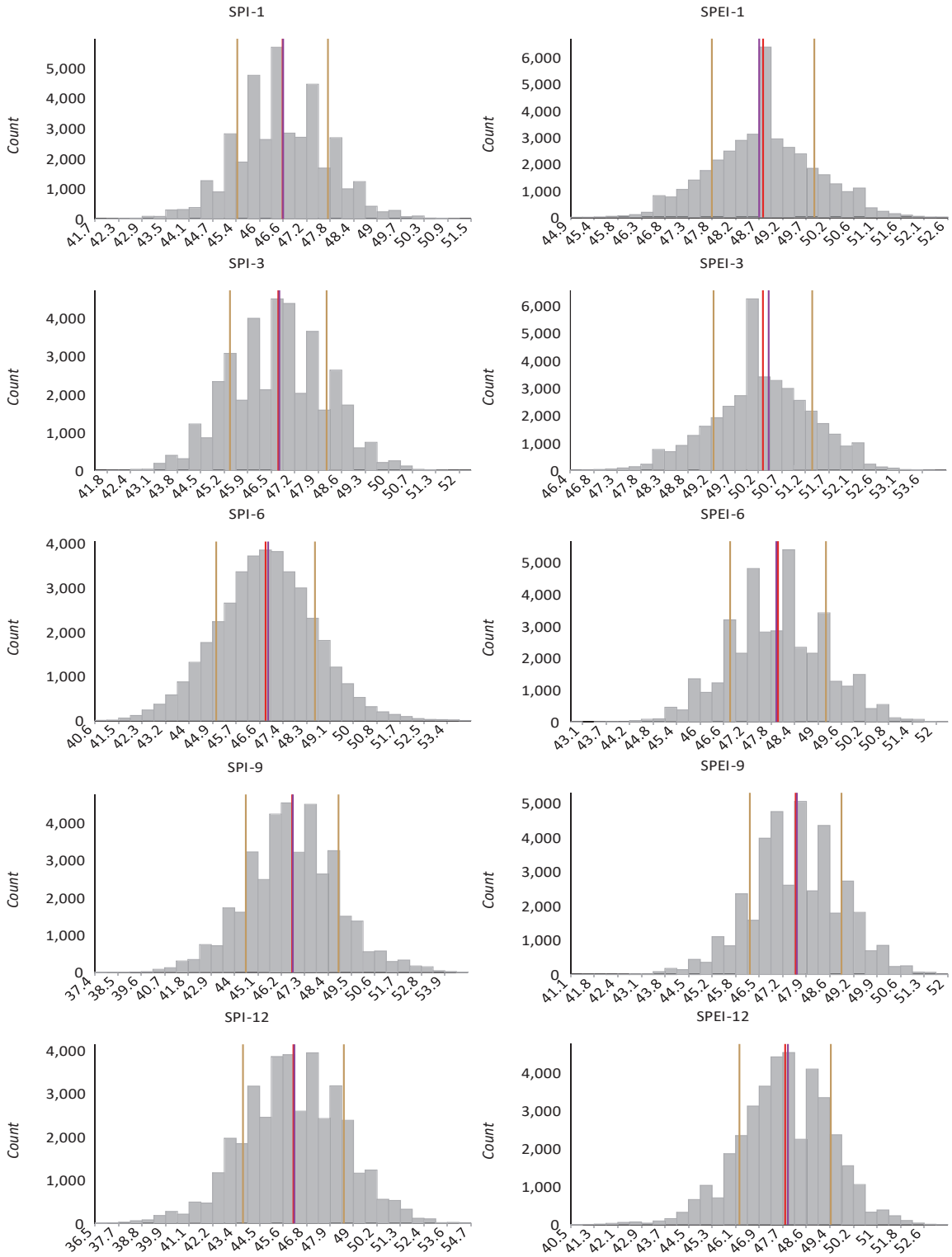

Fig. 2.7 Comparison of the distribution of the number of dry months as a percentage of the total months during the study period, obtained by SPI and SPEI at 1-, 3-, 6-, 9-, and 12-months in the SSRW

2.6 CONCLUDING REMARKS

In this study, the historical drought conditions and evolution were investigated in the South Saskatchewan River Watershed at a fine spatial resolution using a Daymet-gridded dataset in the past 4 decades, based on the indices of SPI and SPEI. The temporal and spatial outputs of SPI and SPEI were compared in order to analyze their performance and degree of agreement.

Based on the results, the region has experienced drought at various severity levels at approximately 50% of the analysis period. On average during the 2001-2010 decade, the geographical area that experienced drought was higher than the other decades. Both indices show that there is a significant increase in the area that is characterized as severe drought and extreme drought in the last two decades of the study period.

The Mann-Kendall trend test was applied on spatiotemporal time series of SPI and SPEI. Both increasing and decreasing trends of drought were detected in various parts of the SSRW. Drought trend maps are similar to the patterns of drought presented by Spinoni et al. (2014), who studied global patterns of drought for 1950-2010 and showed increasing drought severity trends for Alberta. However, the areas identified as having increasing trends are even larger at the longer timescales in the present study. Increasing area with a significant drought trend with the timescale of the drought indices implies that areas in the vicinity of spots with meteorological increasing or decreasing drought trends, at longer timescales, show significant trends of higher order droughts, i.e., hydrological, and agricultural drought. Sun et al. (2012) used a combined drought index to assess agricultural drought in the Canadian Prairies, taking the 2001 drought as an example to

compare drought in different months during the growing season. They showed transition of drought from mild to severe and advancement from smaller areas with severe drought to farther regions, over 6 months (Apr-Sep), from southeastern Alberta to southwestern and southern Saskatchewan, which depicts a basin-wide pattern that apparently follows the South Saskatchewan River. This example shows how the impacts of drought could accumulate over time and extend to adjacent regions and could explain the reason of expansion of areas with increasing or decreasing drought trends in this study at longer timescales.

Both SPI and SPEI at 1-month timescale revealed increasing droughts in the northern parts of the SSRW and decreasing patterns mainly visible in the west and upstream areas in the Rocky Mountain. At longer timescales, the significant increasing drought trends were mostly observed in the downstream plains of the SSRW that encompasses large areas in the northwest, north, middle, and southwest to southeast of the SSRW, where the main agricultural practices are taking place.

Based on the results, SPI and SPEI show similar geographical patterns in both trend detection and analysis of occurrence of drought. However, notable differences were found between the two indices in identifying the drought trends of each cell, as well as the drought occurrence rates of each cell. Overall, including evapotranspiration in the drought analysis resulted in detection of drought in more areas. Also, more areas with increasing drought trends were found within the study region by the SPEI, than the SPI. Including evapotranspiration and using the SPEI in drought analysis made a significant difference in outputs in the study area. Because SPEI is based on the water deficit, it seems to reveal more realistic and reliable outputs.

CHAPTER 3: PROJECTION OF 21ST CENTURY DROUGHT IN THE SOUTH SASKATCHEWAN RIVER WATERSHED

3.1 INTRODUCTION

Drought is a state of the atmosphere with prolonged lack of moisture (Mishra and Singh, 2010) that can detrimentally affect multiple sectors, such as environment, agriculture, and water resources (Bonsal et al., 2011a; Sheffield, 2012; Wang et al., 2021a), through the resulting reduced rainfall and increased drying. This extreme event originates from atmospheric conditions leading to meteorological drought (Zhang and Jia, 2013); but it also involves hydrological, biogeographical, biogeochemical, and human interaction processes (Wang et al., 2021a). Based on IPCC (2012) and IPCC (2021a), more frequent and intense drought events are predicted to happen by the end of 21st century and many studies confirm that on both global and regional scales (Cook et al., 2014; Sheffield and Wood, 2008; Huang et al., 2016; Guo, 2012). Global warming can also impact the water holding capacity of the atmosphere and cause more frequent and severe droughts (Dai et al. 2004; Wang et al. 2021b). Temperature increase is perceived to cause an acceleration of the hydrological cycle that translates into precipitation anomalies (Liu et al. 2018). Although drought is a temporary and recurring event, its increased occurrence and intensification causes irreversible impacts of economies, societies, and ecosystems (Wang et al., 2021a). Based on the most recent projections in the IPCC's Sixth Assessment Report (AR6), the risk of severe droughts is evaluated to be high with 1.5 to 2.0°C warming, which based on AR5 was projected to be more likely to happen at that level of severity by 1.6 to 2.6°C temperature increases (IPCC, 2018).

Drought can deteriorate the soil (Al-Kaisi et al., 2013), accelerate soil erosion (Masroor et al., 2022), set the stage for wildfires (Littell et al., 2016; Chen, 2022), and give rise to outbreaks of insect pests adapted to drought conditions (in Alberta: Grace and Johnson, 1985, Johnson and Worobec, 1989, Johnson, 1989). Severe droughts also can reduce the crops carbon uptake and contribute to more warming (Peters et al., 2018).

Based on the AR6, Western North America (WNA) is prone to more droughts under global climate change than in the past (IPCC, 2021a). Within that region, the Canadian Prairies are particularly susceptible to more intense and longer droughts (Bonsal et al., 2020), driven by high variability and anomaly of precipitation and temperature (Bonsal et al., 2011b). This region, including Alberta, has experienced long and extensive droughts in the past (Grace and Johnson, 1985, Shabbar and Skinner, 2004, Chipanshi et al., 2006, Sun et al., 2012, Stewart et al., 2012, Bonsal et al., 2013, Masud et al., 2015). Spinoni et al. (2014) reported that frequent moderate drought events occurred in this region between 1971-1990 and increased between 1991-2010. There is evidence of increasing trends of droughts in WNA (Sheffield, 2012, Spinoni et al., 2019) and more specifically in parts of the Prairies (Dai et al., 2004, Mousavi et al., 2023). Both the economy and agricultural production of Western Canada and the Prairies have suffered significantly from the impacts of drought in past decades, with imposed billions of dollars in loss (Khandekar, 2004, Shabbar and Skinner, 2004, Sun et al., 2012).

There are several useful indices for drought characterization (Zargar et al., 2011; Svoboda and Fuchs, 2016; Eslamian et al., 2017; Kchouk et al., 2021) among which SPI (introduced by McKee et al., 1993) and SPEI (introduced by Vicente-Serrano et al., 2010) became frequently used in drought studies due to their simplicity, robustness, and multi-

scalar feature that is very useful for studying short-term and long-term droughts. SPI is based on precipitation only and because of acceptable results and relative simplicity it is recommended by the World Meteorological Organization (WMO) for meteorological drought monitoring (Svoboda and Fuchs, 2016). However, SPI does not include responses to temperature or temperature variation, strongly determining factors in the impact of drought on landscapes and living things. Therefore, an adjustment was made by Vincente-Serrano et al. (2010), replacing the precipitation term with moisture deficit that is defined as precipitation minus potential evapotranspiration (PET), thus introducing SPEI. Both indices could be used at different timescales and represent the short-term or longer-term droughts that could be attributed to different characteristics of drought, or the time that the various impacts of drought could be seen in surface water resources, plants, groundwater, pests, erosion, and agricultural production and economy. For example, shorter timescales (1-3 months) are associated with meteorological drought and medium ranges (of 6-12 months) could be representative of a drought that can alter hydrological regime and even agricultural conditions. Longer timescales of the aforementioned drought indices (i.e., 12-24 months) could also be applied to analyze the socio-economic impacts of drought (Pei et al., 2020; Wang et al., 2021a). Mousavi et al. (2023) employed SPI and SPEI to study the drought in the SSRW at different timescales (1-, 3-, 6-, 9-, and 12-months) and showed the longer timescales reveal clearer patterns of increased or decreased drought trends. They found that the SPEI better captures droughts. Also, Gurrapu et al. (2014) showed that SPEI could accurately represent the variability of streamflow in Western Canada.

This study uses the SPEI drought index at different short-term and long-term

timescales to investigate the impact of climate change on drought condition in the South Saskatchewan River Watershed (SSRW). The watershed is a part of the Canadian Prairies that has limited water supply (Sun et al. 2012). The study area is located in the leeward side of the Rocky Mountains and receives low moisture (Bonsal et al., 2013, Chipanshi et al., 2006). Agriculture and related industries are the dominant economic activity in the region with 12 medium to large-sized irrigation districts, which have a large share of regional agricultural production. The Saskatchewan River Basin (SRB) faces with many water security challenges and water consumption for agriculture has increased in the region (Wheater and Gober, 2013). Most of the irrigated lands of Canada are in the Prairies (around 75% of all irrigated lands in Alberta and Saskatchewan) and most of them are located in the south of the SRB where more than 80% of water consumption is for agriculture (Wheater and Gober, 2013). Expansion of irrigation area has not always resulted in an increase in water demand, due to increased efficiencies in water application and management (Bennett et al. 2015). However, there is a limit to efficiencies in water conveyance and storage, and water demand for other purposes in the region will increase with increases in population growth and development (Bennett et al. 2017). Also, current water savings through increased water conveyance efficiency are usually achieved alongside expansions of irrigation in the region. This reliance of the region to water availability, in the condition of increased droughts such as snow drought (Dierauer et al., 2019), or meteorological and hydrological droughts (Mousavi et al., 2023) could lead to more vulnerability and water insecurity (Wheater and Gober, 2013). The previous historical analysis of drought (Chapter 2) showed that the SSRW has experienced increasing drought trends and intensified droughts in recent decades (Mousavi et al., 2023). Due to high dependence of the local communities on agricultural production,

susceptibility of the region to drought, and overall significant vulnerability to impacts on agriculture, environment, and urban systems, it is crucial to understand the future drought conditions under global climate change.

The main objective of this study is to assess the changes in the rates of occurrence of both short-term and long-term droughts under global climate change using a multi-model ensemble of 26 GCMs and three climate change scenarios in the SSRW and identifying the areas that are projected to experience more occurrence or intensification of droughts, compared to base period. These results could improve our understanding of future plausible changes in regional scale and accordingly the preparedness for required adaptation plans.

3.2 STUDY AREA

The South Saskatchewan River Watershed located in Southern Alberta encompasses an area between Canadian Rockies and border of Alberta and Saskatchewan which consists of four sub-basins of Red Deer River, Bow River, Oldman River and South Saskatchewan River (Figure 3.1) with close to 9 Bm^3 total annual flow. The region is one of the most highly populated areas of the province and is home to rural communities, First Nations reserves and communities (Stoney Nakoda, Tsuu T'ina, Siksika, Piikani, and Blood/Blackfoot) and four major cities, Calgary, Red Deer, Lethbridge, and Medicine Hat. The dominant economic activity in the SSRW is agricultural and livestock productions and related industries, which are thus dependent on the environment and the water it provides.

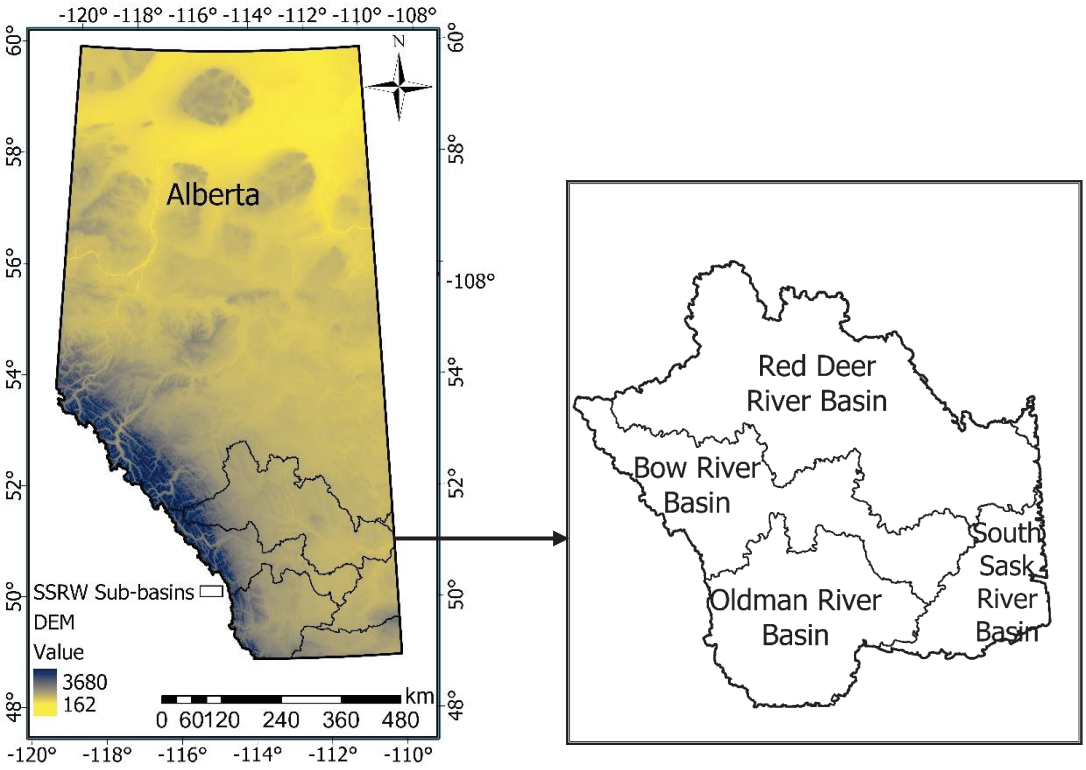

Fig. 3.1 South Saskatchewan River Watershed in Southern Alberta and major sub-basins (Map created by Alberta DEM from Government of Alberta website: https://open.alberta.ca/licence)

3.3 DATASET

In this study, the gridded CMIP6 (Coupled Model Intercomparison Project Phase 6) statistically downscaled maximum and minimum temperature and precipitation dataset is used. We employed a multi-model ensemble of 26 GCMs (CanDCS-U6) at the resolution of 1/12° (~10 km). This dataset covers the temporal range of 1951-2100 with the base period of 1951-2014 based on historical emissions, and future projections based on Shared Socioeconomic Pathways (SSPs) for 2015-2100. The downscaling is based on Bias Correction/Constructed Analogues with Quantile delta mapping algorithm (BCCAQv2) (Cannon et al. 2015; Werner and Cannon, 2016). Table 3.1 represents the list of 26 employed GCMs and their realizations. Projections of temperature and precipitation based on three scenarios of SSP1-2.6, SSP2-4.5, and SSP5-8.5 is used to

compute the drought index and study the changes in rate, intensification and extent of drought affected areas in three 21st century periods (near current: 2015-2030; near future: 2041-2060; and far future: 2071-2100) compared to the base period (1951-1990) in the SSRW.

Table 3.1 Identification of the CMIP6 multi-GCM ensemble of global climate models from CanDCS-U6 (https://climate-scenarios.canada.ca/?page=CanDCS6-data)

Institution	Model Name	Realization
CSIRO-ARCCSS (Australia)	ACCESS-CM2	r1i1p1f1
CSIRO (Australia)	ACCESS-ESM1-5	r1i1p1f1
Beijing Climate Center (China)	BCC-CSM2-MR	r1i1p1f1
Canadian Centre for Climate Modelling and Analysis (Canada)	CanESM5	r1i1p2f1
Euro-Mediterranean Centre for Climate Change (Italy)	CMCC-ESM2	r1i1p1f1
CNRM-CERFACS (France)	CNRM-CM6-1	r1i1p1f2
CNRM-CERFACS (France)	CNRM-ESM2-1	r1i1p1f2
EC-Earth-Consortium (Europe)	EC-Earth3	r4i1p1f1
EC-Earth-Consortium (Europe)	EC-Earth3-Veg	r1i1p1f1
Institute of Atmospheric Physics (China)	FGOALS-g3	r1i1p1f1
NOAA-Geophys. Fluid Dyn. Lab (USA)	GFDL-ESM4	r1i1p1f1
Met Office Hadley Centre and NERC (UK)	HadGEM3-GC31-LL	r1i1p1f3
Institute for Numerical Mathematics (Rus.)	INM-CM4-8	r1i1p1f1
Institute for Numerical Mathematics (Rus.)	INM-CM5-0	r1i1p1f1
Institut Pierre-Simon Laplace (France)	IPSL-CM6A-LR	r1i1p1f1
National Institute of Meteo. Sciences and Korea Meteo. Administration (Korea)	KACE-1-0-G	r2i1p1f1
Korea Institute of Ocean Science and Technology (Korea)	KIOST-ESM	r1i1p1f1
University of Tokyo JAMSTEC, NIES, and AORI (Japan)	MIROC6	r1i1p1f1
University of Tokyo JAMSTEC, NIES, and AORI	MIROC-ES2L	r1i1p1f2

(Japan)		
Max Planck Institute for Meteo. (Germany)	MPI-ESM1-2-HR	r1i1p1f1
Max Planck Institute for Meteo. (Germany)	MPI-ESM1-2-LR	r1i1p1f1
Meteorological Research Institute (Japan)	MRI-ESM2-0	r1i1p1f1
Norwegian Climate Center (Norway)	NorESM2-LM	r1i1p1f1
Norwegian Climate Center (Norway)	NorESM2-MM	r1i1p1f1
Research Center for Env. Changes (Taiwan)	TaiESM1	r1i1p1f1
Met Office Hadley Centre and NERC (UK)	UKESM1-0-LL	r1i1p1f2

3.4 METHODOLOGY

3.4.1 SPEI DROUGHT INDEX

In this part of our study we used the SPEI index, which is deveoped by Vicente-Serrano et al. (2010) and is based the SPI method (proposed by McKee et al., 1993). It was shown in the previous chapter that the SPEI performed better than the SPI in detecting the droughts in the SSRW (Mousavi et al., 2023), as well as other sites (Tan et al., 2015). The calculation procedure of the SPEI and PET are presented Mousavi et al. (2023).

3.4.2 DATA ANALYSIS

Box plots were used to summarize and illustrate future changes under climate change scenarios, compared to the base period (1951-1990). To create these plots we combined the modeled values (for 1951-1990) and the projections (for future periods) of the ensemble of 26 GCMs. We computed the rate of occurrence of drought (as percentage of the whole length of each period) and compared the future rates of occurrence of drought to the base period (1951-1990). The results and differences were mapped in

ArcGIS, to represent the areas with increased or decreased occurrence rates under climate change scenarios in each period compared to the base period (1951-1990). Finally, base period and future projections were compared based on the percentage of the time that drought at different severity levels occured in the SSRW.

3.5 RESULTS AND DISCUSSION

3.5.1 COMPARISON OF DROUGHT IN THE BASE PERIOD AND FUTURE PERIODS UNDER CLIMATE CHANGE

Fig. 3.2 shows the box plots of the drought indices based on three SSP scenarios and four periods. All future periods, based on all three SSP scenarios, show a tendency towards more negative values which based on the SPEI categories, meaning more drought. At the same time, for the base period (1951-1990) the median is just slightly greater than zero, denoting more tendency towards no drought or mild droughts. The box plots and their medians illustrate the shift to more negative values farther in the future (2071-2100). It is clear that there is a relationship between the timescale of the SPEI drought index and severity of droughts, with longer timescales having smaller (more negative) values of the index.

Figures 3.3 to 3.7 represent the average percentage of the time in the SSRW that drought at different severity levels has occurred or is projected to occur for each period and scenario and different timescales of the SPEI index (1-, 3-, 6-, 12-, and 24-months). The results are averaged out from the percentages of drought occurrence obtained by 26 GCMs. For easier comparison, the values of the percentage of time that drought at different severity levels occurred or is projected to occur are also presented in Tables 3.2

to 3.6 for the SPEI at 1-, 3-, 6-, 12-, and 24-months timescales respectively.

Based on Fig. 3.3, in the base period (1951-1990) at 1-month time scale, 54.7% of the times there were no droughts in the SSRW, and the percentage of the times with drought is 33.1% with mild drought, 8.6% with moderate drought, 3.1% with severe drought, and only 0.5% with extreme drought. Under climate change scenarios the percentage of the time that drought (at different severity level) occurs increases to up to 57.1% (SSP1-2.6; 2071-2100). While the percentage of the times with mild drought is almost constant for all scenarios and time periods, the percentages of the time with moderate, severe, and extreme droughts is gradually increasing to up to 13.9% (SSP1-2.6), 8.9% (SSP1-2.6), and 3.3% (SSP1-2.6), respectively, by the end of the century. This could be due to the change in evapotranspiration increase by temperature rise, during the dry periods, when precipitation change cannot offset the increased atmospheric water demand.

Table 3.2 Percentage of the time associated with drought at different severity levels based on SPEI-1month in the base period (1951-1990) and projections for the near current (2015-2030), near future (2041-2060), and far future (2071-2100) periods based on three scenarios (SSP1-2.6, SSP2-4.5, and SSP5-8.5)

Period	Scenario	Drought severity				
		Extreme	Severe	Moderate	Mild	No drought
1951-1990	-	0.5	3.1	8.6	33.1	54.7
2015-2030	SSP1-2.6	0.7	4.2	10.2	34.9	50.0
	SSP2-4.5	0.8	4.4	10.9	34.0	49.9
	SSP5-8.5	0.9	4.7	11.2	34.0	49.3
2041-2060	SSP1-2.6	1.3	5.5	12.4	34.5	46.3
	SSP2-4.5	1.4	5.9	11.9	33.5	47.2
	SSP5-8.5	1.6	6.3	12.1	33.0	47.1
2071-2100	SSP1-2.6	3.3	8.9	13.9	31.0	42.9
	SSP2-4.5	2.4	7.6	13.0	32.3	44.7
	SSP5-8.5	2.5	7.5	12.9	32.6	44.5

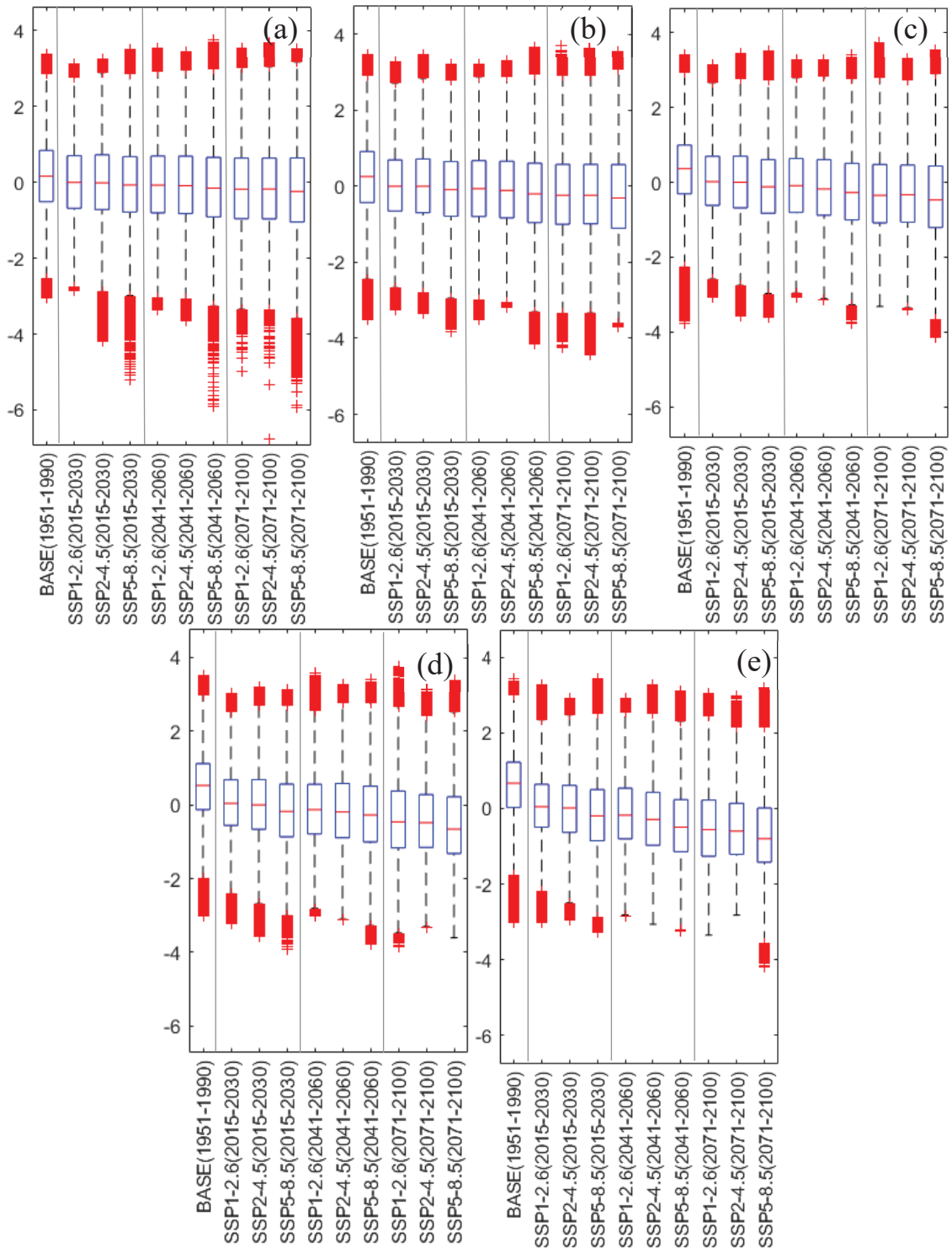

Fig. 3.2 Box plots of the Values of the SPEI index at different timescales for different periods (base period: 1951-1990; near current: 2015-2030; near future: 2041-2060; and far future: 2071-2100) and three climate change scenarios (SSP1-2.6; SSP2-4.5; SSP5-8.5). (a) SPEI-1month; (b) SPEI-3months; (c) SPEI-6months; (d) SPEI-12months; (e) SPEI-24months

Fig. 3.4 shows the percentage of occurrence of drought in the SSRW based on SPEI-3months, with 42.8% of the time the watershed experienced some sort of drought in the base period (1951-1990), 31.3% mild drought, 7.9% moderate drought, 3% severe drought, and 0.6% of the time extreme drought. Based on the results for SPEI-3months, under all climate change scenarios, drought will increase gradually by the end of century, up to 59.8% (based on SSP1-2.6). The increased percentages of the times with mild, moderate, severe, and extreme droughts at 3-months time scale is up to 35.7% (SSP1-2.6; 2015-2030), 14.3% (SSP1-2.6; 2071-2100), 9.4% (SSP1-2.6; 2071-2100), and 3.7% (SSP1-2.6; 2071-2100), respectively.

Table 3.3 Percentage of the time associated with drought at different severity levels based on SPEI-3month in the base period (1951-1990) and projections for the near current (2015-2030), near future (2041-2060), and far future (2071-2100) periods based on three scenarios (SSP1-2.6, SSP2-4.5, and SSP5-8.5)

Period	Scenario	Drought severity				
		Extreme	Severe	Moderate	Mild	No drought
1951-1990	-	0.6	3.0	7.9	31.3	57.2
2015-2030	SSP1-2.6	0.8	3.8	9.7	35.7	50.0
	SSP2-4.5	0.9	4.2	10.4	34.1	50.3
	SSP5-8.5	0.9	4.7	10.8	34.3	49.3
2041-2060	SSP1-2.6	1.5	5.8	12.5	35.0	45.3
	SSP2-4.5	1.6	6.1	11.9	33.9	46.5
	SSP5-8.5	1.9	6.3	12.1	33.5	46.2
2071-2100	SSP1-2.6	3.8	9.4	14.3	32.3	40.2
	SSP2-4.5	2.8	8.0	13.4	32.9	42.9
	SSP5-8.5	2.7	8.0	13.6	32.7	42.9

Similar results obtained by SPEI-6months (Fig. 3.5) indicate that the percentages of mild, moderate, severe, and extreme droughts under climate change scenarios are increasing from 29.4%, 6.9%, 2.5%, and 0.5% in the base period, to up to 35.9% (SSP1-2.6; 2015-2030), 14.5% (SSP2-4.5; 2071-2100), 9% (SSP2-4.5; 2071-2100), and 4.2% (SSP1-2.6; 2071-2100), respectively. Overall, under climate change scenarios, an increase

in the times attributed with drought occurence is projected, from 39.3% in the base period (1951-1990), to 50.5% (SSP5-8.5) in near current (2015-2030), 56.5% (SSP1-2.6) in near future (2041-2060), and 63.9% (SSP1-2.6) in far future (2071-2100) periods.

Table 3.4 Percentage of the time associated with drought at different severity levels based on SPEI-6month in the base period (1951-1990) and projections for the near current (2015-2030), near future (2041-2060), and far future (2071-2100) periods based on three scenarios (SSP1-2.6, SSP2-4.5, and SSP5-8.5)

Period	Scenario	Drought severity				
		Extreme	Severe	Moderate	Mild	No drought
1951-1990	-	0.5	2.5	6.9	29.4	60.7
2015-2030	SSP1-2.6	0.6	3.4	9.2	35.9	50.9
	SSP2-4.5	0.9	4.2	10.3	33.7	51.0
	SSP5-8.5	0.9	4.3	11.0	34.2	49.5
2041-2060	SSP1-2.6	1.5	5.9	13.3	35.7	43.5
	SSP2-4.5	1.8	6.4	12.0	34.8	45.1
	SSP5-8.5	1.8	6.5	13.0	34.6	44.1
2071-2100	SSP1-2.6	4.2	10.5	16.3	32.9	36.1
	SSP2-4.5	2.9	9.0	14.5	33.6	40.0
	SSP5-8.5	3.2	8.7	14.0	33.8	40.4

Results of percentage of the times with drought at 12-months timescale (Fig. 3.6) indicate 34.1% of the time drought occurred in the base period (1951-1990) with 26.3% mild drought, 5.6% moderate drought, 1.9% severe drought, and 0.3% extreme drought; under climate change scenarios (ensemble) this would increase up to 37.8% (SSP1-2.6; 2041-2060), 19% (SSP1-2.6; 2071-2100), 12.1% (SSP1-2.6; 2071-2100), and 4.7% (SSP1-2.6; 2071-2100) for mild, moderate, severe, and extreme droughts, repectively. The maximum percentage of the times with drought are increasing from 29.9% in the base period (1951-1990) to 50% (SSP5-8.5) in near current (2015-2030), 62.7% (SSP1-2.6) in near future (2041-2060), and 75% (SSP1-2.6) in the far future (2071-2100).

Table 3.5 Percentage of the time associated with drought at different severity levels based on SPEI-12month in the base period (1951-1990) and projections for the near current (2015-2030), near future (2041-2060), and far future (2071-2100) periods based on three scenarios (SSP1-2.6, SSP2-4.5, and SSP5-8.5)

Period	Scenario	Drought severity				
		Extreme	Severe	Moderate	Mild	No drought
1951-1990	-	0.3	1.9	5.6	26.3	65.9
2015-2030	SSP1-2.6	0.3	2.7	8.3	36.8	51.9
	SSP2-4.5	0.8	4.1	9.6	34.7	50.8
	SSP5-8.5	0.9	4.4	10.2	34.8	49.7
2041-2060	SSP1-2.6	1.5	6.5	14.3	37.8	39.9
	SSP2-4.5	1.9	6.2	12.0	36.2	43.7
	SSP5-8.5	1.8	7.0	14.2	36.2	40.8
2071-2100	SSP1-2.6	4.7	12.1	19.1	34.1	30.0
	SSP2-4.5	3.3	10.2	16.2	34.5	35.7
	SSP5-8.5	3.4	9.9	15.4	35.0	36.3

Percentages of time with drought obtained by SPEI-24months are presented in Fig. 3.7, with SSRW experiencing drought at 24-months time scale at 29.9% of the time in the base period (1951-1990); with 24.3% mild drought, 4.2% moderate drought, 1.3% severe drought, and 0.2% extreme drought. Those percentages under climate change are projected to increase up to 75% (SSP1-2.6; 2071-2100), with each individual category of drought increase up to 40.1% (SSP1-2.6; 2041-2060) for mild drought, 21.9% (SSP1-2.6; 2071-2100) for moderate drought, 14.9% (SSP1-2.6; 2071-2100) for severe drought, and 4% (SSP1-2.6; 2071-2100) for extreme drought.

Table 3.6 Percentage of the time associated with drought at different severity levels based on SPEI-24month in the base period (1951-1990) and projections for the near current (2015-2030), near future (2041-2060), and far future (2071-2100) periods based on three scenarios (SSP1-2.6, SSP2-4.5, and SSP5-8.5)

Period	Scenario	Drought severity				
		Extreme	Severe	Moderate	Mild	No drought
1951-1990	-	0.2	1.3	4.2	24.3	70.1
2015-2030	SSP1-2.6	0.3	2.2	6.6	38.7	52.3
	SSP2-4.5	0.6	3.9	9.2	34.2	52.1
	SSP5-8.5	0.9	3.9	9.9	35.3	50.0
2041-2060	SSP1-2.6	1.6	5.8	15.2	40.1	37.3
	SSP2-4.5	1.6	6.4	13.1	37.3	41.7
	SSP5-8.5	2.0	7.5	14.9	37.5	38.2
2071-2100	SSP1-2.6	4.0	14.9	21.9	34.2	25.0
	SSP2-4.5	3.4	11.9	17.7	34.2	32.7
	SSP5-8.5	3.3	11.5	16.1	37.2	31.9

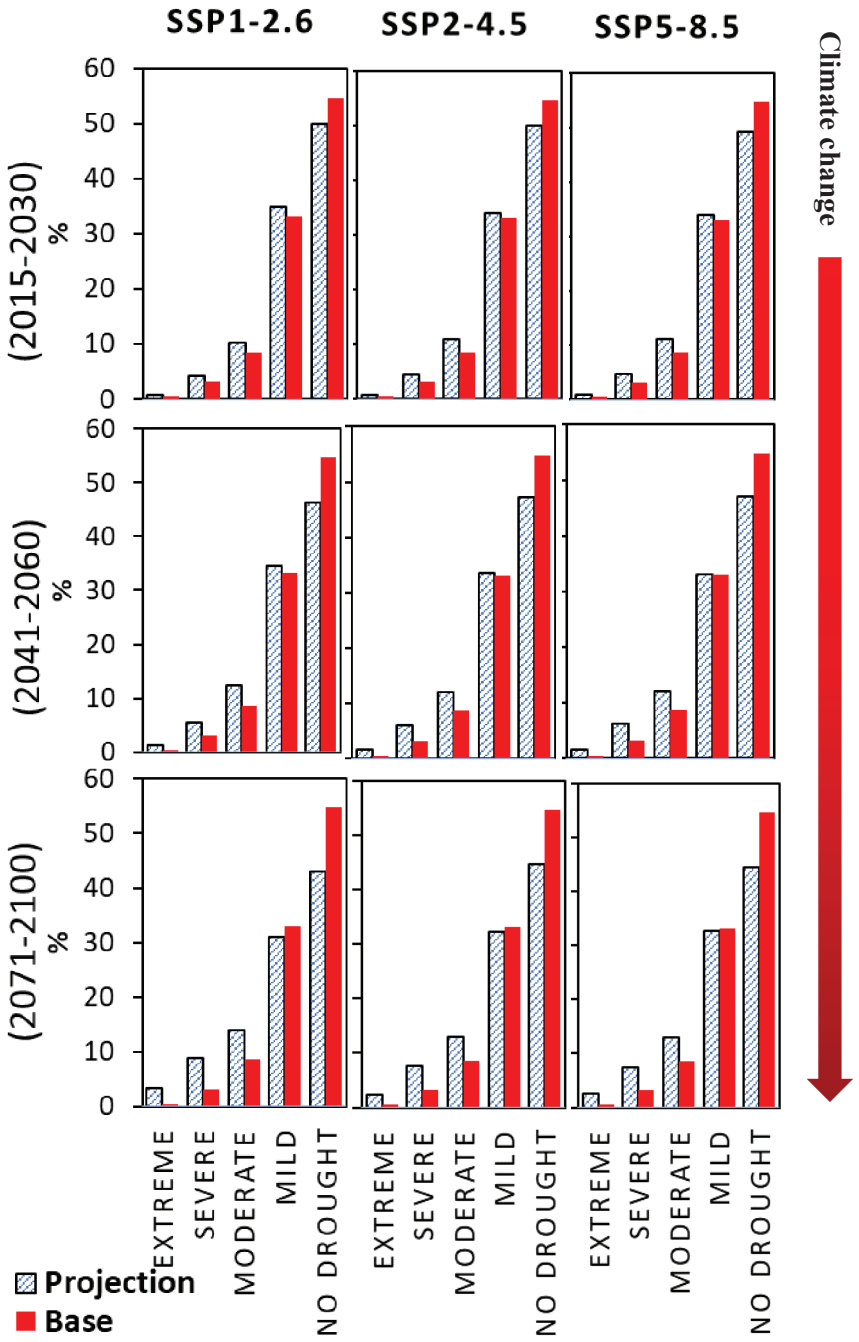

Fig. 3.3 Results of SPEI-1month: Comparison of the percentage of the time that drought (at different severity levels) occurred in the base period (1951-1990) with projections for three periods of near current (2015-2030), near future (2041-2060), and far future (2071-2100) based on three scenarios (SSP1-2.6, SSP2-4.5, and SSP5-8.5)

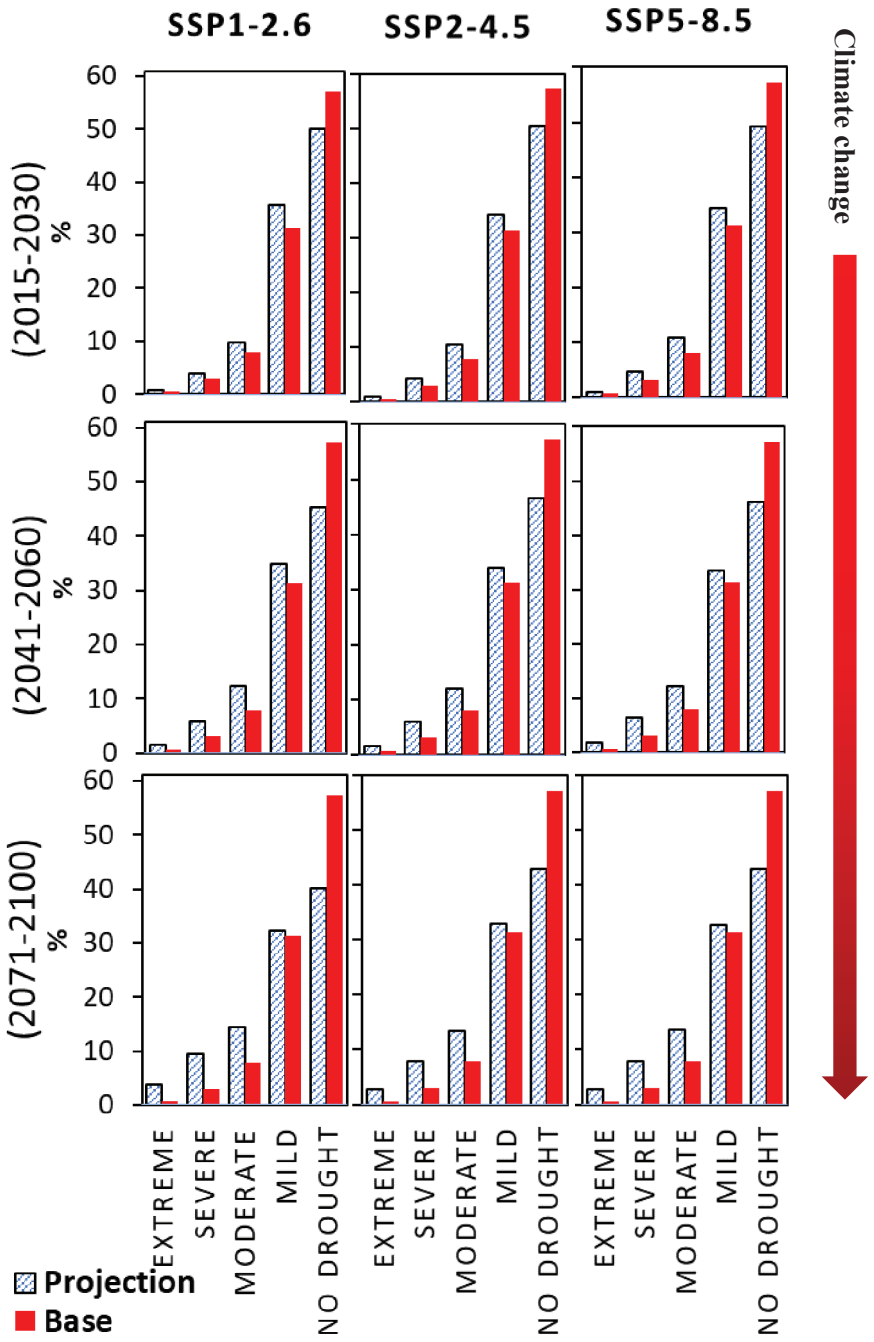

Fig. 3.4 Results of SPEI-3month: Comparison of the percentage of the time that drought (at different severity levels) occurred in the base period (1951-1990) with projections for three periods of near current (2015-2030), near future (2041-2060), and far future (2071-2100) based on three scenarios (SSP1-2.6, SSP2-4.5, and SSP5-8.5)

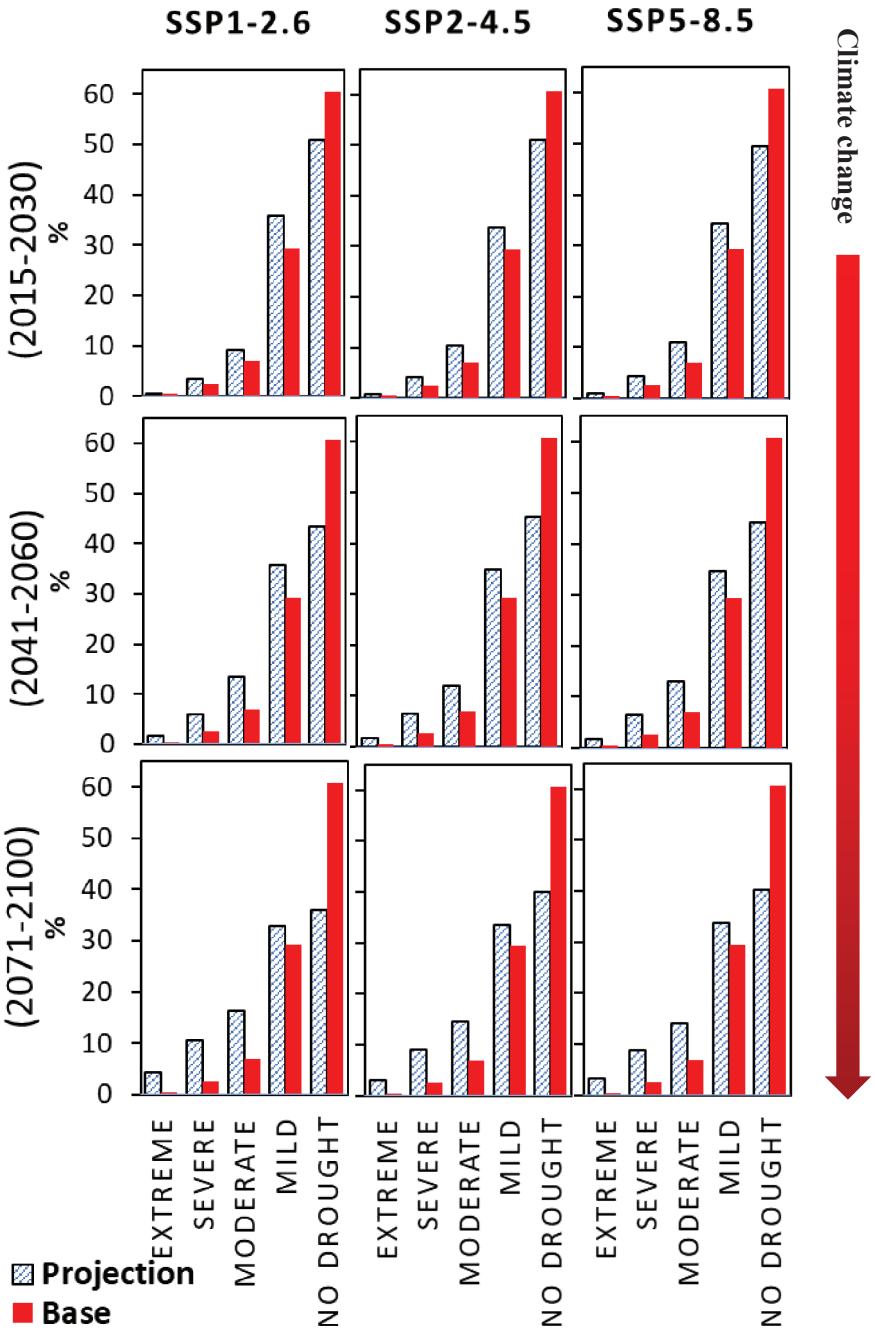

Fig. 3.5 Results of SPEI-6month: Comparison of the percentage of the time that drought (at different severity levels) occurred in the base period (1951-1990) with projections for three periods of near current (2015-2030), near future (2041-2060), and far future (2071-2100) based on three scenarios (SSP1-2.6, SSP2-4.5, and SSP5-8.5)

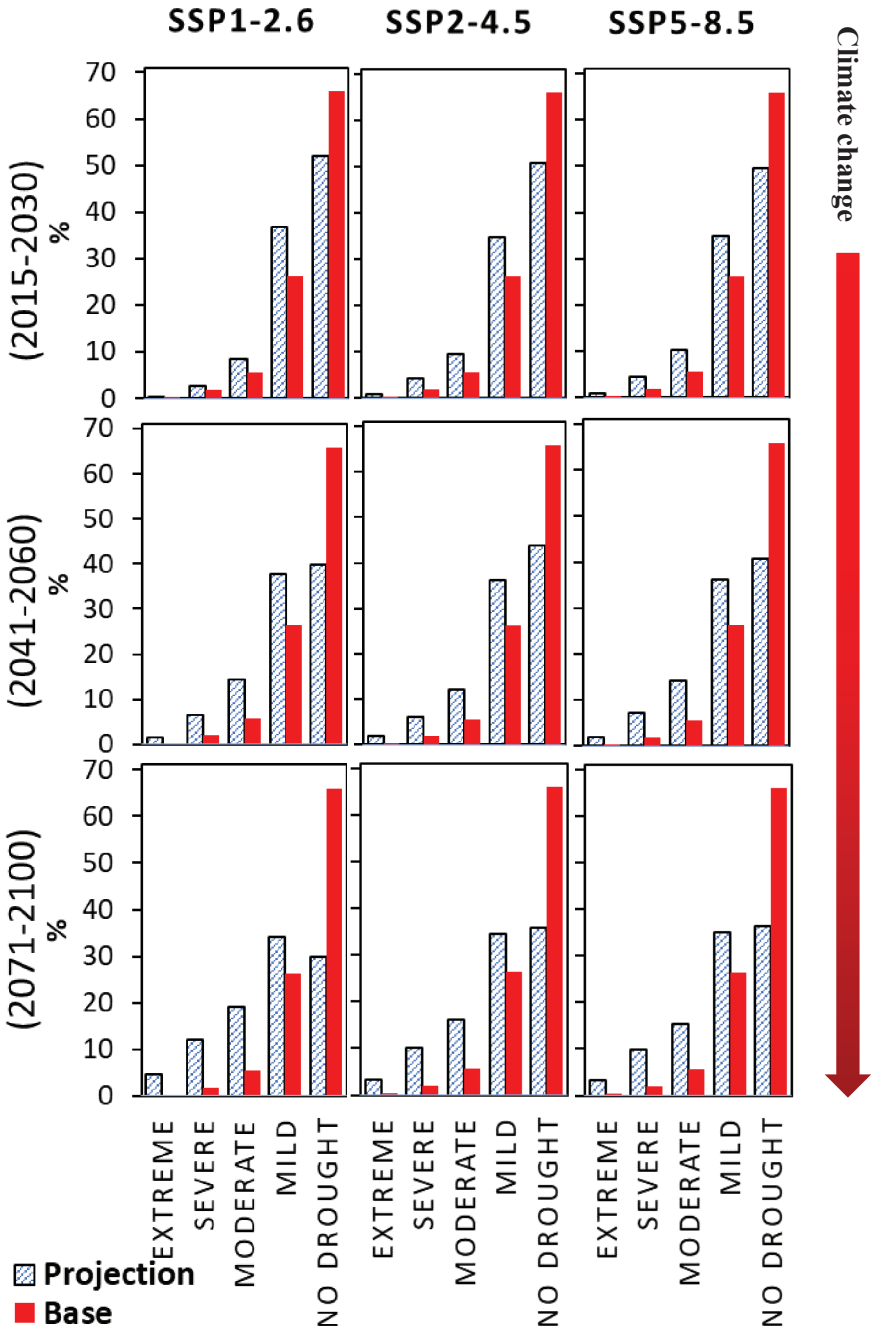

Fig. 3.6 Results of SPEI-12month: Comparison of the percentage of the time that drought (at different severity levels) occurred in the base period (1951-1990) with projections for three periods of near current (2015-2030), near future (2041-2060), and far future (2071-2100) based on three scenarios (SSP1-2.6, SSP2-4.5, and SSP5-8.5)

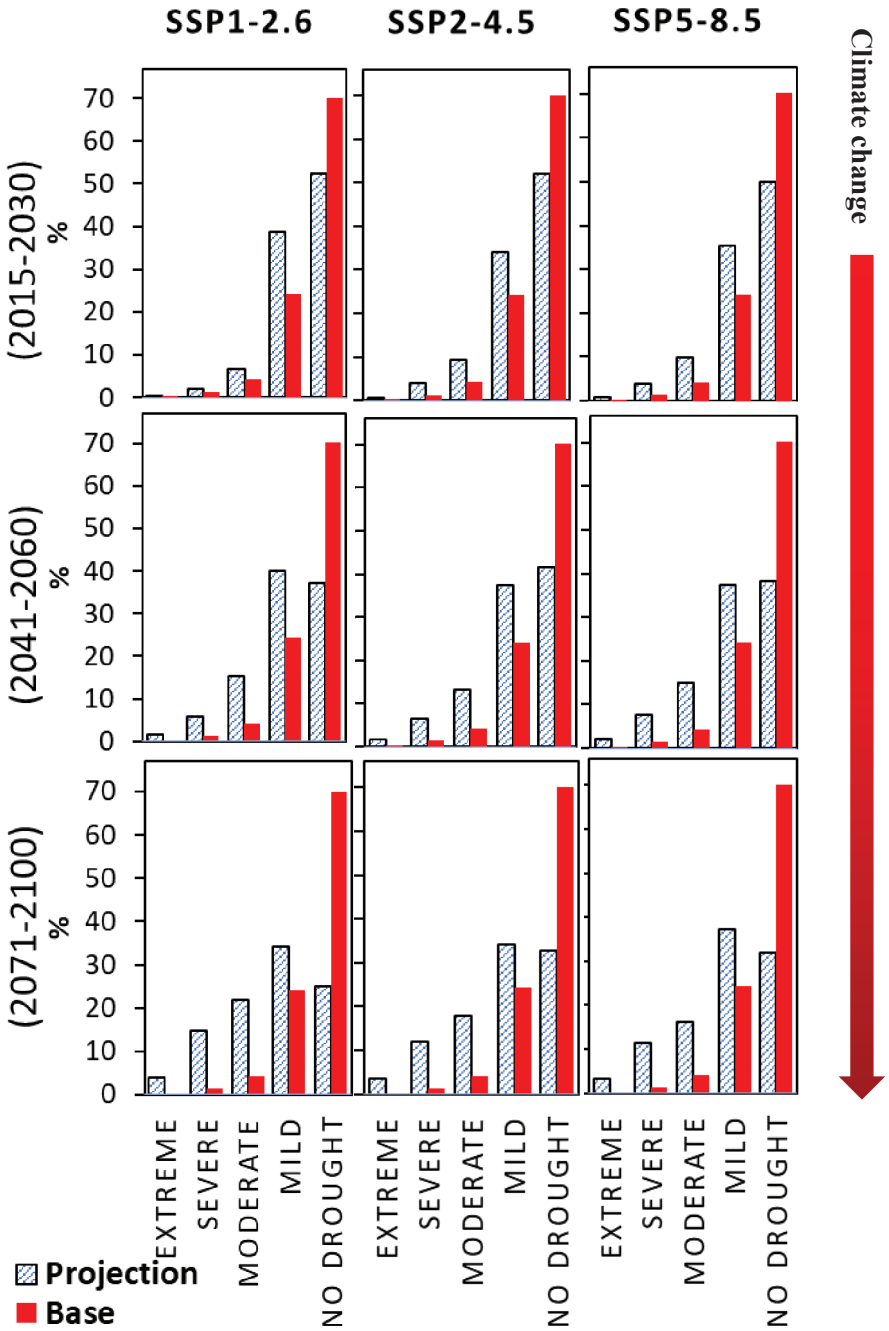

Fig. 3.7 Results of SPEI-24month: Comparison of the percentage of the time that drought (at different severity levels) occurred in the base period (1951-1990) with projections for three periods of near current (2015-2030), near future (2041-2060), and far future (2071-2100) based on three scenarios (SSP1-2.6, SSP2-4.5, and SSP5-8.5)

3.5.2 FUTURE CHANGES IN OCCURRENCE RATES OF DROUGHT UNDER CLIMATE CHANGE

Figures 3.8 to 3.12 show and compare the rates of occurrence of drought based on

the SPEI drought index at different time scales (1-, 3-, 6-, 9-, 12-, and 24-months) in the basin, based on different scenarios and different periods of time, or simply the percentage of the time where the SPEI index value is below zero.

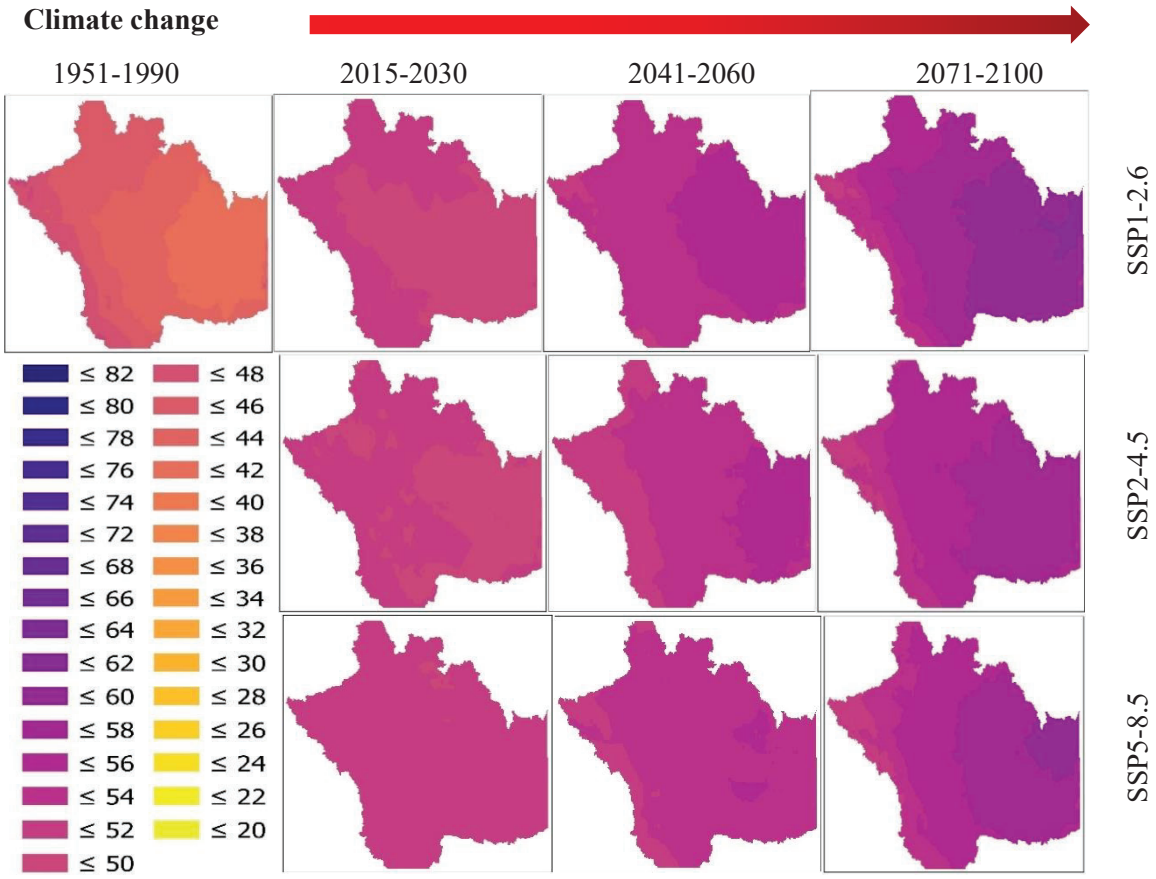

Fig. 3.8 Drought occurrence rates: percentage (%) of the total selected time period for which (based on the SPEI-1month index) drought (at different severity levels) has happened in the base period (1951-1990) or is projected to happen in future periods (near current: 2015-2030; near future: 2041-2060; and far future: 2071-2100)

For SPEI-1month in the base period (1951-1990) (Fig. 3.8), the rate of drought occurrence in the basin varies between 40.4% and 48.9% which is higher in the Rocky Mountains and the western portion of the SSRW, and lower in the eastern parts, which includes downstream of Red Deer Basin and Bow River Basin. The projected rates of drought occurrence for all scenarios in the near current period (2015-2030) is between 48.6% and 51.9%; in the near future (2041-2060) it is between 49.9% and 55.9%; and in

the far future (2071-2100) it is between 48.6% (SSP1-2.6; 2015-2030) and 60.6% (SSP1-2.6; 2071-2100). The rate of occurrence of drought is projected to increase closer to the end of the century (2071-2100), as well as the range of variability of occurrence rates within the basin. Based on the projections it is obvious that by moving from west to the east in the SSRW, the rates of drought occurrence increases, with lowest rates in the Rockies and north of the watershed and higher rates in the South Saskatchewan River Basin (the southeastern part of SSRW) and downstream of Red Deer and Bow River Basins.

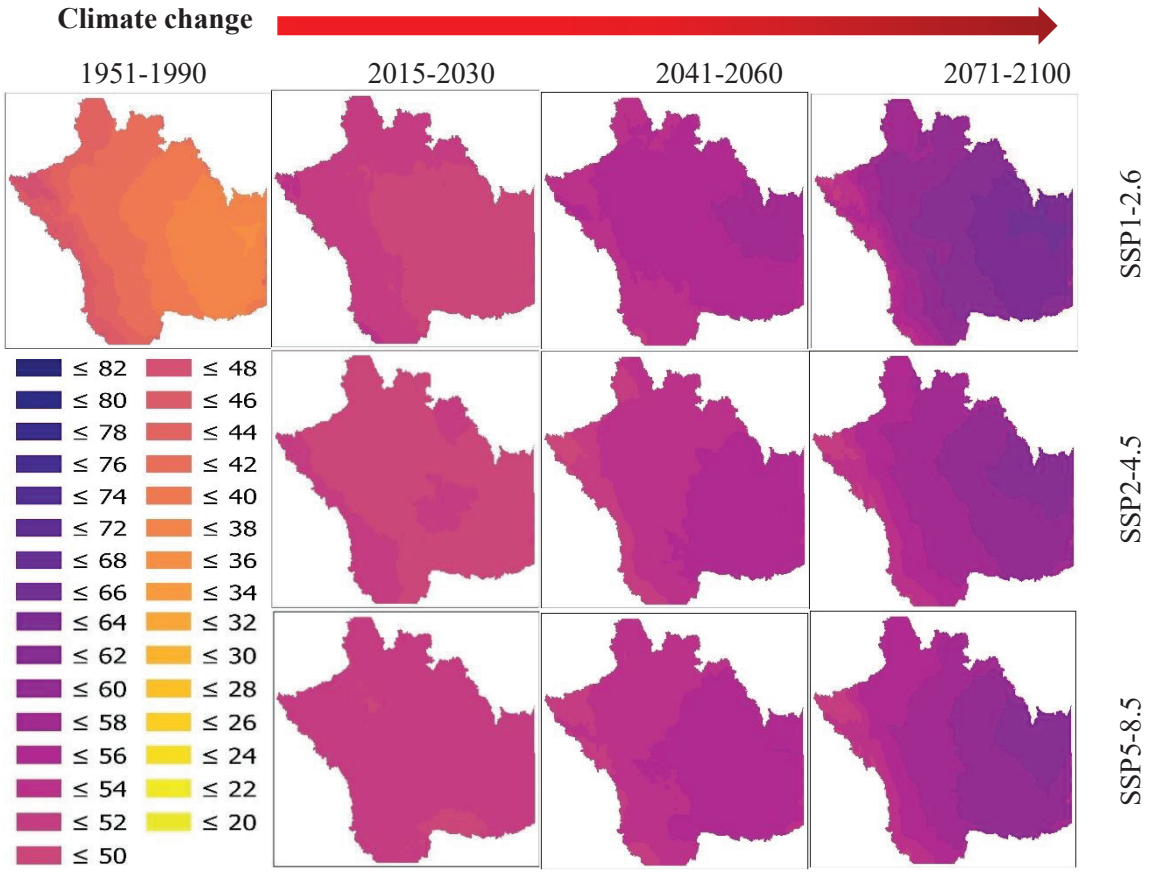

Fig. 3.9 Drought occurrence rates: percentage (%) of the total selected time period for which (based on the SPEI-3month index) drought (at different severity levels) has happened in the base period (1951-1990) or is projected to happen in future periods (near current: 2015-2030; near future: 2041-2060; and far future: 2071-2100)

As shown in Fig. 3.9, the rate of drought occurrence based on SPEI-3months in

the base period (1951-1990) ranges from 35.6% to 47.7%, which is lower in the Rocky Mountains and parts of the Oldman River Basin, and increases eastward, as most parts of the basin especially in the downstream of the Red Deer and Bow River basins and South Saskatchewan River Basin experienced higher rates of drought at 3-months timescale. Projections show a range between 48.4% (SSP1-2.6; 2015-2030) and 64.7% (SSP1-2.6; 2071-2100) of drought occurrence rates at 3-months timescale that reaches the highest rate at 2071-2100 based on the SSP1-2.6. The range of projected values is larger at later time periods. Unlike for the base period, regions closer to the Rocky Mountains and headwaters of Red Deer River, Bow River, and Oldman River Basins are experiencing less frequency of drought, while the eastern parts, mainly the downstream of Red Deer and Bow River Basins and most parts of the South Saskatchewan River Basin have higher projected drought rates.

At the SPEI-6months time scale (Fig. 3.10), the rate of drought occurrence of the base period (1951-1990) is between 33.9% and 49.2%, higher in the upstream areas of the basins and mountainous parts, and lower in other parts of the SSRW, especially in the east side and areas in the downstream of Red Deer and Bow River Basins and most parts of the South Saskatchewan River Basin. The climate change ensemble models and scenario projections suggest rates of drought occurrence between 47.4% (SSP1-2.6; 2015-2030) and 69.7% (SSP1-2.6; 2071-2100), which is lower in the west and north and increases eastward and in lower parts of the river basins in the SSRW. The far future period (2071-2100) is projected to have higher rates of drought occurrence with higher variability.

Fig. 3.11 shows the range of drought occurrence based on the SPEI-12months

which is between 24.2% and 43.9% in the base period (1951-1990).

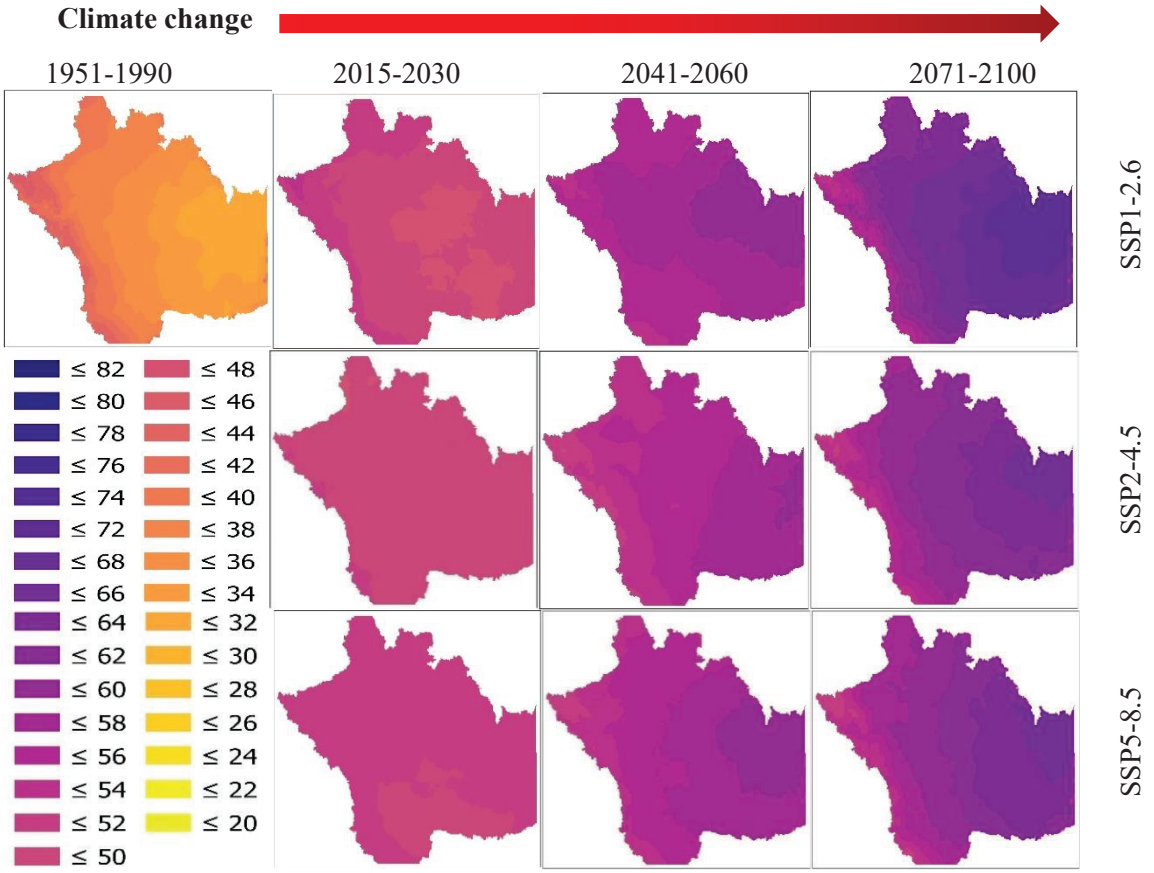

Fig. 3.10 Drought occurrence rates: percentage (%) of the total selected time period for which (based on the SPEI-6month index) drought (at different severity levels) has happened in the base period (1951-1990) or is projected to happen in future periods (near current: 2015-2030; near future: 2041-2060; and far future: 2071-2100)

Projections based on SPEI-12months show a range of 47.2% (SSP2-4.5; 2015-2030) to 75.6% (SSP1-2.6; 2071-2100) for drought occurrence rates in the SSRW. The rates are obviously higher in most parts of the basin based on projections of SSP1-2.6 at 2071-2100 period. It is clear that at 2071-2100 the rates of drought occurrence are significantly higher than lower time scales of the SPEI index. Drought is projected to happen very frequently during 2071-2100 in the downstream areas of the Red Deer and Bow River Basins and parts of the South Saskatchewan River Basin. The highest 12-month drought occurrence rates are projected by SSP1-2.6 in the far future period (2071-2100).

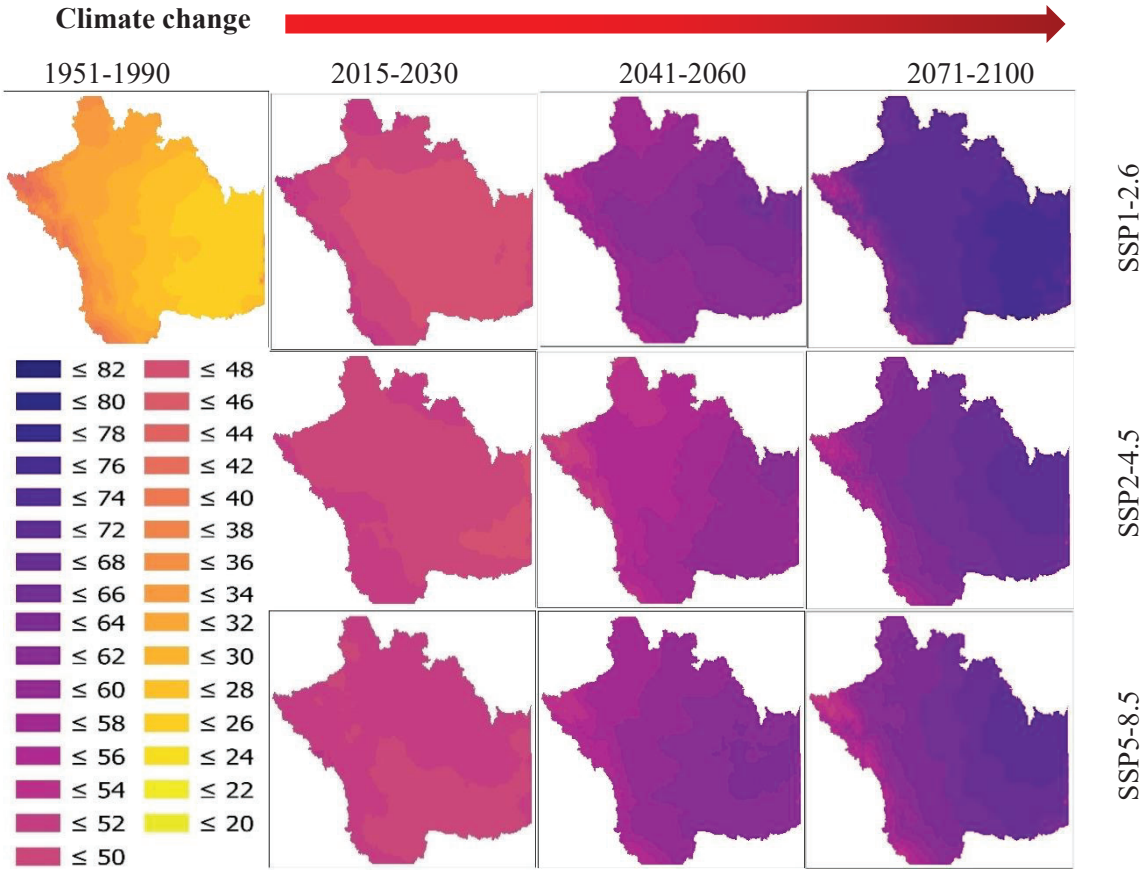

Fig. 3.11 Drought occurrence rates: percentage (%) of the total selected time period for which (based on the SPEI-12month index) drought (at different severity levels) has happened in the base period (1951-1990) or is projected to happen in future periods (near current: 2015-2030; near future: 2041-2060; and far future: 2071-2100)

The rates of drought occurrence based on SPEI at 24-month timescale are presented in Fig. 3.12. For the base period (1951-1990), the rates range from 17.5% to 42.7% in the SSRW, which is less than 20% in eastern parts of the watershed and increases towards the west to even more than 40%. In the near current period (2015-2030), the rates are lower in central and southern parts of the watershed with lowest rate of projected drought occurrence (44.4%) for SSP1-2.6. The rate of drought occurrence is significantly higher in the 2071-2100, peaking at 80.8% for SSP1-2.6. Highest rates of projected drought occurrence are evident at 2071-2100 in the downstream of the river basins in the SSRW and most parts of the South Saskatchewan River basin. The rates of

projected drought occurrence are lower in the west and mountainous parts of the SSRW.

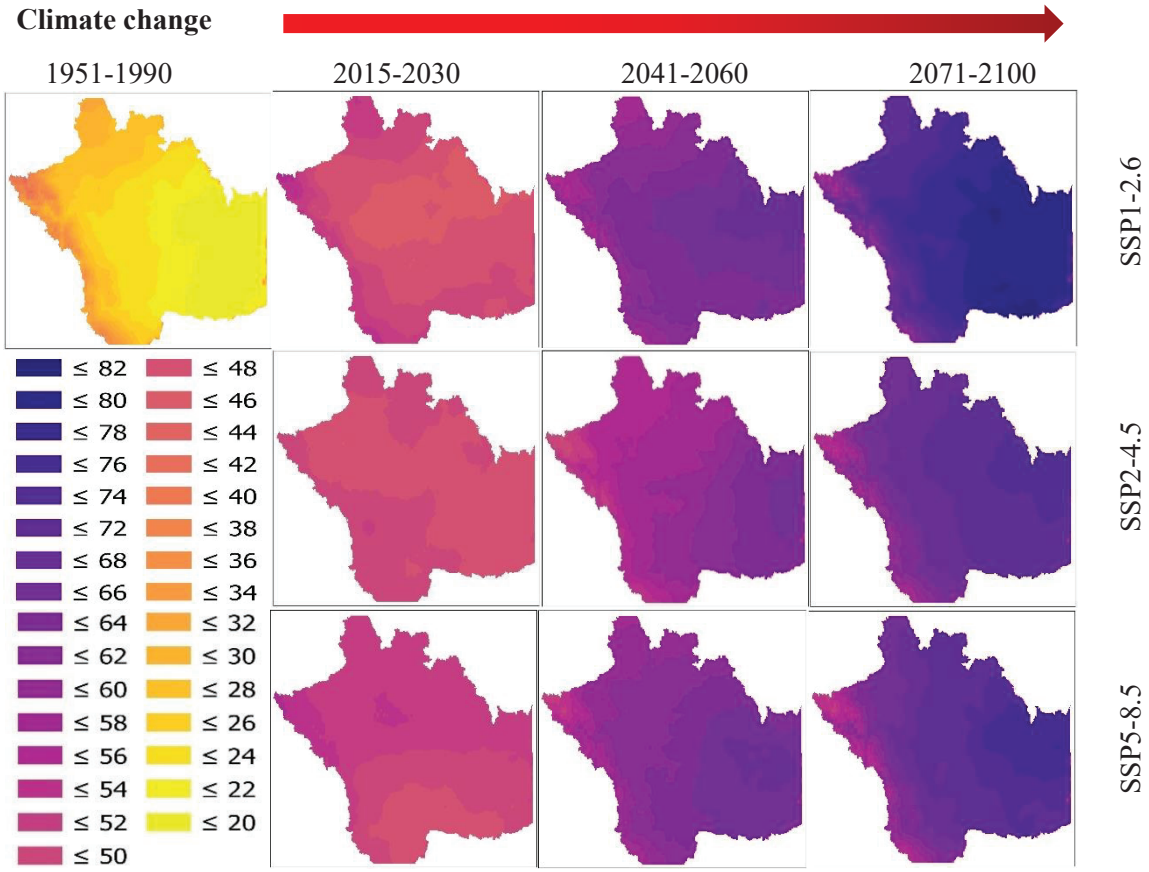

Fig. 3.12 Drought occurrence rates: percentage (%) of the total selected time period for which (based on the SPEI-24month index) drought (at different severity levels) has happened in the base period (1951-1990) or is projected to happen in future periods (near current: 2015-2030; near future: 2041-2060; and far future: 2071-2100)

Table 3.7 summarizes the range of drought occurrence rates, based on SPEI (at different time scales), in the base period (1951-1990) and also based on projections under different climate change scenarios (SSP1-2.6; SSP2-4.5; and SSP5-8.5) in future time horizons. It is evident that the range of the values and (in most cases) the percentage of drought occurrence increases with time scale and at later time horizons.

Table 3.7 Range of the rate of drought occurrence based on SPEI at different time scales in the base period (1951-1990) or as is projected to happen in future periods (near current: 2015-2030; near future: 2041-2060; and far future: 2071-2100)

Period	Scenario	Timescale									
		1-month		3-months		6-months		12-months		24-months	
		Min	Max	Min	Max	Min	Max	Min	Max	Min	Max
1951-1990	-	40	49	36	48	34	49	24	44	17	43
2015-2030	SSP1-2.6	47	52	48	53	47	52	46	53	44	55
	SSP2-4.5	49	51	49	51	48	51	47	51	46	50
	SSP5-8.5	50	52	49	52	49	52	49	52	46	55
2041-2060	SSP1-2.6	51	56	52	57	52	60	54	64	54	67
	SSP2-4.5	50	55	49	56	50	59	48	61	47	65
	SSP5-8.5	50	54	50	56	50	59	51	63	50	67
2071-2100	SSP1-2.6	51	61	50	65	51	70	52	76	54	81
	SSP2-4.5	51	58	50	61	51	65	52	70	52	74
	SSP5-8.5	50	59	49	61	49	65	49	71	50	76

3.6 CONCLUDING REMARKS

Our findings based on the multi-model ensemble of 26 CMIP6 GCMs and three climate change scenarios (SSP1-2.6; SSP2-4.5; SSP5-8.5) and calculated SPEI indices at different timescales (1-, 3-, 6-, 12-, and 24-months) showed that under climate change, drought conditions in the selected time periods (near current: 2015-2030; near future: 2041-2060; and far future: 2071-2100) will change significantly from the base period. This change is shifting the average SPEI index values from more positive values towards more negative values, denoting more drought conditions from reduced rain and increased evaporation in connection to the increasing temperatures.

It was found that not only will the drought occurrence increase under climate change scenarios, but also the severity of the droughts will increase somewhat for all time scales of the SPEI (i.e., 1-,3-, 6-, 12-, and 24-months). This increase is greater for the longer time scales of the SPEI drought index. This could be explained by accumulation of

the impacts of drought that are occurring at longer timescales. As was shown in Chapter 2, the areas in the vicinity of places with increased drought also showed the same pattern at longer timescales, resulting in detection of increasing trends of drought in larger areas.

Based on the projections, occurrence of more severe and extreme drought events will become more prevalent under all three SSP climate change scenarios and for all future time horizons, with the most severe drought events occurring at the end of the century (2071-2100). Based on these results, the severe and extreme droughts, which were rarely occurring in the region in the base period of 1951-1990, will increase significantly in the 2041-2060 period with occurrence rates of severe drought increasing, and in 2071-2100 when both severe and extreme droughts will increase, and consequently areas with "no drought" condition will decrease. The rates of mild and moderate drought occurrences will increase significantly at SPEI time scales of 3-months and higher. These increases in the rates of drought occurrence at different severity levels result in an overall dramatic increase in drought occurrence rates in the SSRW in the near and distant future.

Based on these results, the severity of drought is increasing with the timescale of the SPEI drought index. Also, the range of variability of projected drought occurrence increases at higher time scales of the SPEI drought index and at later periods.

Mapping the rate of occurrence of drought showed that the spatial pattern of projected drought frequency is distinguishable from and opposite to that of the base period (1951-1990). As in the base period, more droughts were occurring in the western parts of the watershed, within or close to mountainous areas of the basin, while based on future projections, the occurrence rates of drought are higher in the downstream of the

river basins or the SSRW and more towards the eastern parts of the watershed.

Among studied climate change scenarios, SSP1-2.6 showed more drought occurrence rates based on SPEI at different timescales, followed by the SSP5-8.5 and SSP2-4.5. This result could be further investigated by changes in the precipitation and its impact of the SPEI drought condition, as this index is sensitive to both temperature and precipitation change.

CHAPTER 4: ANALYSIS OF THE TEMPERATURE-RELATED EXTREME EVENTS IN THE SOUTH SASKATCHEWAN RIVER WATERSHED UNDER CLIMATE CHANGE

4.1 INTRODUCTION

The impacts of human activities on intensification of climate extremes in different parts of the globe are irrefutable (Batibeniz et al., 2023). Extreme weather events can be deadly, costly, and a driver of demographic changes. In the current condition of climate change, we are witnessing some extreme events more frequently or more intensively that were rare previously. Already, seven of the highest global average temperatures ever recorded are in July 2023, with numerous regional upper temperature records broken, and then broken a short time later. These complicated and combined-effects marginal events, known as extreme events, are costly and can endanger humans, wildlife, and the environment, as well as result in extensive economic losses and setbacks to sustainability. Combinations of these events could result in disastrous situation like coincidence of drought and heatwaves (Batibeniz et al., 2023) that can increase the risk of wildfire, erosion, and pest outbreaks, with greater exposure to human populations (Batibeniz et al., 2023). The other concern comes from observing more back-to-back extreme events of one type or of different types, which may vary, such as floods, droughts, and heatwaves. These could significantly impact different sectors, such as healthcare, agriculture, forestry, parkland, wildlife, and infrastructure, and as a result impose heavy costs on people and governments (Bell et al., 2018). An example of such concurrent events is the wildfire of Fort McMurray in Alberta in 2016 that a preceding drought before a heatwave event caused a devastating wildfire that led to the fire to advance much further and faster

and evacuation of large population from the area (French et al. 2019). Also, concurrent and frequent heatwaves and dry conditions not only prohibits the crop development but also imposes stresses on livestock and workers (Raymond et al., 2020). The result could be significant shortage of food productions and higher prices (Raymond et al., 2020). This combination of processes and connectivity of extreme events that can lead to more severe consequences is known as compound events (Raymond et al., 2020; Zscheischler et al., 2018).

Increase in the magnitude and frequency of occurrence of extreme daily temperatures, recorded Tmax and Tmin values, are expected under climate change and the results can impact the hydrologic cycle acceleration and intensification, crops growth and development (Liu et al., 2018). The increase in Tmin is projected to be more pronounced (Liu et al., 2018).

Almazroui et al. (2021), using an ensemble of 31 CMIP6 GCMs, studied changes in precipitation and temperature over United States, Central America, and Caribbean in three future time zones and compared it with a selected base period of 1995-2014. Their results showed that temperature can rise by up to 6° C, and precipitation will increase by 10-30% in US and decrease by 10-40% in Central America and Caribbean, with the greatest increase in higher latitudes. These changes can have considerable impacts in the environment, cities, economies, and societies.

These facts have led to introducing new methods and indices which enable us to analyze these phenomena and assess their social, economic, and environmental impacts and also to monitor them in order to be prepared. Due to the importance of studying

extreme events and need for unified definitions and methods of analysis, the World Meteorological Organization Commission on Climatology and the Climate Variability and Prediction (WMO CCI/CLIVAR) Expert Team on Climate Change Detection, Monitoring and Indices introduced 27 extreme climate indicators known as ETCCDI (Expert Team on Climate Change Detection, Monitoring and Indices) indices (Peterson, 2001; Alexander et al. 2006; Brown et al. 2010; Perkins, 2015). ETCCDI indices have been employed by researchers, managers, governments, and organizations. We compared the temperature-related extreme events in the past and future by utilizing ETCCDI indices to study the extreme events in the SSRW.

The main objectives of this chapter are to explore the projected impact of climate change in SSRW on (1) the annual count of the days with extreme cold or hot temperatures and duration of cold or warm spells; (2) the monthly pattern of daily temperature range (DTR); (3) the monthly pattern of extremely high or low temperatures; and (4) annual count of days with temperatures suitable for vegetation growth and development, known as growing season length (GSL).

4.2 STUDY AREA

The South Saskatchewan River Watershed in Southern Alberta consists of four sub-basins which drain an area of 112,800 km^2 (Figure 4.1). This watershed is located between latitudes of 52º 58′ 6″and 48º 59′ 50″ and longitudes of 110º 0′ 3″ and 116º 35′ 55″ and includes parts of the Canadian Rocky Mountains in the west and parts of the Canadian Prairies further east in Southern Alberta. The main land uses are agricultural, mainly annual crop production, pastures, and ranching. There are 12 major irrigation

districts, four major cities (Calgary, Red Deer, Lethbridge, and Medicine Hat), and many rural communities in the area. As described in Chapter 3, it also contains Kainai Sahkoi - the largest First Nation Reserve of Canada (Blood 148), and other indigenous communities and territories, First Nations reserves and communities (Stoney Nakoda, Tsuu T'ina, Siksika, and Piikani, are located in this region. The main rivers of the four sub-basins of this watershed are Red Deer, Bow River, Oldman River, and South Saskatchewan River, with total annual discharge of 8.8 Bm3.

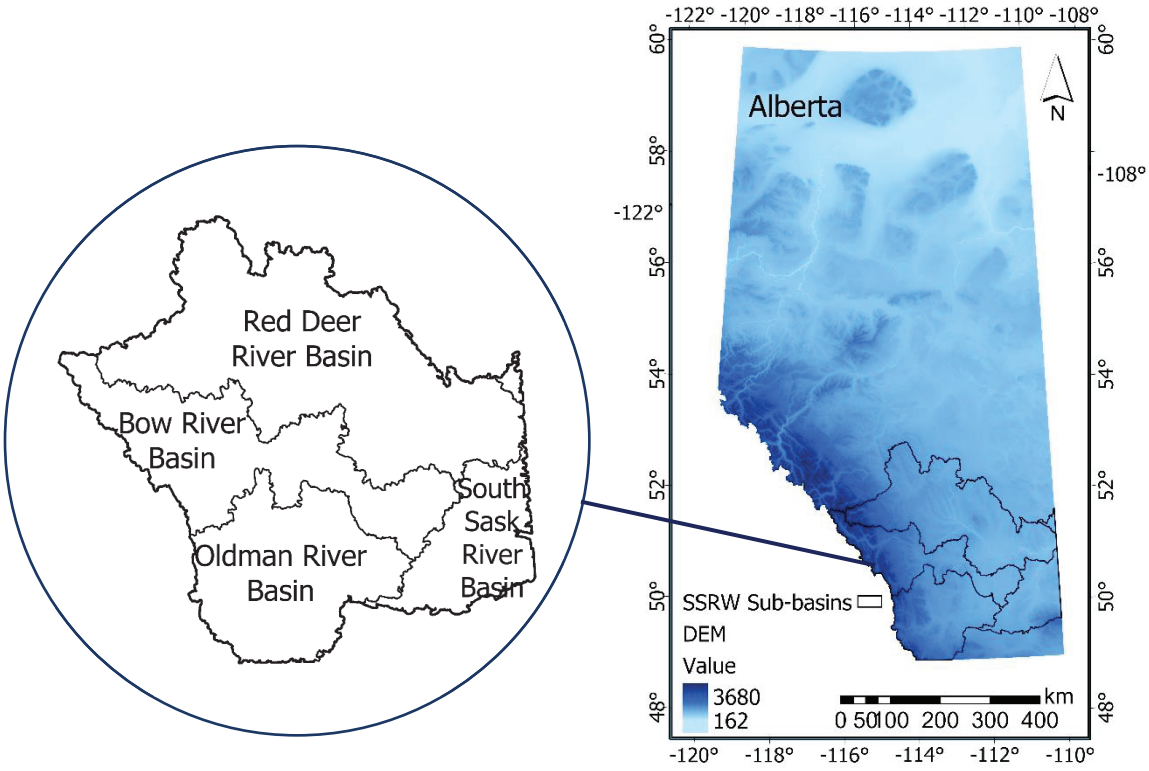

Fig. 4.1 Map of the study area and location of the SSRW sub-basins in Alberta (Mapped by Arc GIS Pro software and Alberta DEM from Government of Alberta website: https://open.alberta.ca/licence)

4.3 DATASET

In this study the CMIP6 statistically downscaled climate indices (CanDCS-U6) was used. This dataset provides the downscaled indices at 1/12° (~10 km) grid resolution

from 1950-2100 with base period of 1951-1990 and future projections based on three Shared Socioeconomic Pathways (SSPs) for 2015-2100 period. The downscaling is based on Bias Correction/Constructed Analogues with Quantile delta mapping algorithm (BCCAQv2) (Cannon et al. 2015; Werner and Cannon, 2016). The multi-GCM ensemble of 26 GCMs (Table 4.1) and three scenarios of SSP1-2.6, SSP2-4.5, and SSP5-8.5 is employed to investigate variations of extreme temperature related indices in SSRW in near current period of 2015-2030, and two future periods of 2041-2060 and 2071-2100 compared to the base period of 1951-1990.

Table 4.1 Identification of the CMIP6 multi-GCM ensemble of global climate models adopted form CanDCS-U6 (https://climate-scenarios.canada.ca/?page=CanDCS6-indices)

Institution	**Model Name**	**Realization**
CSIRO-ARCCSS (Australia)	ACCESS-CM2	r1i1p1f1
CSIRO (Australia)	ACCESS-ESM1-5	r1i1p1f1
Beijing Climate Center (China)	BCC-CSM2-MR	r1i1p1f1
Canadian Centre for Climate Modelling and Analysis (Canada)	CanESM5	r1i1p2f1
Euro-Mediterranean Centre for Climate Change (Italy)	CMCC-ESM2	r1i1p1f1
CNRM-CERFACS (France)	CNRM-CM6-1	r1i1p1f2
CNRM-CERFACS (France)	CNRM-ESM2-1	r1i1p1f2
EC-Earth-Consortium (Europe)	EC-Earth3	r4i1p1f1
EC-Earth-Consortium (Europe)	EC-Earth3-Veg	r1i1p1f1
Institute of Atmospheric Physics (China)	FGOALS-g3	r1i1p1f1
NOAA-Geophys. Fluid Dyn. Lab (USA)	GFDL-ESM4	r1i1p1f1
Met Office Hadley Centre and NERC (UK)	HadGEM3-GC31-LL	r1i1p1f3
Institute for Numerical Mathematics (Rus.)	INM-CM4-8	r1i1p1f1
Institute for Numerical Mathematics (Rus.)	INM-CM5-0	r1i1p1f1
Institut Pierre-Simon Laplace (France)	IPSL-CM6A-LR	r1i1p1f1

National Institute of Meteo. Sciences and Korea Meteo. Administration (Korea)	KACE-1-0-G	r2i1p1f1
Korea Institute of Ocean Science and Technology (Korea)	KIOST-ESM	r1i1p1f1
University of Tokyo JAMSTEC, NIES, and AORI (Japan)	MIROC6	r1i1p1f1
University of Tokyo JAMSTEC, NIES, and AORI (Japan)	MIROC-ES2L	r1i1p1f2
Max Planck Institute for Meteo. (Germany)	MPI-ESM1-2-HR	r1i1p1f1
Max Planck Institute for Meteo. (Germany)	MPI-ESM1-2-LR	r1i1p1f1
Meteorological Research Institute (Japan)	MRI-ESM2-0	r1i1p1f1
Norwegian Climate Center (Norway)	NorESM2-LM	r1i1p1f1
Norwegian Climate Center (Norway)	NorESM2-MM	r1i1p1f1
Research Center for Env. Changes (Taiwan)	TaiESM1	r1i1p1f1
Met Office Hadley Centre and NERC (UK)	UKESM1-0-LL	r1i1p1f2

4.4 METHODOLOGY

4.4.1 EXTREME CLIMATE INDICES

There are 16 temperature-related indices proposed by the ETCCDI that could be a good representative of extreme temperatures and heat. These indices are based on daily maximum and minimum temperatures (Alexander et al., 2006). These indices were introduced and applied on a global scale by Alexander et al. (2006) and also been applied in the Fourth Assessment Report of the Intergovernmental Panel on Climate Change (AR4 IPCC) (http://www.clivar.org/workshops-extremes-indices). The complete list of the ETCCDI indices and their definitions are available at (http://etccdi.pacificclimate.org/list_27_indices.shtml). Our analysis of recent changes in extreme climate in the SSRW, is based on the ETCCDI temperature-related indices listed

in Table 4.2. Some of these indices are appropriate tools for application in agriculture such as frost days, icing days, and growing season length (Brown et al. 2010). Here we also used an additional threshold-based index (SU30) to study very hot summer days.

Table 4.2 List of ETCCDI temperature-related indices used in this study

Index	Description	Unit
DTR	Daily temperature range	°C
GSL	Growing season length	days/year
FD	Number of frost days	days/year
ID	Number of icing days	days/year
SU	Number of summer days (> 25°C)	days/year
SU30	Number of summer days (> 30°C)	days/year
TR	Number of tropical nights	days/year
CSDI	Cold spell duration index	days/year
WSDI	Warm spell duration index	days/year
TXx	Monthly maximum value of daily maximum temperature (TX)	°C
TNx	Monthly maximum value of daily minimum temperature (TN)	°C
TXn	Monthly minimum value of TX	°C
TNn	Monthly minimum value of TN	°C
TN10p	Percentage of days when TN < 10^{th} percentile	% of days in month
TX10p	Percentage of days when TX < 10^{th} percentile	% of days in month
TN90p	Percentage of days when TN > 90^{th} percentile	% of days in month
TX90p	Percentage of days when TX > 90^{th} percentile	% of days in month

4.4.2 DATA ANALYSIS

In this chapter we use box plots and maps to present and compare differences between the base period (1951-1990) and future projections under climate change scenarios. The plots and maps present output of combined data obtained from 26 GCMs

for each scenario in each period. The maps are based on the differences between future values of the index compared to the base period (1951-1990) and presented in the form of percentages and values. For monthly indices only the box plot and monthly patterns of change is provided for the base and future periods.

4.5 RESULTS AND DISCUSSION

4.5.1 COMPARISON OF THE ANNUAL EXTREME TEMPERATURE INDICIES IN THE BASE PERIOD AND FUTURE PERIODS UNDER CLIMATE CHANGE

Average values of extreme annual indices in the base period (1951-1990) and projections for the near current (2015-2030) and two future periods (2041-2060 and 2071-2100) under SSP1-2.6, SSP2-4.5, SSP5-8.5 scenarios are presented in Table 4.3. Figures 4.2 and 4.3 depict numbers of extreme warm or cold days. It is evident that because of warming, the number of summer days (SU) on an annual basis increases from 36 days (in 1951-1990) to up to 58 days (based on SSP5-8.5) in near current period (2015-2030), and is projected to increase further up to 76 days (based on SSP5-8.5) in the mid-century (2041-2060), and up to 104 days (based on SSP5-8.5) in the far future (2071-2100). The same increasing pattern is shown for the number of hot days (SU30) in a year that on average based on the higher emission scenario (SSP5-8.5) increases from 8 days in the base period (1951-1990) to 20, 64 and 62 days in near current (2015-2030), mid-century (2041-2060) and far future (2071-2100) periods, respectively. The number of tropical nights (TR) is projected to increase based on SSP5-8.5 in the far future period (2071-2100), as the $TR_{SSP5-8.5}$ is projected to reach up to 13 nights during a year (on average) that compared to the base (1951-1990) and near current (2015-2030) periods, with zero

tropical nights, shows a substantial increase.

Table 4.3 Average values of extreme annual indices in the base period (1951-1990) and projections for the near current (2015-2030) and two future periods (2041-2060 and 2071-2100) under SSP1-2.6, SSP2-4.5, SSP5-8.5 scenarios

		SSP1-2.6			SSP2-4.5			SSP5-8.5		
Index	**1951-1990**	**2015-2030**	**2041-2060**	**2071-2100**	**2015-2030**	**2041-2060**	**2071-2100**	**2015-2030**	**2041-2060**	**2071-2100**
ID	80	71	65	63	72	65	58	71	61	47
FD	204	186	177	175	187	174	162	186	168	138
CSDI	8	4	3	3	4	2	1	4	2	0
SU	36	56	66	68	57	69	80	58	76	104
SU30	8	18	25	26	19	27	37	20	34	62
TR	0	0	0	0	0	0	0	0	0	4
WSDI	7	20	33	38	21	36	57	22	47	102
GSL	174	191	200	202	190	202	212	190	207	235

Number of icing days (ID) which on average were 80 days in a year, are projected to decrease remarkably in the near current period (2015-2030) to 71 days (SSP1-2.6 and SSP5-8.5) and to be as low as 58 and 47 days (both based on SSP5-8.5) in the mid-century (2041-2060) and far future (2071-2100) periods, respectively. The number of frost days (FD) also is projected to decrease from 204 days a year (on average) to the lowest projected values of 175, 162 and 138 (all based on SSP5-8.5) in the near current (2015-2030), mid-century (2041-2060) and far future (2071-2100) periods, respectively. The number of icing days and frost days during the winter season is important for agriculture as it can limit some weeds and pests in the fields. Also, this reduction of number of cold days (ID and FD) under climate change means, depending on the timing of frost days, there might be possibility to have longer growing season permitting cultivation of certain winter crops that can tolerate light frosts.

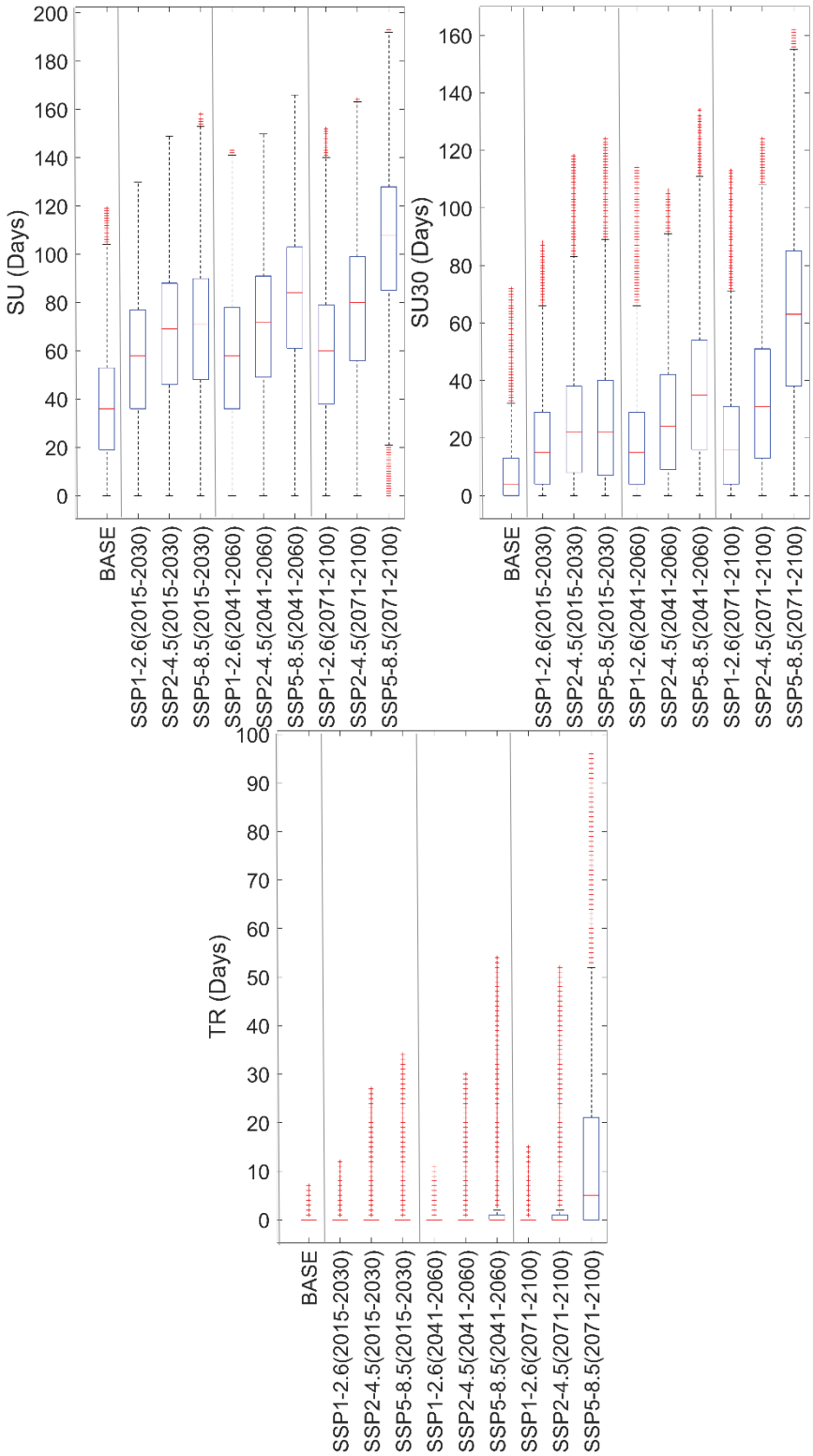

Fig. 4.2 Box plot of the SU, SU30 and TR in the base period (1951-1990) and projections for the near current (2015-2030) and two future periods (2041-2060 and 2071-2100) under SSP1-2.6, SSP2-4.5, SSP5-8.5 scenarios

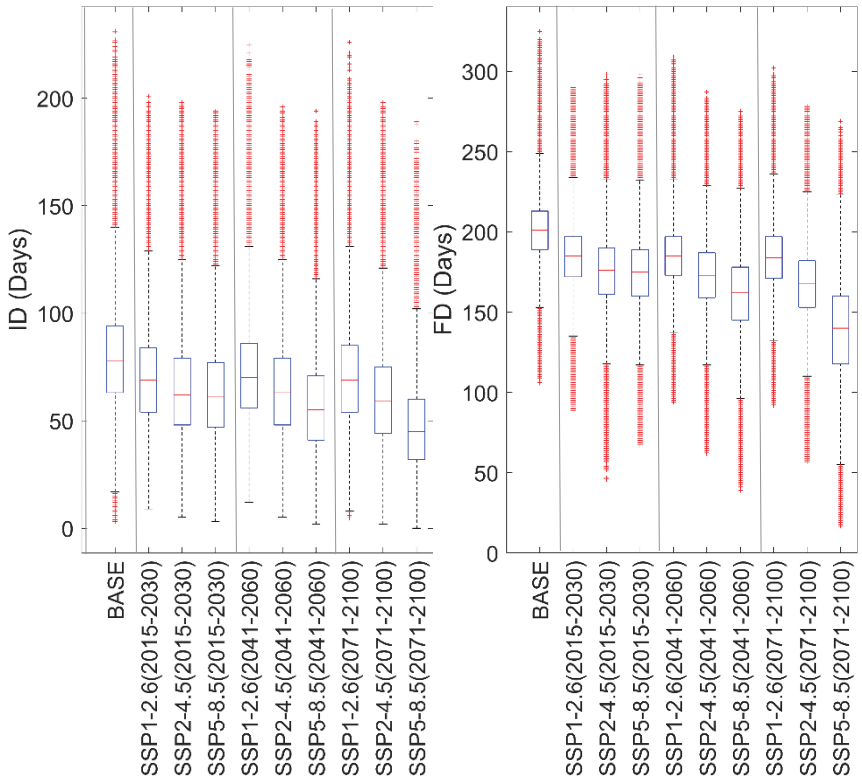

Fig. 4.3 Box plot of the ID and FD in the base period (1951-1990) and projections for the near current (2015-2030) and two future periods (2041-2060 and 2071-2100) under SSP1-2.6, SSP2-4.5, SSP5-8.5 scenarios

On average, GSL in the base period (1951-1990) is 174 days. The results (Figure 4.4) show considerable increases in growing season length by around 17 days (for all scenarios) in the near current period (2015-2030) compared to the base period (1951-1990). The growing season length (GSL) is expected to increase further to a significantly longer period under all three climate change scenarios in the near future (2041-2060) [$GSL_{SSP1\text{-}2.6}$= 200; $GSL_{SSP2\text{-}4.5}$= 202; $GSL_{SSP5\text{-}8.5}$= 207] and the far future (2071-2100) [$GSL_{SSP1\text{-}2.6}$= 202; $GSL_{SSP2\text{-}4.5}$= 212; $GSL_{SSP5\text{-}8.5}$= 235]. On the one hand, it might seem favorable for agricultural productions as a longer growing season length will permit growing cultivars with higher yield potential, as well as the possibility to cultivate a larger variety of crops. But on the other hand, longer growing seasons will increase crop water demand and thus contribute to the occurrence of more severe droughts and will

likely also result in more and earlier agricultural pests, as they are ectothermic, with greater growth, development, survival, and feeding in slightly warmer conditions. Other negative impacts due to increasing growing season lengths are already addressed by agricultural services, for instance increased fall season droughts that cause soil erosion and cold season fires, for example in Lethbridge County.

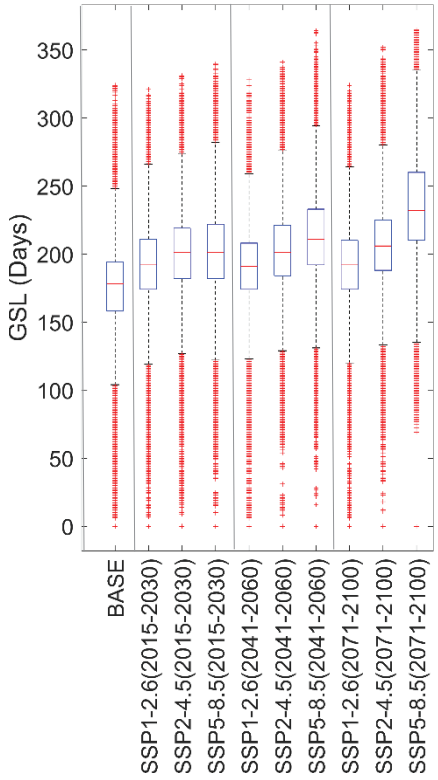

Fig. 4.4 Box plot of the GSL in the base period (1951-1990) and projections for the near current (2015-2030) and two future periods (2041-2060 and 2071-2100) under SSP1-2.6, SSP2-4.5, SSP5-8.5 scenarios

Figure 4.5 shows the dramatic increases of WSDI from 7 days (on average) in the base period (1951-1990) to more than 20 days (all scenarios) in the near current period (2015-2030). The WSDI is almost tripled in the near current period (2015-2030) compared to the base period (1951-1990) and is projected to increase much further by the mid-century (2041-2060) to [$WSDI_{SSP1\text{-}2.6}$= 33; $WSDI_{SSP2\text{-}4.5}$= 36; $WSDI_{SSP5\text{-}8.5}$= 47] and at the end of the century (2071-2100) to [$WSDI_{SSP1\text{-}2.6}$= 38; $WSDI_{SSP2\text{-}4.5}$= 57; $WSDI_{SSP5\text{-}}$

$_{8.5}$= 110]. By contrast, the CSDI which was 8 days (on average) in the base period (1951-1990) is almost halved in the near current period (2015-2030) to 4 days (for all scenarios) and is projected to decrease to less than 3 days (on average) for both the near future (2041-2060) and the far future (2071-2100).

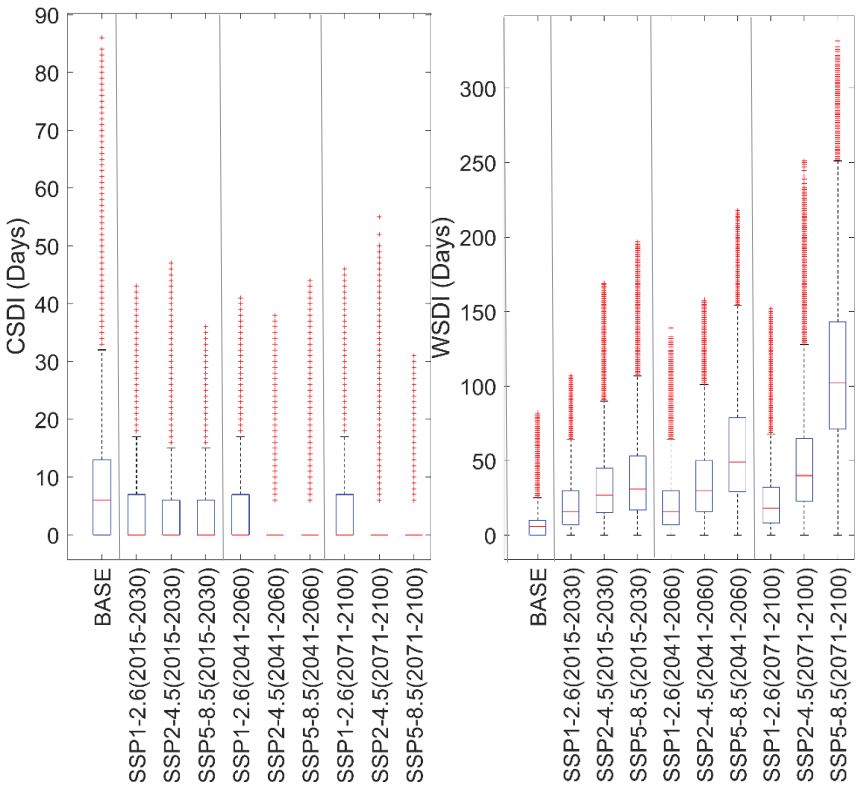

Fig. 4.5 Box plot of the CSDI and WSDI in the base period (1951-1990) and projections for the near current (2015-2030) and two future periods (2041-2060 and 2071-2100) under SSP1-2.6, SSP2-4.5, SSP5-8.5 scenarios

4.5.2 COMPARISON OF THE MONTHLY EXTREME TEMPERATURE INDICIES IN THE BASE PERIOD AND FUTURE PERIODS UNDER CLIMATE CHANGE

In this section we discuss the variations of the projected values based on the medians of the monthly extreme indices compared to the base period (1951-1990). Figures 4.6 to 4.14 show the range and variability of the index values as represented by

box plots for each scenario and time horizon. Each group of data represented by a box is constructed by the values of the indices from the ensemble of 26 GCMs.

Based on Figure 4.6, the warming pattern of TNn (monthly minimum temperature) is evident for all the scenarios in all months. Based on SSP1-2.6, TNn of colder months (i.e., NDJFM) increases by 4-5°C in 2041-2060 and 2071-2100, compared to the base period (1951-1990). The increase of TNn in warmer months is around 2-4°C. The SSP2-4.5 also shows the same pattern as SSP1-2.6, however, the TNn values are slightly higher. Based on SSP5-8.5, TNn shows a warming of ~3°C in 2015-2030, 6°C in 2041-2060, and 9-10°C in 2071-2100. Warming of TNn in warmer months (JJAS) occur at a lower rate of around 1°C in 2015-2030, 3°C in 2041-2060, and ~7-8°C in 2071-2100.

Figure 4.7 shows the box plot of TNx. Based on SSP1-2.6, the TNx values in cold months (DJF) are between -2.5 to -2.0°C, and up to around 0°C values in 2071-2100. The warmer months (JJA) experience approximately 1°C of warming of TNx per period, approximately increasing the TNx by 3°C by 2071-2100, based on SSP1-2.6.

TNx as projected by SSP5-8.5 in colder months (DJF) tends to be above 0°C closer to the end of the century, at the period of 2071-2100. Also, in warmer months an increase of 6-8°C in TNx is projected by SSP5-8.5.

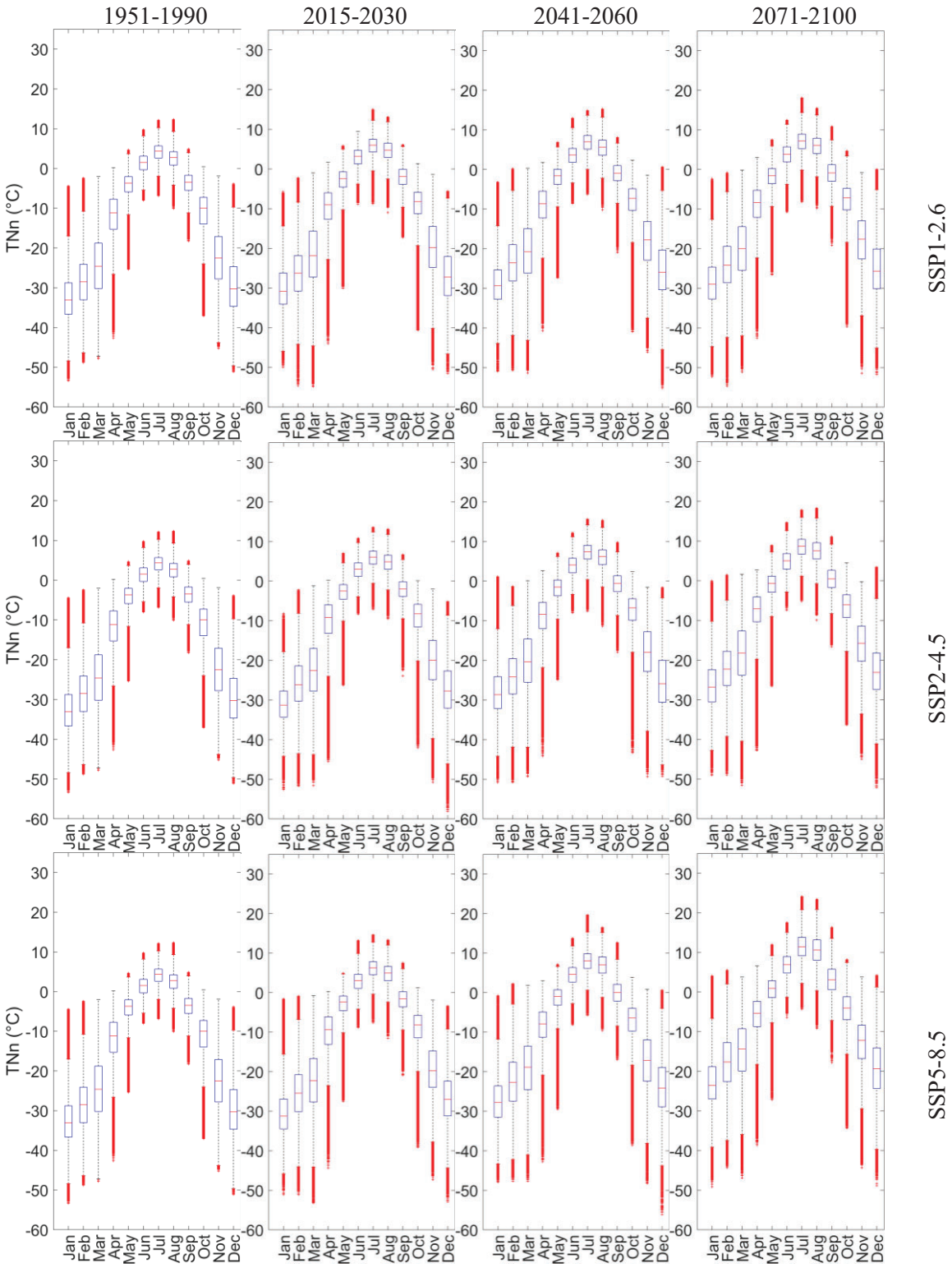

Fig. 4.6 Box plot of TNn in the base period (1951-1990) and projections for the near current (2015-2030) and two future periods (2041-2060 and 2071-2100) under SSP1-2.6, SSP2-4.5, SSP5-8.5 scenarios

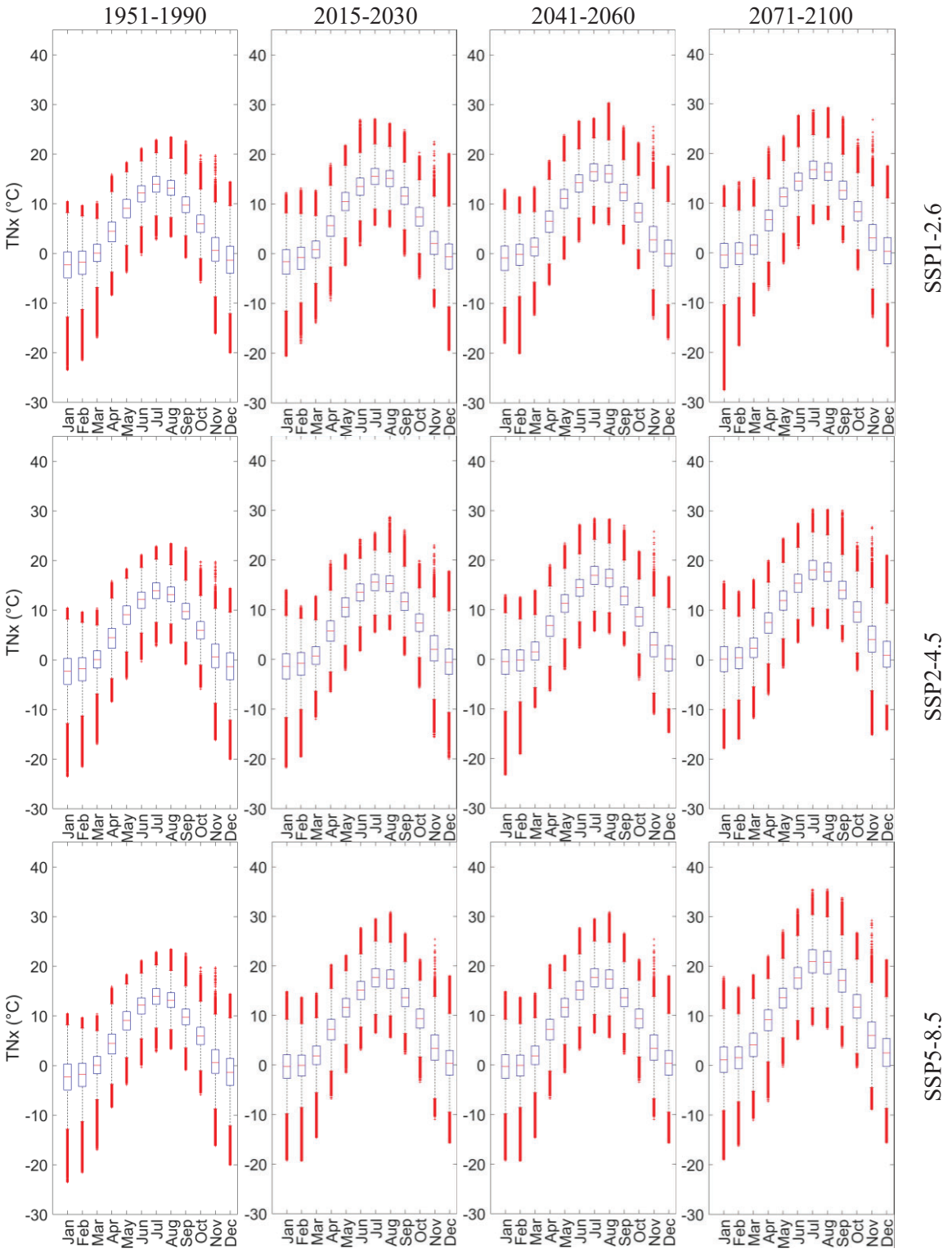

Fig. 4.7 Box plot of TNx in the base period (1951-1990) and projections for the near current (2015-2030) and two future periods (2041-2060 and 2071-2100) under SSP1-2.6, SSP2-4.5, SSP5-8.5 scenarios

Figure 4.8 shows that values of TN10p (percentage of days when the minimum temperature for the day is less than the lower tenth percentile) in the base period (1951-1990) for colder months (October to April) is between 6-7%; while in warmers months it is around 10%. Projected TN10p values (percentage of days when the minimum temperature for the day is below the tenth percentile) are 0% for all scenarios in 2041-2060 and 2071-2100 periods. Based on SSP5-8.5, not only the median in the 2071-2100 is 0 but also the whole range is 0, meaning no temperature values are in the lowest 10^{th} percentile of TN. For the near current period (2015-2030) the values of the TN10p hover around 3% in most of the months (except warmer months).

Based on Figure 4.9, TN90p in the base period (1951-1990) is around 6% (ranging from 3 to 17%) and it clearly increases in all periods based on all applied scenarios. TN90p values increase in later time periods. They are smaller for SSP1-2.6 and greater for SSP5-8.5. TN90p increase is greater in warmer months of the year as for the SSP1-2.6 it reaches up to 26%, 40%, and 46% in near current (2015-2030), near future (2041-2060) and far future (2071-2100), respectively; the values are 27%, 44%, and 68% for SSP2-4.5, and 25%, 60%, and 97% for SSP5-8.5. The variabilities of the projected values of TN90p also increase dramatically with time.

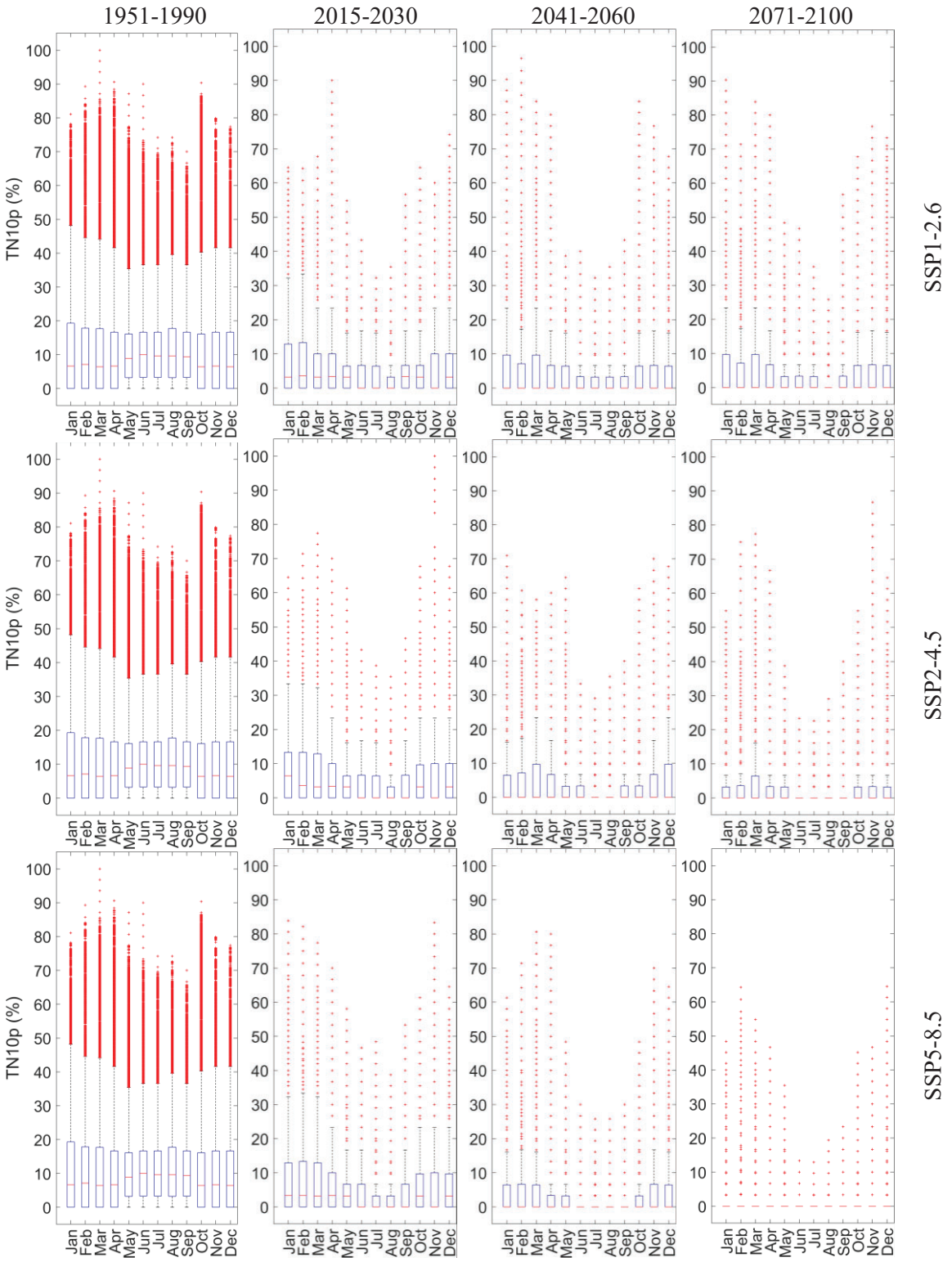

Fig. 4.8 Box plot of TN10p in the base period (1951-1990) and projections for the near current (2015-2030) and two future periods (2041-2060 and 2071-2100) under SSP1-2.6, SSP2-4.5, SSP5-8.5 scenarios

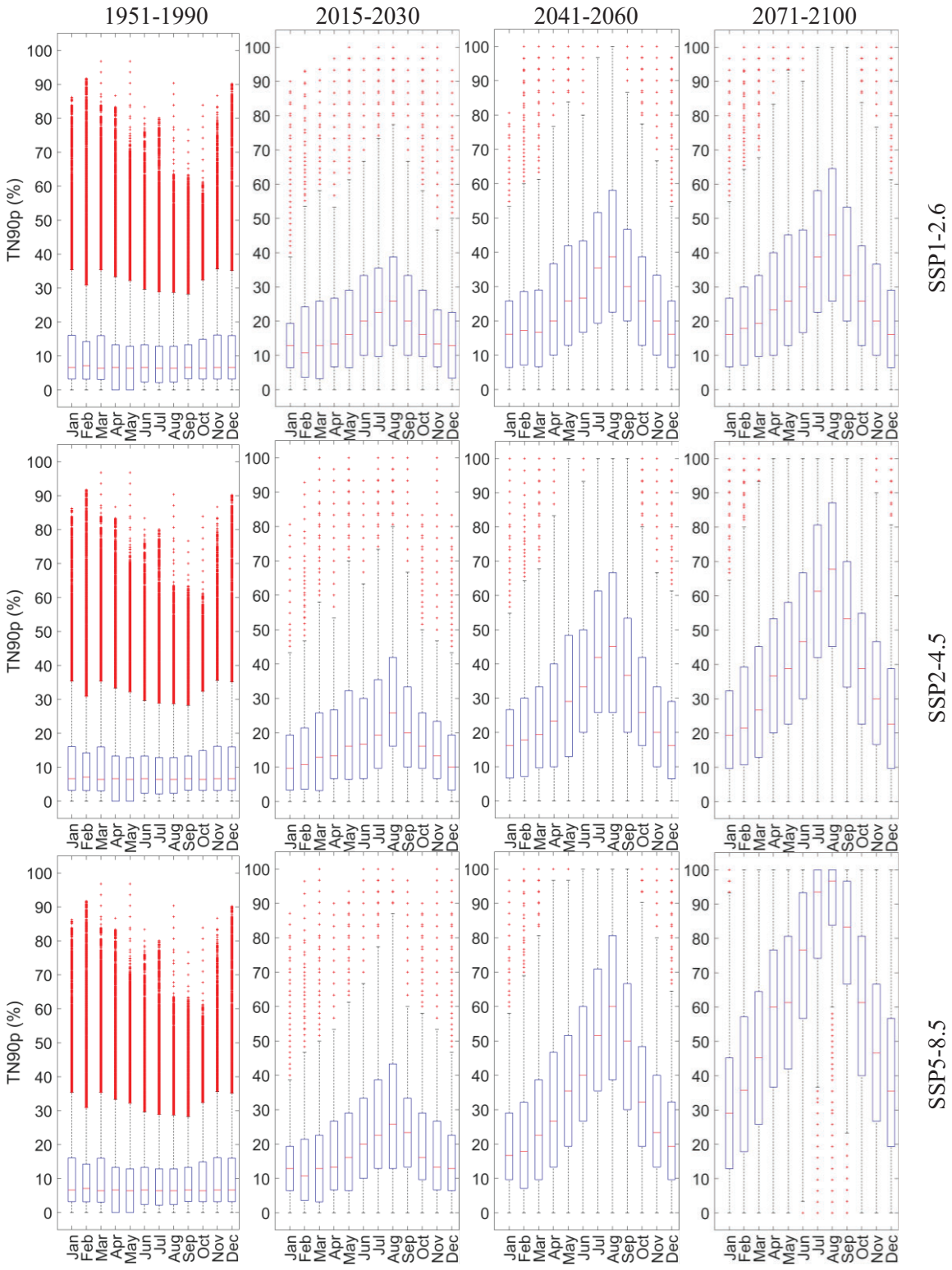

Fig. 4.9 Box plot of TN90p in the base period (1951-1990) and projections for the near current (2015-2030) and two future periods (2041-2060 and 2071-2100) under SSP1-2.6, SSP2-4.5, SSP5-8.5 scenarios

Figure 4.10 shows the TXn in base period (1951-1990) and its projections. Based on SSP1-2.6, approximately 4-5°C of warming in colder months (DJF) and ~4°C of warming in warmer months (JJA) is projected for the far future period. Also, a 1.0-1.5°C of warming of TXn is projected to occur per period. SSP2-4.5 shows a very similar pattern to SSP1-2.6, with around 1°C higher TXn values for the SSP2-4.5 compared to SSP1-2.6. Based on SSP5-8.5, TXn increases more dramatically than the two other scenarios, as in warmer months at the end of the century the TXn is projected to be 9-10°C higher than the base period (1951-1990); and in colder months the warming is about 7-9°C. In the near current period (2015-2030), the temperature increase of the colder months is between 1-3°C and is ~4°C in near future (2041-2060). Warmer months of the year are projected to experience an increase of 2°C and 4°C in near current (2015-2030) and near future (2041-2060), respectively.

Figure 4.11 compares the TXx as projected by three scenarios compared to the base period (1951-1990). Projections show that TXx increased slightly in the near current (2015-2030) compared to the base period (1951-1990) for all the scenarios and the maximum increase is projected by SSP5-8.5 in the 2015-2030 period which is about 2°C warming in warm months of July and August. The increase of TXx for colder months in the near (2041-2060) and far future (2071-2100) compared to the base period (1951-1990) is below 2°C for SSP1-2.6 and SSP2-4.5. But based on SSP1-2.6, the warming is around 3°C and 4°C higher in warm months of the near future (2041-2060) and far future (2071-2100), respectively.

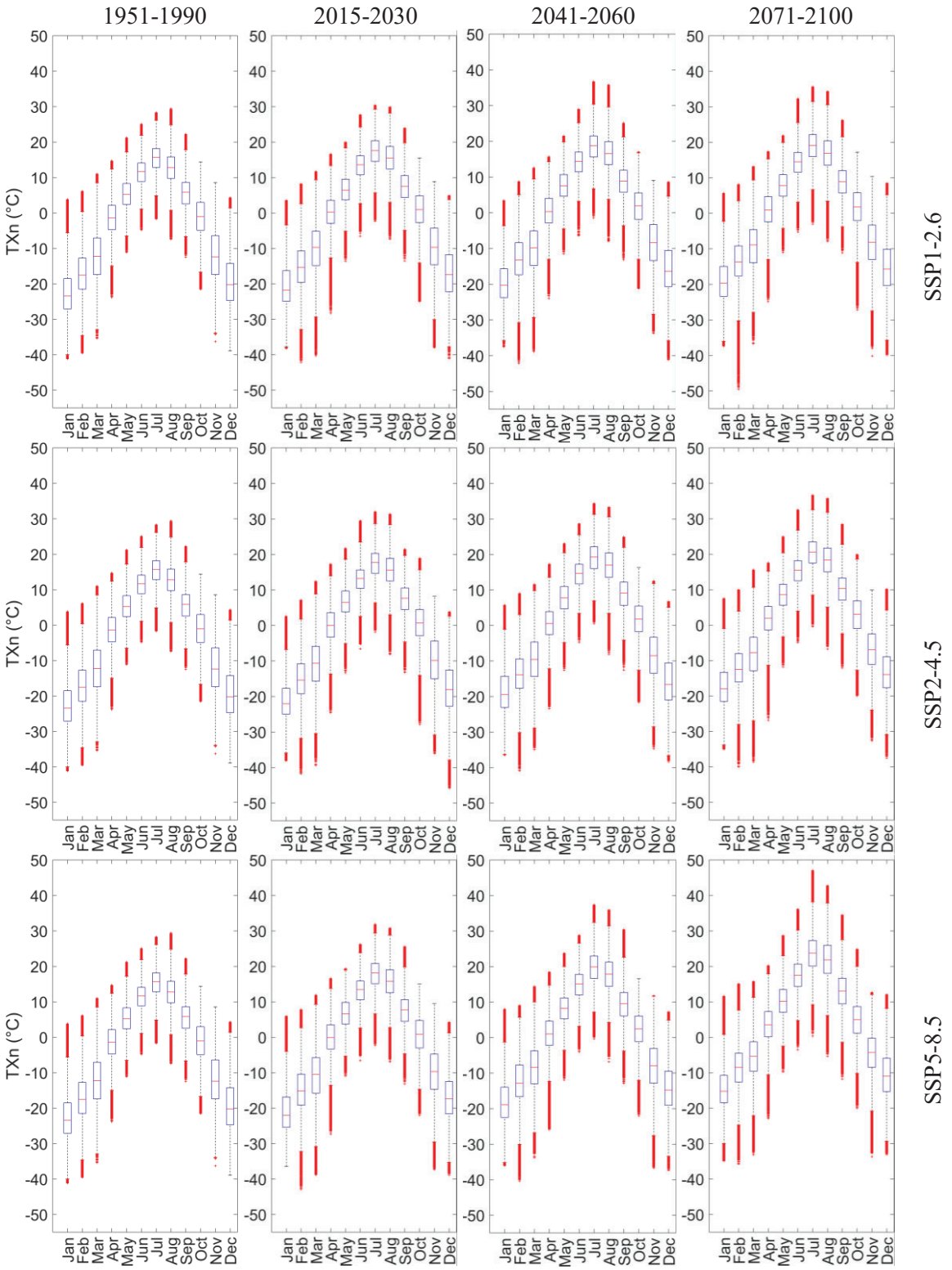

Fig. 4.10 Box plot of TXn in the base period (1951-1990) and projections for the near current (2015-2030) and two future periods (2041-2060 and 2071-2100) under SSP1-2.6, SSP2-4.5, SSP5-8.5 scenarios

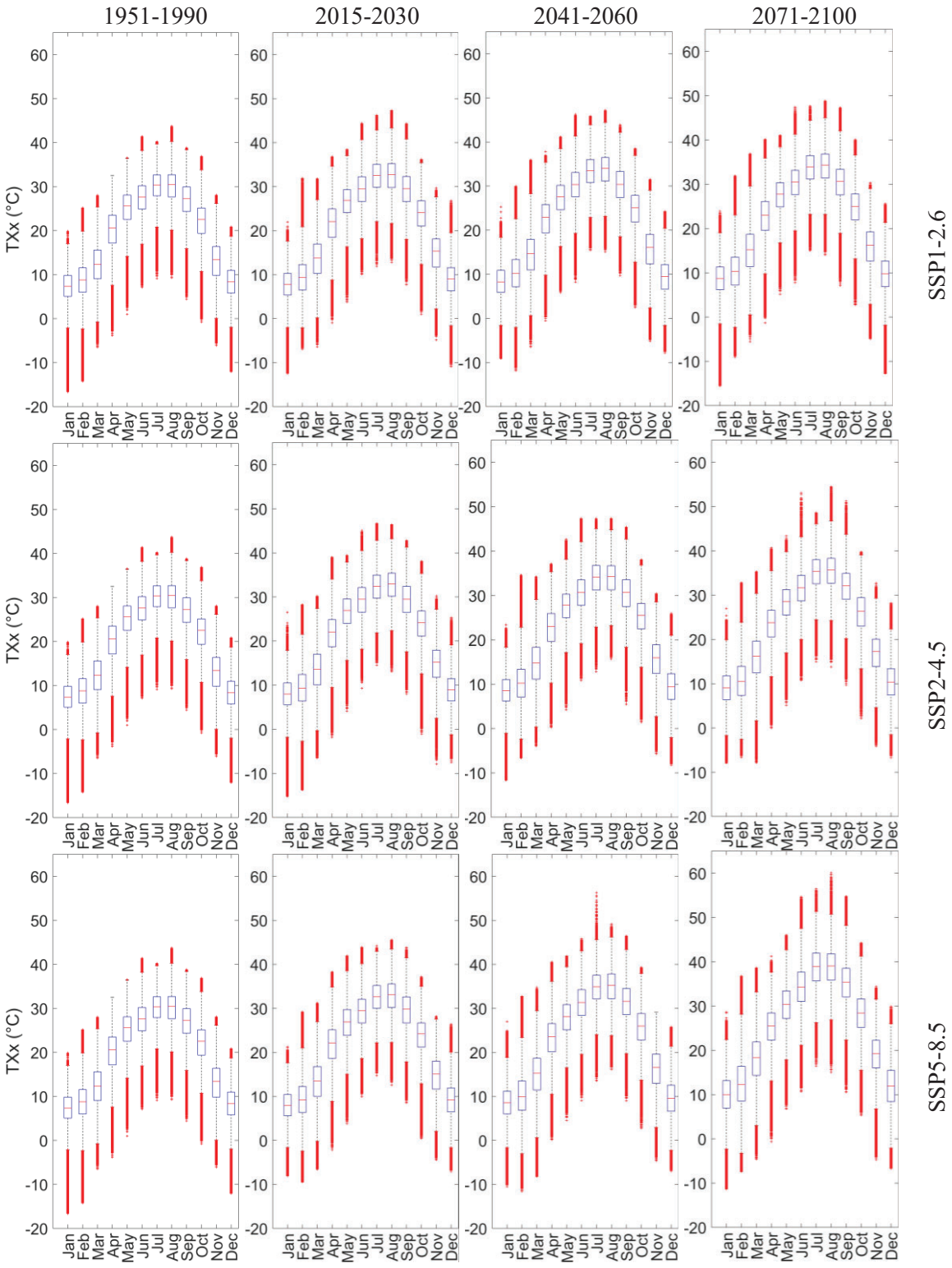

Fig. 4.11 Box plot of TXx in the base period (1951-1990) and projections for the near current (2015-2030) and two future periods (2041-2060 and 2071-2100) under SSP1-2.6, SSP2-4.5, SSP5-8.5 scenarios

The increases of TXx in warm months in the near (2041-2060) and far future (2071-2100), projected by SSP2-4.5, are 3°C and ~5°C, respectively, are shown. Warming of TXx projected by SSP5-8.5 is more dramatic in the near (2041-2060) and far future (2071-2100), which in these two periods is around 5°C and ~9°C higher than in the base period (1951-1990) in warm months, and around 2°C and 4°C higher than the base period (1951-1990) in cold months.

As presented in Figure 4.12, the TX10p ranges around 10% in warmer months (JJAS) and 7% in other months. TX10p tends to be 0% at 2041-2060 and 2071-2100, with a few exceptions (being around 3%) observed between the months of January to May. For the near current period (2015-2030), however, TX10p values are between 3-6% in all cases (except one 0% value for the month of July based on SSP5-8.5). The range and variability of TX10p is decreasing as we move towards the end of the century.

Unlike TX10p, the range of variabilities of TX90p increases by time (Figure 4.13). The TX90p values are almost constant and around 6% in the base period (1951-1990) and increase over time. The increased TX90p in projected periods shows a seasonal pattern, which is greater closer to the end of the century, and for SSP5-8.5. In the near current period (2015-2030), almost all months show an increase in TX90p, but it stays below 20% (except in one case). The increase in TX90p is greater for warmer months as for near future (2041-2060) and far future (2071-2100) periods, it hits 30% and ~33% based on SSP1-2.6, 33%, and 45% based on SSP2-4.5, and 49% and 74% based on SSP5-8.5.

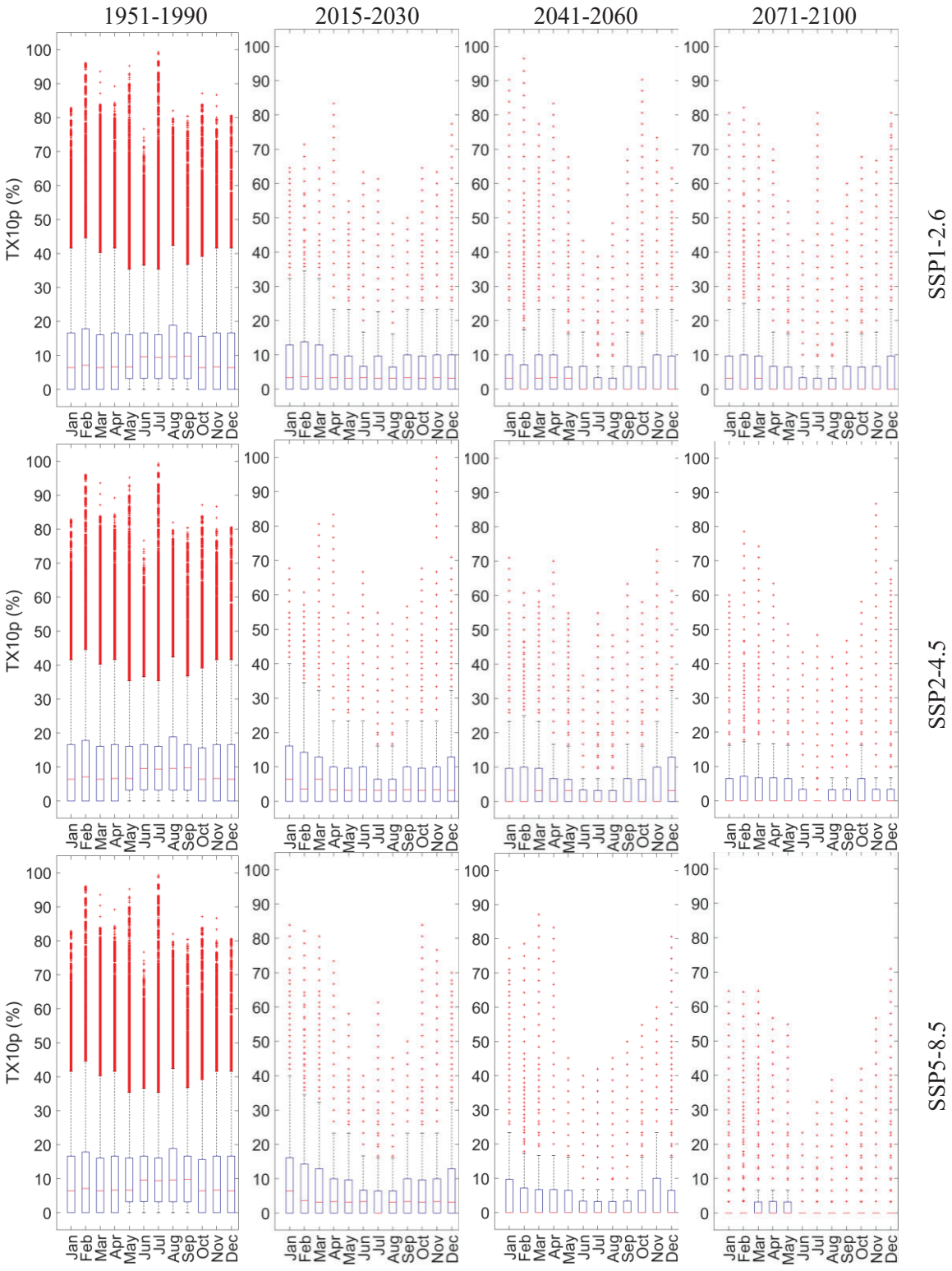

Fig. 4.12 Box plot of TX10p in the base period (1951-1990) and projections for the near current (2015-2030) and two future periods (2041-2060 and 2071-2100) under SSP1-2.6, SSP2-4.5, SSP5-8.5 scenarios

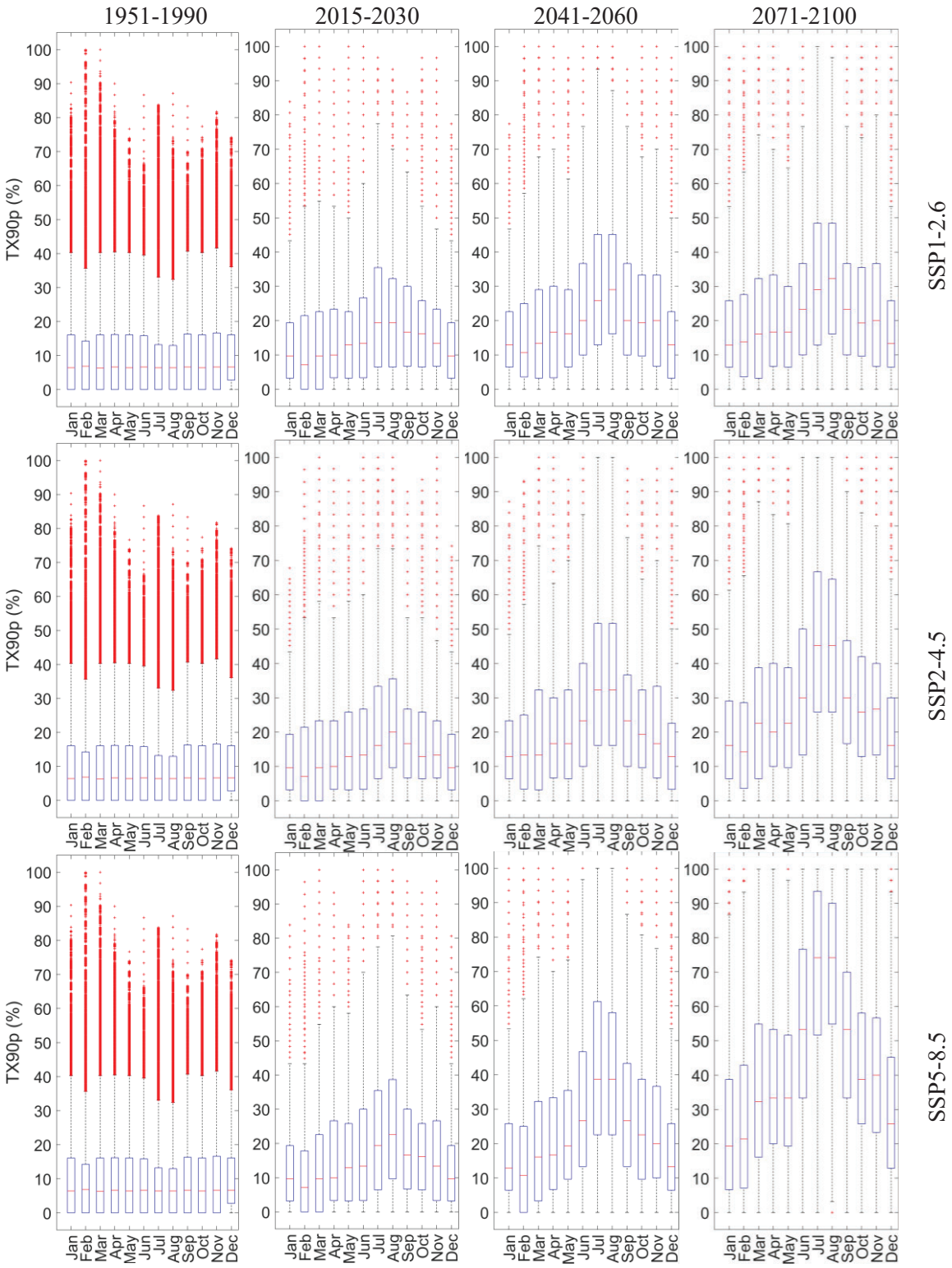

Fig. 4.13 Box plot of TX90p in the base period (1951-1990) and projections for the near current (2015-2030) and two future periods (2041-2060 and 2071-2100) under SSP1-2.6, SSP2-4.5, SSP5-8.5 scenarios

Based on Figure 4.14, and all three scenarios, the DTR decreases slightly as we move towards the end of the century as in the cold months (DJF) based on projections of SSP1-2.6 for far future period (2071-2100) it decreases by around 1-2°C, compared to the base period (1951-1990). DTR of cold months (DJF) at the end of century, projected by SSP5-8.5, is up to 3°C smaller than the DTR of the base period (1951-1990). As shown in Figure 4.14, DTR of warmer months based on SSP1-2.6 and SSP2-4.5 is slightly higher than the base period (1951-1990). The difference of the future projected DTR and DTR of the base period (1951-1990) in warm months at far future period (2071-2100) for SSP5-8.5 is greater than two other scenarios and is between 1-1.5°C.

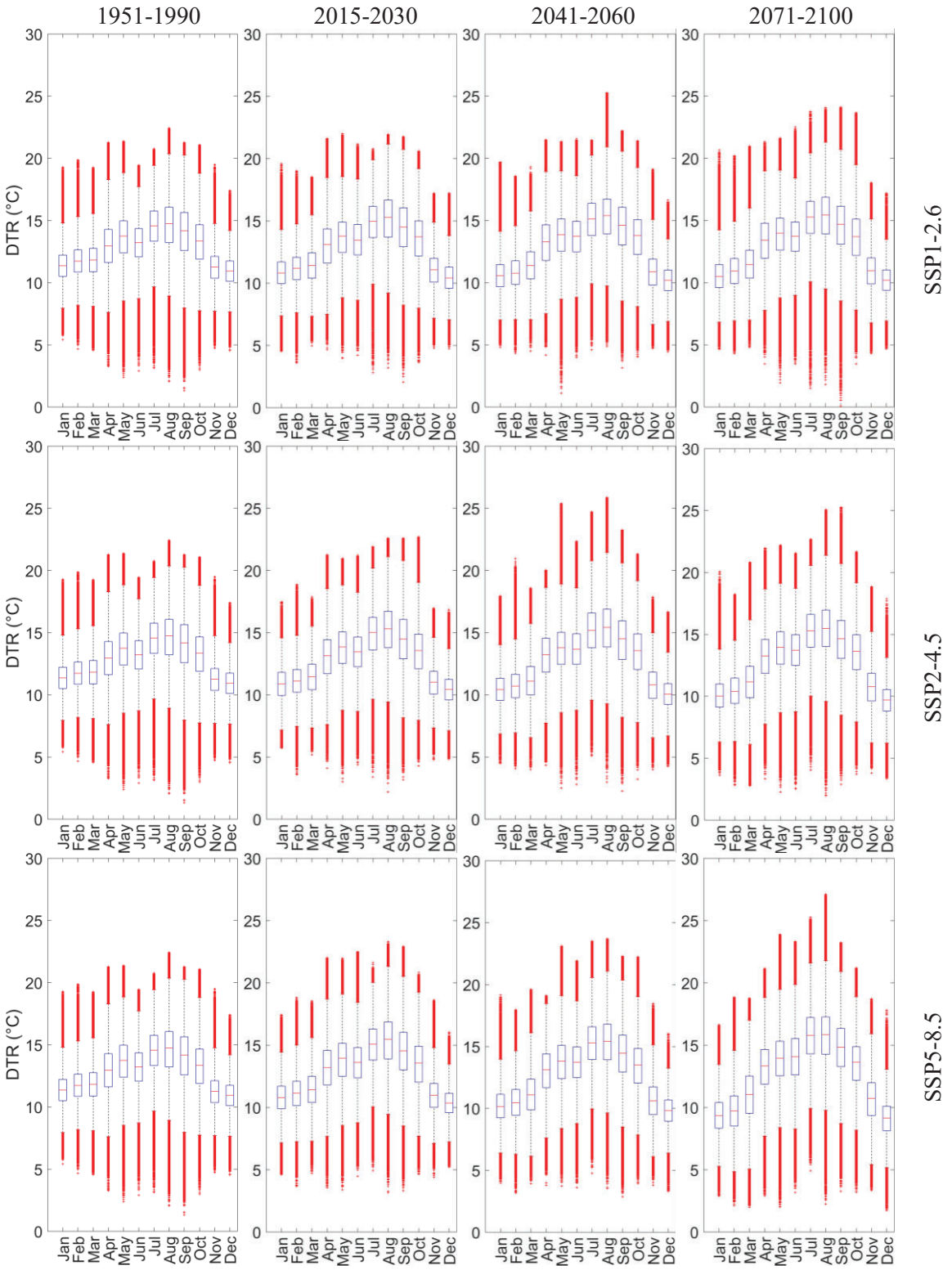

Fig. 4.14 Box plot of DTR in the base period (1951-1990) and projections for the near current (2015-2030) and two future periods (2041-2060 and 2071-2100) under SSP1-2.6, SSP2-4.5, SSP5-8.5 scenarios

4.6 CONCLUDING REMARKS

In this chapter future projections of temperature extreme events were studied and analyzed. Applied indices clearly show the considerable impacts of global warming in the near current period (2015-2030) compared to the base period (1951-1990). Also, under all climate change scenarios, the results indicate intensification of such extreme events by the end of the century. The impacts of these changes in the temperature extreme events could be explored within different systems such as urban systems and environmental and agricultural systems.

Urban systems: Increased temperature and related extreme events could have some implications for the urban water and power supply sectors as the demands for both resources will increase. Increased numbers of hot and very hot days based on SU and SU30 combined with overall increased minimum and maximum temperatures in warmer months of the year can cause challenges for health care services as those with background health issues or elderly people could be exposed to excess heat (Bell et al. 2018) that cannot be dissipated without air conditioning. The minimum temperature, which usually occurs at nights, and maximum temperature during the day will rise and during warmer summer days can put people with chronic issues at higher risk as overall higher rates of mortality is expected under climate change (Gasparrini, 2017).

Agricultural and environmental systems: Increase in the number of extreme warm days can cause water stress of crops and other vegetation, prohibit their full development, and greatly reduce yields. Certain crops and at different stages of development could have different responses to the heat and water deficit. Rainfed

agriculture is also more vulnerable against higher temperatures and water stress. High sensitivity to heat in the root zone of wheat (Wang et al., 2007) and low tolerance of the potato to water deficit (Van Loon, 1981) are examples of crops that are extensively cultivated in Southern Alberta and can have reduced yield under environmental stressors.

Seasonal patterns of the maximum and minimum temperature and the percentage of days that fall within the thresholds of above the 90^{th} percentile and below the 10^{th} percentile of both TX and TN, show increased temperatures, smaller number of cold days, and a greater number of warmer days. In addition to higher minimum and maximum temperatures, the daily temperature range (DTR) is projected to decrease in colder months of the year and slightly increase in warmer months, under climate change scenarios.

Dierauer et al. (2019) showed that higher mean winter temperature is increasing the risk of snow droughts in WNA, and around 27% of the non-glaciated snowpack in the Western US and southwestern Canada is prone to medium to high snow drought risk. However, under +2° C forcing, the Canadian Rockies showed lower susceptibility to warm snow drought, but the risk of warm and dry snow drought was considerable. Warmer winter months can cause snow events to start later and melt during the winter season, or occurrence of mixed rain and snow events in wintertime may occur, reducing the accumulation of snow (Dierauer et al., 2019). The resulting effect on snow is critical in the SSRW, where the spring and summer discharges of all the river basins are dependent to snowmelt. Warm snow droughts also can increase the risk of flood events. Earlier thawing of the snowpack related to temperature increase is also associated with increased risk of wildfire (Westerling et al., 2006), less carbon uptake (Hu et al., 2010;

Winchell et al., 2016), and negative ecological impacts in the mountains (Harpold, 2016).

All in all, the projected changes in the extreme temperature related indices, based on all three climate change scenarios, suggest a significant increase in temperature and warm spells and number of days with extreme warm temperatures. This can cause increased food and water insecurity and jeopardize the sustainable economic revenue of the region. It can also impose health risks and overburden the healthcare sector.

The rise in the crop water demands with projected increased temperature, and longer growing season, can contribute to more dryness and impact the environment and wildlife.

Considerable change that is projected to occur in most of the temperature indices, will impact the water cycle by increased evapotranspiration and more surface water consumption. Also, during hot long periods, known as heat waves, the suitable condition for local and regional convective precipitation will be negatively impacted. However, the impact of temperature change on geographically wider precipitation change should be studied along with the global climate model projections for the future time horizons. Based on the projections, an increase in the global amount of precipitation is expected (Tabari, 2020) because of increased evaporation over surface water and increased water holding capacity of the atmosphere. Although the regional impacts and interactions of temperature and precipitation will change, the effects of global changes on local precipitation should be explored.

CHAPTER 5: SUMMARY AND CONCLUSIONS

This study was designed as an effort to address the current and future states of the impact of climate change on extent, duration, and likelihood of extreme weather events in the South Saskatchewan River Watershed in Southern Alberta, and identify the areas that are prone to drought events. A second objective was to investigate the degree to which the characteristics and likelihood of these extreme events could vary under global climate change. In particular, in Chapters 2 to 4 we discussed these main objectives and corresponding research efforts:

1- Studying the historical and future changes of drought in the South Saskatchewan River Watershed using two drought indices, comparing the drought occurrence rates in the past four decades, and identifying and mapping the areas that showed significant trends of drought.

2- Investigating the impacts of climate change on drought conditions in the study area using three SSP (Shared Socioeconomic Pathways, from the IPCC Sixth Assessment Report) climate change scenarios (SSP1-2.6, SSP2-4.5, and SSP5-8.5) in three time horizons (near current: 2015-2030; near future: 2041-2060; and far future: 2071-2100) and compare the results with the base period (1951-1990).

3- Investigating the impact of climate change on temperature-related extreme events in the study area using three SSP climate change scenarios (SSP1-2.6, SSP2-4.5, and SSP5-8.5) in three time horizons (near current: 2015-2030; near future: 2041-2060; and far future: 2071-2100) and compare the results with the base period (1951-1990).

4- Identifying areas most vulnerable to the extent and duration of drought, and possible range of variabilities of these extreme events within the study area under climate change condition.

This information is important to be considered for adapting to the environmental challenges of climatic change and variability. Advance warning of expectations could increase the resiliency of local communities and decrease vulnerability against the damaging and unpleasant consequences of climatic change. Awareness and quantitative forecasting would allow better preparedness of the healthcare sector, urban development plans, power supply, and infrastructure design in order to prevent/reduce the disaster-level losses.

In Chapter 2, we assessed the previous state and change of the historical drought conditions in the SSRW. In this part of the study, we used Daymet gridded dataset to calculate two drought indices of SPI and SPEI at different timescales of 1-, 3-, 6-, 9- and 12-month(s). Our findings showed that the SPEI (taking evapotranspiration into account) performed better in detecting drought conditions than the SPI. By analyzing the drought in the historical period (1980-2018) in the study area, we found that the rate of occurrence of drought has increased and also the area affected with more severe and extreme droughts have increased in recent decades. The Mann-Kendall trend test applied to monthly gridded drought values showed both increasing and decreasing drought trends have occurred in the four decades of the study period. Decreasing trends are found mainly in the upstream of the Bow River Basin and mainly in the vicinity of the Rocky Mountains. Larger areas have seen increased drought trends in the recent four decades (1980-2018), mainly in downstream portions of the watershed, especially in parts of the

south, southeast, east, central, and northern areas of the SSRW. The mapped areas attributed to increased drought and the intensity of drought condition were greater in proportion to the timescales of the indices.

In Chapter 3 we discussed the future possible drought conditions in the study area based on the SPEI drought index at 5 timescales (1-, 3-, 6-, 12- and 24-month(s)) in the near current and two future periods (2015-2030; 2041-2060; 2071-2100), obtained by an ensemble of 26 GCMs and 3 SSP climate change scenarios (SSP1-2.6; SSP2-4.5; and SSP5-8.5) to cover a range of possibilities regarding future emissions and impacts on short-term and long-term drought conditions in the SSRW. Results were compared to the selected (1951-1990) base period. We used a CMIP6 (Coupled Model Intercomparison Project, Phase 6) ensemble of gridded temperature and precipitation values from CanDCS-U6 (Canadian Downscaled Climate Scenarios – Univariate CMIP6). Our findings showed a shift from more positive and closer to zero values of the SPEI index in the base period (1951-1990), denoting no drought or mild drought conditions, to more negative values projected for near current (2015-2030) and future periods (2041-2060 and 2071-2100). As we move forward toward the end of the century, increased occurrence rates and intensification of the drought events were projected to occur under all the applied scenarios. It was found that the projected occurrence rates under different applied climate change scenarios do not differ significantly and are only slightly higher under SSP1-2.6.

The spatial pattern of drought under climate change conditions differs from that of the base period. In the historical base period, more drought occurrence rates were detected closer to the western boundaries of the SSRW and mountainous areas of the

Rocky range in Southern Alberta, while the future projections in 2041-2060 and 2071-2100 show that eastern parts of the SSRW are more prone to experience more droughts than other parts of the watershed. The projections show that the highest rates of drought occurrence and severity is associated with the SSP1-2.6 scenario in which global CO_2 emissions are reduced moderately rapidly, reaching net-zero after 2050.

Chapter 4 describes the plausible changes in temperature-related extreme events in the SSRW under climate change based on CMIP6 projections of extreme temperature indices of the CanDCS-U6 ensemble of 26 GCMs and 3 SSP scenarios (SSP1-2.6; SSP2-4.5; and SSP5-8.5), in near current (2015-2030) and two future time periods (2041-2060; and 2071-2100), which are compared to the values of the base period (1951-1990).

Our results showed that the annual count of the extreme warm (Tmax>25°C) and number of hot (Tmax>30°C) summer days increase considerably based on the projections of all three scenarios, while the number of days with lower temperatures (i.e., frost days and icing days) will decline significantly in all three periods compared to the base period (1951-1990). Numbers of tropical nights is only projected to increase under highest emission scenario (SSP5-8.5) for the period 2071-2100. The length of the growing season is projected to increase substantially. Other changes include notable increase in WSDI (warm spell duration index) and decrease in CSDI (cold spell duration index) under climate change condition. Monthly patterns of the indices that show extreme cold or warm temperatures in a month also confirm increased extreme warmer temperatures and milder extreme cold temperatures, compared to the base period (1951-1990). The greatest changes of the extreme temperature related events in the SSRW are projected to occur under SSP5-8.5 (high emissions scenario, sometimes referred to as ‘business as usual’)

and closer to the end of the 21st century.

5.1 RECOMMENDATIONS FOR FUTURE RESEARCH

In this study we employed drought and temperature- extreme weather event indices and an ensemble of 26 CMIP6 GCMs and 3 SSP scenarios to assess the future changes in the extent and likelihood of extreme weather events in the South Saskatchewan River Watershed.

1- Drought conditions and change over time could be different at different locations, so we recommend that region-specific studies be conducted in other areas. Specifically in the Canadian Prairies, which have a generally dry grassland biome and climate, understanding the pattern of change and areas prone to increased drought severity can help local communities, farmers, and planners by providing scientific background to increase resiliency. Using longer time periods of historical data can help with understanding of long-term changes and variabilities of drought condition. However, accessing long-term data with adequate accuracy, consistency over time, and good spatial coverage might be a constraint in many regions.

2- Our findings based on the SPEI drought index showed that the more significant increase in drought frequency is plausible under SSP1-2.6 (or lower warming). As this index is sensitive to changes in both precipitation and temperature, we recommend use of SPEI to describe and assess drought under climate change.

3- Since extreme events could show different patterns in different regions, it is crucial that regional studies being carried out in different regions to obtain region-

specific results and prepare the adaptation plans based on them.

4- Results of the climate change studies are highly dependent on the choice of applied GCMs. There is an ongoing effort in improvement of the precision of these models. Due to high importance of the extreme events and the impacts they can have on the environment and our societies, it is crucial to use the most reliable data when studying the extreme events. In this study we employed the most recent available outputs of the CMIP6 project. The information presented in this dissertation is currently reliable but should be updated as other data become available.

5- In Chapters 3 and 4 of this study we analyzed the future changes of drought and extreme temperatures. As drought and extreme high temperatures can have disastrous impacts, it is recommended that a separate study focus on the compound impacts of these two extreme events.

6- There are reports of occurrence or increased risk of wildfires under concurrent drought and heatwaves. Many recent studies focus on combined impact of drought and extreme heat, as they can superimpose each other and have more disastrous impacts. Like causing severe stress for vegetation and lack of moisture in the environment, that can cause the fire damage potential to be increased and cause the fire to advance further and faster in the absence of moisture in the environment. Studying the attribution and associated risk of these extreme events to wildfires under climate change is crucial and will help better understanding of future risks and detection of areas that are at higher risk.

7- In Chapter 4 we studied the extreme temperature related indices and analyzed the possible changes in future decades compared to the base period (1951-1990). Due to importance of extreme precipitation events, it is recommended that another study focuses on the precipitation extreme events in the study area.

8- Based on the findings of this study on the extent and likelihood of extreme events under climate change, along with other reports by other researchers, and observing the patterns of change in precipitation and temperature regimes, it is apparent that climate change has impacted the region, like other regions, and will have future impacts. Climate change impacts can have irreversible economic and societal consequences; therefore, it is important to assess the possible socio-economic and demographic changes derived by this reality of the near future.

REFERENCES

AghaKouchak, A., Cheng, L., Mazdiyasni, O., & Farahmand, A. (2014). Global warming and changes in risk of concurrent climate extremes: Insights from the 2014 California drought. *Geophysical Research Letters, 41*(24), 8847-8852.

Ajjur, S. B., & Al-Ghamdi, S. G. (2021). Global hotspots for future absolute temperature extremes from CMIP6 models. *Earth and Space Science, 8*(9), e2021EA001817.

Alexander, L. V., Zhang, X., Peterson, T. C., Caesar, J., Gleason, B., Klein Tank, A. M. G., Haylock, M., Collins, D., Trewin, B., Rahimzadeh, F., Tagipour, A., Rupa Kumar, K., Revadekar, J., Griffiths, G., Vincent, L., Stephenson, D. B., Burn, J., Aguilar, E., Brunet, M., Taylor, M., New, M., Zhai, P., Rusticucci, M., & Vazquez-Aguirre, J. L. (2006). Global observed changes in daily climate extremes of temperature and precipitation. *Journal of Geophysical Research, 111*(D5), D05109-n/a. https://doi.org/10.1029/2005JD006290

Al-Kaisi, M. M., Elmore, R. W., Guzman, J. G., Hanna, H. M., Hart, C. E., Helmers, M. J., Hodgson, E. W., Lenssen, A. W., Mallarino, A. P., Robertson, A. E., & Sawyer, J. E. (2013). Drought impact on crop production and the soil environment: 2012 experiences from Iowa. *Journal of Soil and Water Conservation, 68*(1), 19-24A. https://doi.org/10.2489/jswc.68.1.19A

Allen, R. G., Pereira, L. S., Raes, D., & Smith, M. (1998). Crop evapotranspiration-Guidelines for computing crop water requirements-FAO Irrigation and drainage paper 56. FAO, Rome, 300(9), D05109. Chapter 2.

Almazroui, M., Islam, M. N., Saeed, F., Saeed, S., Ismail, M., Ehsan, M. A., Diallo, I., O'Brien, E., Ashfaq, M., Martínez-Castro, D., Cavazos, T., Cerezo-Mota, R., Tippett, M. K., Gutowski, W. J., Alfaro, E. J., Hidalgo, H. G., Vichot-Llano, A., Campbell, J. D., Kamil, S., Ur Rashid, I., Sylla, M. B., Stephenson, T., Taylor, M., Barlow, M. (2021). Projected changes in temperature and precipitation over the United States, central America, and the Caribbean in CMIP6 GCMs. *Earth Systems and Environment, 5*(1), 1-24. https://doi.org/10.1007/s41748-021-00199-5

Bandyopadhyay, N., Bhuiyan, C., & Saha, A. K. (2016). Heat waves, temperature extremes and their impacts on monsoon rainfall and meteorological drought in Gujarat, India. *Natural Hazards (Dordrecht), 82*(1), 367-388. https://doi.org/10.1007/s11069-016-2205-4

Batibeniz, F., Ashfaq, M., Diffenbaugh, N. S., Key, K., Evans, K. J., Turuncoglu, U. U., & Önol, B. (2020). Doubling of US population exposure to climate extremes by 2050. *Earth's Future*, *8*(4), e2019EF001421.

Beguería, S., Vicente-Serrano, S. M., Reig, F., & Latorre, B. (2014). Standardized precipitation evapotranspiration index (SPEI) revisited: Parameter fitting, evapotranspiration models, tools, datasets and drought monitoring. *International*

Journal of Climatology, 34(10), 3001-3023. https://doi.org/10.1002/joc.3887

Bell, J. E., Brown, C. L., Conlon, K., Herring, S., Kunkel, K. E., Lawrimore, J., Luber, G., Schreck, C., Smith, A. & Uejio, C. (2018). Changes in extreme events and the potential impacts on human health. Journal of the Air & Waste Management Association, 68(4), 265-287.

Bennett, D. R., Riewe, R. V., Entz, T., & Woods, S. A. (2015). Water conveyance and on-farm irrigation system efficiency gains in southern Alberta irrigation districts from 1999 to 2012. *Canadian Water Resources Journal/Revue Canadienne des ressources hydriques*, *40*(2), 173-186.

Bennett, D. R., Phillips, R. J., & Gallagher, C. W. (2017). Water available for future growth and economic development in southern Alberta. *Canadian Water Resources Journal/Revue Canadienne des ressources hydriques*, *42*(2), 193-202.

Bonsal, B. R., Wheaton, E. E., Meinert, A., & Siemens, E. (2011a). Characterizing the surface features of the 1999-2005 Canadian Prairie drought in relation to previous severe twentieth century events. *Atmosphere-Ocean, 49*(4), 320-338. https://doi.org/10.1080/07055900.2011.594024

Bonsal, B. R., Wheaton, E. E., Chipanshi, A. C., Lin, C., Sauchyn, D. J., & Wen, L. (2011b). Drought research in Canada: A review. *Atmosphere-Ocean, 49*(4), 303-319. https://doi.org/10.1080/07055900.2011.555103

Bonsal, B. R., Aider, R., Gachon, P., & Lapp, S. (2013). An assessment of Canadian Prairie drought: Past, present, and future. *Climate Dynamics, 41*(2), 501-516. https://doi.org/10.1007/s00382-012-1422-0

Bonsal, B. R., Cuell, C., Wheaton, E., Sauchyn, D. J., & Barrow, E. (2017). An assessment of historical and projected future hydro-climatic variability and extremes over southern watersheds in the Canadian Prairies. *International Journal of Climatology, 37*(10), 3934-3948. https://doi.org/10.1002/joc.4967

Bonsal, B., Liu, Z., Wheaton, E., & Stewart, R. (2020). Historical and projected changes to the stages and other characteristics of severe Canadian Prairie droughts. *Water (Basel), 12*(12), 3370. https://doi.org/10.3390/w12123370

Brown, P. J., Bradley, R. S., Keimig, F. T. (2010) Changes in Extreme Climate Indices for the Northeastern United States, 1870–2005. *Journal of Climate, 23*(24), 6555-6572. doi:10.1175/2010jcli3363.1

Bush, E., Lemmen, D. S. (2019). Canada's changing climate report. Government of Canada, Environment and Climate Change Canada.

Cannon, A. J., Sobie, S. R., & Murdock, T. Q. (2015). Bias correction of GCM precipitation by quantile mapping: how well do methods preserve changes in quantiles and extremes?. *Journal of Climate, 28*(17), 6938-6959.

Chen, A. (2022). Evaluating the relationships between wildfires and drought using machine learning. *International Journal of Wildland Fire, 31*(3), 230-239. https://doi.org/10.1071/WF21145

Chipanshi, A. C., Findlater, K. M., Hadwen, T., & O'Brien, E. G. (2006). Analysis of consecutive droughts on the Canadian Prairies. *Climate Research, 30*(3), 175-187. https://doi.org/10.3354/cr030175

Cook, B. I., Smerdon, J. E., Seager, R., & Coats, S. (2014). Global warming and 21st century drying. *Climate Dynamics, 43*(9-10), 2607-2627. https://doi.org/10.1007/s00382-014-2075-y

Dai, A., Trenberth, K. E., & Qian, T. (2004). A global dataset of palmer drought severity index for 1870–2002: Relationship with soil moisture and effects of surface warming. *Journal of Hydrometeorology, 5*(6), 1117-1130. https://doi.org/10.1175/JHM-386.1

Danandeh Mehr, A., & Vaheddoost, B. (2020). Identification of the trends associated with the SPI and SPEI indices across Ankara, Turkey. *Theoretical and Applied Climatology*, *139*(3-4), 1531-1542.

Dierauer, J. R., Allen, D. M., & Whitfield, P. H. (2019). Snow drought risk and susceptibility in the western United States and southwestern Canada. *Water Resources Research, 55*(4), 3076-3091. https://doi.org/10.1029/2018WR023229

Droogers, P., & Allen, R. G. (2002). Estimating reference evapotranspiration under inaccurate data conditions. *Irrigation and Drainage Systems, 16*(1), 33-45. https://doi.org/10.1023/A:1015508322413

Eslamian, S., Ostad-Ali-Askari, K., Singh, V. P., Dalezios, N. R., Ghane, M., Yihdego, Y., & Matouq, M. (2017). A review of drought indices. *Int. J. Constr. Res. Civ. Eng, 3*, 48-66.

Faramarzi, M., Abbaspour, K. C., Lu, W., Fennell, J., Zehnder, A. J., & Goss, G. G. (2017). Uncertainty based assessment of dynamic freshwater scarcity in semi-arid watersheds of Alberta, Canada. Journal of Hydrology: Regional Studies, 9, 48-68.

French, J., Kokoszka, P., Stoev, S., & Hall, L. (2019). Quantifying the risk of heat waves using extreme value theory and spatio-temporal functional data. *Computational Statistics & Data Analysis, 131*, 176-193. https://doi.org/10.1016/j.csda.2018.07.004

Gasparrini, A., Guo, Y., Sera, F., Vicedo-Cabrera, A. M., Huber, V., Tong, S., de Sousa Zanotti Stagliorio Coelho, M., Nascimento Saldiva, P.H., Lavigne, E., Matus Correa, P. and Valdes Ortega, N., Kan, H., Osorio, S., Kyselý, J., Urban, A., Jaakkola, J. J. K., Ryti, N. R. I., Pascal, M., Goodman, P. G., Zeka, A., Michelozzi, P., Scortichini, M., Hashizume, M., Honda, Y., Hurtado-Diaz, M., Cruz, J. C., Seposo, X., Kim, H., Tobias, A., Iñiguez, C., Forsberg, B., Åström, D.

Q., Ragettli, M. S., Guo, Y. L., Wu, C-f, Zanobetti, A., Schwartz, J., Bell, M. L., Dang, T. N., Van, D. D., Heaviside, C., Vardoulakis, S., Hajat, S., Haines, A. & Armstrong, B. (2017). Projections of temperature-related excess mortality under climate change scenarios. *Lancet Planet Health 1*: e360–e367.

Grace, B., & Johnson, D. L. (1985). The drought of 1984 in southern Alberta: its severity and effects. *Canadian Water Resources Journal*, *10*(2), 28-38.

Grumm, R. H. (2011). The central European and Russian heat event of July–August 2010. *Bulletin of the American Meteorological Society, 92*(10), 1285-1296. https://doi.org/10.1175/2011BAMS3174.1

Grinder, B., Paterson, B. (2010). South Saskatchewan River Basin in Alberta water supply study summary. Alberta Agriculture and Rural Development, & South Saskatchewan River Basin Water Supply Steering Committee (Alta.), Government of Alberta.

Guo, S. (2012). The meteorological disaster risk assessment based on the diffusion mechanism. *Journal of Risk Analysis and Crisis Response (JRACR), 2*(2), 124–130. https://doi.org/10.2991/jracr.2012.2.2.5

Gurrapu, S., Chipanshi, A., Sauchyn, D., & Howard, A. (2014, February). Comparison of the SPI and SPEI on predicting drought conditions and streamflow in the Canadian Prairies. In *Proceedings of the 28th Conference on Hydrology* (pp. 2-6). Atlanta, GA, USA: American Meteorological Society.

Hargreaves, G. H., Samani, Z. A. (1985). Reference crop evapotranspiration from temperature. *Applied Engineering in Agriculture, 1*(2), 96-99. https://doi.org/10.13031/2013.26773

Hargreaves, G. H. (1994). Defining and using reference evapotranspiration. *Journal of irrigation and drainage engineering*, *120*(6), 1132-1139.

Hargreaves, G. H., & Allen, R. G. (2003). History and evaluation of Hargreaves evapotranspiration equation. *Journal of Irrigation and Drainage Engineering, 129*(1), 53-63. https://doi.org/10.1061/(ASCE)0733-9437(2003)129:1(53)

Harpold, A. A. (2016). Diverging sensitivity of soil water stress to changing snowmelt timing in the western U.S. *Advances in Water Resources, 92*, 116-129. https://doi.org/10.1016/j.advwatres.2016.03.017

Hong, X., Guo, S., Xiong, L., & Liu, Z. (2015). Spatial and temporal analysis of drought using entropy-based standardized precipitation index: A case study in Poyang Lake basin, China. *Theoretical and Applied Climatology, 122*(3-4), 543-556. https://doi.org/10.1007/s00704-014-1312-y

Hu, J. I. A., Moore, D. J., Burns, S. P., & Monson, R. K. (2010). Longer growing seasons lead to less carbon sequestration by a subalpine forest. *Global Change Biology,*

16(2), 771-783.

Huang, J., Yu, H., Guan, X., Wang, G., & Guo, R. (2016). Accelerated dryland expansion under climate change. *Nature climate change, 6*(2), 166-171.

IPCC (2012) Field, C. B., Barros, V., Stocker, T. F., Qin, D., Dokken, D. J., Ebi, K. L., Mastrandrea, M. D., Mach, K. J., Plattner, G., -K., Allen, S. K., Tignor, M., & Midgley, P. M. (Eds.), *Managing the risks of extreme events and disasters to advance climate change adaptation: Special report of the intergovernmental panel on climate change*. Cambridge University Press. https://doi.org/10.1017/CBO9781139177245

IPCC (2018) Masson-Delmotte, V., Zhai, P., Pörtner, H. O., Roberts, D., Skea, J., Shukla, P. R., Pirani, A., Moufouma-Okia, W., Péan, C., Pidcock, R., Connors, S., Matthews, J. B. R., Chen, Y., Zhou, X., Gomis, M. I., Lonnoy, E., Maycock, T., Tignor, M., & Waterfield, T. (Eds.). *Global Warming of 1.5°C. An IPCC Special Report on the impacts of global warming of 1.5°C above pre-industrial levels and related global greenhouse gas emission pathways, in the context of strengthening the global response to the threat of climate change, sustainable development, and efforts to eradicate poverty*. Cambridge University Press, Cambridge, UK and New York, NY, USA, 616 pp. https://doi.org/ 10.1017/9781009157940

IPCC (2021a) Masson-Delmotte, V., Zhai, P., Pirani, A., Connors, S. L., Péan, C., Berger, S., Caud, N., Chen, Y., Goldfarb, L., Gomis, M. I., Huang, N., Leitzell, K., Lonnoy, E., Matthews, J. B. R., Maycock, T. K., Waterfield, T., Yelekçi, O., Yu, R., & Zhou, B. (Eds.). *Summary for Policymakers. In: Climate Change 2021: The Physical Science Basis. Contribution of Working Group I to the Sixth Assessment Report of the Intergovernmental Panel on Climate Change* Cambridge University Press, Cambridge, United Kingdom and New York, NY, USA, pp. 3−32, doi:10.1017/9781009157896.001.

IPCC (2021b) Masson-Delmotte, V., P. Zhai, A. Pirani, S.L. Connors, C. Péan, S. Berger, N. Caud, Y. Chen, L. Goldfarb, M.I. Gomis, M. Huang, K. Leitzell, E. Lonnoy, J.B.R. Matthews, T.K. Maycock, T. Waterfield, O. Yelekçi, R. Yu, and B. Zhou (Eds.). *Climate Change 2021: The Physical Science Basis. Contribution of Working Group I to the Sixth Assessment Report of the Intergovernmental Panel on Climate Change.* Cambridge University Press, Cambridge, United Kingdom and New York, NY, USA, 2391 pp. doi:10.1017/9781009157896

Johnson, D. L. (1989) Spatial analysis of the relationship of grasshopper outbreaks to soil classification. *Estimation and analysis of insect populations* (pp. 347-359). Springer New York. https://doi.org/10.1007/978-1-4612-3664-1_24

Johnson, D. L., & Worobec, A. (1988). Spatial and temporal computer analysis of insects and weather: grasshoppers and rainfall in Alberta. *The Memoirs of the Entomological Society of Canada*, *120*(S146), 33-48.

Kchouk, S., Melsen, L. A., Walker, D. W., & van Oel, P. R. (2021). A review of drought

indices: Predominance of drivers over impacts and the importance of local context. *Nat. Hazards Earth Syst. Sci. Discuss*, 1-28.

Khandekar, M. L. (2004). *Canadian Prairie drought: A climatological assessment.* (No. no. T/787;T/787;). Edmonton: Alberta Environment.

Li, X., He, B., Quan, X., Liao, Z., & Bai, X. (2015). Use of the standardized precipitation evapotranspiration index (SPEI) to characterize the drying trend in southwest China from 1982–2012. *Remote Sensing*, *7*(8), 10917-10937.

Li, W., Duan, L., Wang, W., Wu, Y., Liu, T., Quan, Q., Chen, X., Yin, H., & Zhou, Q. (2021). Spatiotemporal characteristics of drought in a semi-arid grassland over the past 56 years based on the standardized precipitation index. *Meteorology and Atmospheric Physics*, 133(1), 41-54. https://doi.org/10.1007/s00703-020-00727-4

Littell, J. S., Peterson, D. L., Riley, K. L., Liu, Y., & Luce, C. H. (2016). A review of the relationships between drought and forest fire in the United States. *Global change biology*, *22*(7), 2353-2369.

Liu, S., Huang, S., Xie, Y., Huang, Q., Leng, G., Hou, B., Zhang, Y., & Wei, X. (2018). Spatial-temporal changes of maximum and minimum temperatures in the Wei River Basin, China: Changing patterns, causes and implications. *Atmospheric Research*, *204*, 1-11.

Luterbacher, J., Dietrich, D., Xoplaki, E., Grosjean, M., & Wanner, H. (2004). European seasonal and annual temperature variability, trends, and extremes since 1500. *Science*, *303*(5663), 1499-1503.

Masroor, M., Sajjad, H., Rehman, S., Singh, R., Rahaman, M. H., Sahana, M., Ahmed, R., Avtar, R. (2022). Analysing the relationship between drought and soil erosion using vegetation health index and RUSLE models in Godavari middle sub-basin, India. *Geoscience Frontiers*, *13*(2), 101312.

Masud, M. B., Khaliq, M. N., & Wheater, H. S. (2015). Analysis of meteorological droughts for the Saskatchewan River Basin using univariate and bivariate approaches. *Journal of Hydrology*, *522*, 452-466.

Mazdiyasni, O., & AghaKouchak, A. (2015). Substantial increase in concurrent droughts and heatwaves in the United States. *Proceedings of the National Academy of Sciences*, *112*(37), 11484-11489.

McKee, T. B., Doesken, N. J., & Kleist, J. (1993, January). The relationship of drought frequency and duration to time scales. In *Proceedings of the 8th Conference on Applied Climatology* (Vol. 17, No. 22, pp. 179-183).

Mehdipoor, H., Zurita-Milla, R., Izquierdo-Verdiguier, E., & Betancourt, J. L. (2018). Influence of source and scale of gridded temperature data on modelled spring onset patterns in the conterminous United States. *International journal of*

climatology, *38*(14), 5430-5440.

Mishra, A. K., & Singh, V. P. (2010). A review of drought concepts. *Journal of Hydrology*, *391*(1-2), 202-216.

Mourtzinis, S., Edreira, J. I. R., Conley, S. P., & Grassini, P. (2017). From grid to field: Assessing quality of gridded weather data for agricultural applications. *European Journal of Agronomy*, *82*, 163-172.

Mousavi, R., Sabziparvar, A. A., Marofi, S., Ebrahimi Pak, N. A., & Heydari, M. (2015). Calibration of the Angström-Prescott solar radiation model for accurate estimation of reference evapotranspiration in the absence of observed solar radiation. *Theoretical and Applied Climatology*, *119*, 43-54.

Mousavi, R. S., Marofi, S., Gupta, H. V., & Ahmadizadeh, M. (2019). Statistical analysis of discharge fluctuations in a semiarid basin using effective atmospheric teleconnections: Dez River Basin in Iran. *Journal of Hydrologic Engineering*, *24*(7), 05019012.

Mousavi, R., Johnson, D., Kroebel, R., & Byrne, J. (2023). Analysis of historical drought conditions based on SPI and SPEI at various timescales in the South Saskatchewan River Watershed, Alberta, Canada. *Theoretical and Applied Climatology*, 153, 873–887.

O'Brien, E. G., & Stroich, J. (2005). Concept of defining drought in Canada: an evaluation of drought indicators for application in the agricultural landscapes of Canada. *National Land and Water Information Service (NLWIS), Agriculture and Agri-Food Canada (AAFC)*.

Parente, J., Pereira, M. G., Amraoui, M., & Fischer, E. M. (2018). Heat waves in Portugal: Current regime, changes in future climate and impacts on extreme wildfires. *Science of the total environment*, *631*, 534-549.

Pei, Z., Fang, S., Wang, L., & Yang, W. (2020). Comparative analysis of drought indicated by the SPI and SPEI at various timescales in inner Mongolia, China. *Water*, *12*(7), 1925.

Penman, H. L. (1948). Natural evaporation from open water, bare soil and grass. *Proceedings of the Royal Society of London. Series A. Mathematical and Physical Sciences*, *193*(1032), 120-145.

Perkins, S. E. (2015). A review on the scientific understanding of heatwaves—Their measurement, driving mechanisms, and changes at the global scale. *Atmospheric Research*, *164*, 242-267.

Peters, W., van der Velde, Ivar R, van Schaik, E., Miller, J. B., Ciais, P., Duarte, H. F., van der Laan-Luijkx, Ingrid T, van der Molen, Michiel K, Scholze, M., Schaefer, K., Vidale, P. L., Verhoef, A., Warlind, D., Zhu, D., Tans, P. P., Vaughn, B., &

White, J. W. C. (2018). Increased water-use efficiency and reduced CO_2 uptake by plants during droughts at a continental scale. *Nature Geoscience, 11*(10), 744-748. https://doi.org/10.1038/s41561-018-0212-7

Peterson, T., Folland, C., Gruza, G., Hogg, W., Mokssit, A., & Plummer, N. (2001). *Report on the activities of the working group on climate change detection and related rapporteurs* (p. 143). Geneva: World Meteorological Organization.

R Core Team (2020) R: A language and environment for statistical computing. R Foundation for Statistical Computing, Vienna, Austria. https://www.R-project.org/

Raymond, C., Horton, R. M., Jakob, Z., Olivia, M., Amir, A., Balch, J., Bowen, S. G., Camargo, S. J., Hess, J., Kai, K., Oppenheimer, M., Ruane, A. C., Wahl, T., & White, K. (2020). Understanding and managing connected extreme events. *Nature Climate Change, 10*(7), 611-621. https://doi.org/10.1038/s41558-020-0790-4

Sabziparvar, A. A., Mousavi, R., Marofi, S., Ebrahimipak, N. A., & Heidari, M. (2013). An improved estimation of the Angstrom–Prescott radiation coefficients for the FAO56 Penman–Monteith evapotranspiration method. *Water Resources Management*, *27*, 2839-2854.

Shabbar, A., & Skinner, W. (2004). Summer drought patterns in Canada and the relationship to global sea surface temperatures. *Journal of Climate*, *17*(14), 2866-2880.

Sheffield, J., & Wood, E. F. (2008). Projected changes in drought occurrence under future global warming from multi-model, multi-scenario, IPCC AR4 simulations. *Climate dynamics*, *31*, 79-105.

Sheffield, J., Wood, E. F., & Roderick, M. L. (2012). Little change in global drought over the past 60 years. *Nature*, *491*(7424), 435-438.

Spinoni, J., Naumann, G., Carrao, H., Barbosa, P., & Vogt, J. (2014). World drought frequency, duration, and severity for 1951–2010. *International Journal of Climatology*, *34*(8), 2792-2804.

Spinoni, J., Vogt, J. V., Naumann, G., Barbosa, P., & Dosio, A. (2018). Will drought events become more frequent and severe in Europe?. *International Journal of Climatology*, *38*(4), 1718-1736.

Spinoni, J., Barbosa, P., De Jager, A., McCormick, N., Naumann, G., Vogt, J. V., Magni, D., Masante D. & Mazzeschi, M. (2019). A new global database of meteorological drought events from 1951 to 2016. *Journal of Hydrology: Regional Studies*, *22*, 100593.

Stewart, R. E., Bonsal, B. R., Harder, P., Henson, W., & Kochtubajda, B. (2012). Cold and hot periods associated with dry conditions over the Canadian Prairies. *Atmosphere-ocean*, *50*(3), 364-372.

Sun, L., Mitchell, S. W., & Davidson, A. (2012). Multiple drought indices for agricultural drought risk assessment on the Canadian Prairies. *International Journal of Climatology*, *32*(11), 1628-1639.

Svoboda, M. D., & Fuchs, B. A. (2016). Handbook of drought indicators and indices. *Drought and water crises* (2nd ed., pp. 155-208). CRC Press. https://doi.org/10.1201/b22009-11

Swain, D. L., Tsiang, M., Haugen, M., Singh, D., Charland, A., Rajaratnam, B., & Diffenbaugh, N. S. (2014). The extraordinary California drought of 2013/2014: Character, context, and the role of climate change. *Bulletin of the American Meteorological Society*, *95*(9), S3.

Tabari, H. (2020). Climate change impact on flood and extreme precipitation increases with water availability. *Scientific reports*, *10*(1), 13768.

Tan, C., Yang, J., & Li, M. (2015). Temporal-spatial variation of drought indicated by SPI and SPEI in Ningxia Hui Autonomous Region, China. *Atmosphere*, *6*(10), 1399-1421.

Tefera, A. S., Ayoade, J. O., & Bello, N. J. (2019). Comparative analyses of SPI and SPEI as drought assessment tools in Tigray Region, Northern Ethiopia. *SN Applied Sciences*, *1*, 1-14.

Thornthwaite, C. W. (1948). An approach toward a rational classification of climate. *Geographical review*, *38*(1), 55-94.

Thornton, P. E., Running, S. W., & White, M. A. (1997). Generating surfaces of daily meteorological variables over large regions of complex terrain. *Journal of hydrology*, *190*(3-4), 214-251.

Thornton, P. E., Thornton, M. M., Mayer, B. W., Wei, Y., Devarakonda, R. S., Vose, R. S., & Cook, R. B. (2017). Daymet: Daily Surface Weather Data on a 1-km Grid for North America, Version 3 ORNL DAAC Oak Ridge Tenn.

Tran, T. V., Tran, D. X., Myint, S. W., Latorre-Carmona, P., Ho, D. D., Tran, P. H., & Dao, H. N. (2019). Assessing spatiotemporal drought dynamics and its related environmental issues in the Mekong River Delta. *Remote Sensing*, *11*(23), 2742.

Van Loon, C. D. (1981). The effect of water stress on potato growth, development, and yield. American potato journal, 58, 51-69.

Vicente-Serrano, S. M., Beguería, S., & López-Moreno, J. I. (2010). A multiscalar drought index sensitive to global warming: the standardized precipitation evapotranspiration index. *Journal of climate*, *23*(7), 1696-1718.

Walton, D., & Hall, A. (2018). An assessment of high-resolution gridded temperature datasets over California. *Journal of Climate*, *31*(10), 3789-3810.

Wang, H., Lemke, R., Goddard, T., & Sprout, C. (2007). Tillage and root heat stress in wheat in central Alberta. *Canadian Journal of Soil Science, 87*(1), 3-10.

Wang, Q., Zeng, J., Qi, J., Zhang, X., Zeng, Y., Shui, W., Xu, Z., Zhang, R., Wu, X., & Cong, J. (2021a). A multi-scale daily SPEI dataset for drought characterization at observation stations over mainland China from 1961 to 2018. *Earth System Science Data*, *13*(2), 331-341.

Wang, T., Tu, X., Singh, V. P., Chen, X., & Lin, K. (2021b). Global data assessment and analysis of drought characteristics based on CMIP6. *Journal of Hydrology*, *596*, 126091.

Werner, A. T., & Cannon, A. J. (2016). Hydrologic extremes–an intercomparison of multiple gridded statistical downscaling methods. *Hydrology and Earth System Sciences, 20*(4), 1483-1508.

Westerling, A. L., Hidalgo, H. G., Cayan, D. R., & Swetnam, T. W. (2006). Warming and earlier spring increase western US forest wildfire activity. *science*, *313*(5789), 940-943.

Wheater, H., & Gober, P. (2013). Water security in the Canadian Prairies: science and management challenges. *Philosophical Transactions of the Royal Society A: Mathematical, Physical and Engineering Sciences*, *371*(2002), 20120409.

Wheaton, E., Kulshreshtha, S., Wittrock, V., & Koshida, G. (2008). Dry times: hard lessons from the Canadian drought of 2001 and 2002. *The Canadian Geographer/Le Géographe Canadien*, *52*(2), 241-262.

Winchell, T. S., Barnard, D. M., Monson, R. K., Burns, S. P., & Molotch, N. P. (2016). Earlier snowmelt reduces atmospheric carbon uptake in midlatitude subalpine forests. *Geophysical Research Letters*, *43*(15), 8160-8168.

Xu, B., Arain, M. A., Black, T. A., Law, B. E., Pastorello, G. Z., & Chu, H. (2020). Seasonal variability of forest sensitivity to heat and drought stresses: a synthesis based on carbon fluxes from North American forest ecosystems. *Global change biology*, *26*(2), 901-918.

Yang, M., Yan, D., Yu, Y., & Yang, Z. (2016). SPEI-based spatiotemporal analysis of drought in Haihe River Basin from 1961 to 2010. *Advances in Meteorology*, *2016*, 1-10.

Yang, Y., Gan, T. Y., & Tan, X. (2020). Spatiotemporal changes of drought characteristics and their dynamic drivers in Canada. *Atmospheric Research*, *232*, 104695.

Zargar, A., Sadiq, R., Naser, B., & Khan, F. I. (2011). A review of drought indices. Environmental Reviews, 19(NA), 333-349. https://doi.org/10.1139/a11-013

Zhang, A., & Jia, G. (2013). Monitoring meteorological drought in semiarid regions using multi-sensor microwave remote sensing data. *Remote sensing of Environment*, *134*, 12-23.

Zhang, Q., Qi, T., Singh, V. P., Chen, Y. D., & Xiao, M. (2015). Regional frequency analysis of droughts in China: a multivariate perspective. *Water Resources Management*, *29*, 1767-1787.

Zscheischler, J., Westra, S., Van Den Hurk, B. J., Seneviratne, S. I., Ward, P. J., Pitman, A., AghaKouchak, A., Bresch, D.N., Leonard, M., Wahl, T., & Zhang, X. (2018). Future climate risk from compound events. *Nature Climate Change*, *8*(6), 469-477.